Finite-Time Output Feedback Tracking Control for Autonomous Underwater Vehicles

Shihua Li, *Senior Member, IEEE*, Xiangyu Wang, and Lijun Zhang, *Member, IEEE*

***Abstract*—In this paper, the finite-time output feedback trajectory tracking control problem for autonomous underwater vehicles (AUVs) is investigated. The vehicle model is constructed in six degrees of freedom and the vehicle attitude is represented by quaternions to avoid representation singularities. The control design consists of three steps. First, by using the finite-time control technique, two global finite-time stabilizing controllers based on state feedback are proposed for the vehicle translational and rotational tracking error subsystems, respectively. Second, considering the estimation problem of the vehicle translational velocities, a global finite-time convergent observer is employed to reconstruct the information of the vehicle translational velocities. Finally, based on the proposed state feedback controllers and the finite-time convergent observer, a finite-time output feedback trajectory tracking control scheme for AUVs is derived. Global finite-time stability of the closed-loop system is rigorously proved by using Lyapunov theory. Compared with the conventional backstepping control scheme via output feedback, the proposed finite-time output feedback control scheme offers not only a faster convergence rate but also a higher tracking accuracy for trajectory tracking control of AUVs. Simulations demonstrate the effectiveness of the proposed control scheme.**

***Index Terms*—Autonomous underwater vehicles (AUVs), finite-time control, finite-time convergent observer, output feedback control, trajectory tracking control.**

I. Introduction

In the past few years, control of autonomous underwater vehicles (AUVs) has been a field of increasing interest, including both control of individual AUV systems [1]–[9], [11], [15]–[17] and cooperative control of multiple AUVs [18]–[21]. This is motivated by various applications of AUVs, such as geological surveying, pipeline inspection, and diver support. As many of the applications require AUVs to operate in environments with obstacles and hazards, it is imperative that their motion be accurately controlled in six degrees of freedom (DOFs). However, due to highly nonlinear and strongly coupled dynamics of AUVs and the environmental disturbances (such as currents, waves, etc.), it is a great challenge to provide high accuracy motion control for AUVs.

Generally speaking, there are two important issues in the motion control literature for AUVs. One is to develop a motion control scheme under the condition that all the states of AUVs in 6 DOFs are measurable, which yields a full state feedback control scheme. In this respect, recently, numerous nonlinear control methods have been utilized to achieve improved performances for motion control of AUVs. In [1] and [2], the sliding mode control techniques were applied to motion control of AUVs. In [3], the backstepping control approach was employed to design a model-based control scheme for path following of a kind of underactuated AUVs. In [4], an AUV docking approach based on fuzzy control was presented. In [5], an H_∞ control design approach was presented for motion control of AUVs. In [6]–[9], the adaptive control methods were utilized for motion control of AUVs to improve robustness of the control systems against parameter uncertainties.

To implement the aforementioned control schemes, full state information of the AUV, including the position and orientation (or attitude) in the inertial reference frame and the velocities in the body-fixed reference frame, needs to be measured. Usually, this information can be measured by using some equipment, e.g., an inertial navigation system (INS) consisting of a measurement part (IMU) and software that computes position and attitude in the inertial reference frame from the measurements [10]. Specifically, an AUV can be equipped with a compass module (including a biaxial electrolytic inclinometer and a triaxial magnetometer system [11]) to measure its attitude in the inertial reference frame, and angular velocities can be measured by an angular rate sensor. As for positioning, the typical positioning systems include the acoustic ultrashort baseline (USBL) system [4], acoustic long baseline (LBL) system [12], global positioning system (GPS) [13], and INS [14]. Under different work situations, different techniques can be chosen or combined together to get the positions of AUVs with very good accuracy. Turning to measurements of the translational velocities, usually, these velocities can be obtained by the Doppler velocity log (DVL) [14]. However, in some cases, due to economic and other practical limitations, AUVs may not be equipped with DVLs. Even when an AUV is equipped with a DVL, the measured translational velocities by DVL may be not adequately accurate because of measurement noises.

Correspondingly, the other important issue is to investigate motion control for AUVs with inaccurate or without translational velocity measurements. In such cases, a simple way to

Manuscript received October 27, 2011; revised July 18, 2013; accepted June 08, 2014. Date of publication July 09, 2014; date of current version July 10, 2015. This work was supported by the National Natural Science Foundation of China under Grants 61074013 and 61174047; by the Science Foundation for Distinguished Young Scholars of Jiangsu Province under Grant BK20130018; by the Scientific Research Foundation of Graduate School of Southeast University under Grant YBJJ1213; and by the Graduate Innovation Program of Jiangsu Province, China.

Guest Editor: M. Seto.

S. Li and X. Wang are with the School of Automation, Southeast University, Nanjing, Jiangsu 210096, China and also with the Key Laboratory of Measurement and Control of Complex Systems of Engineering, Ministry of Education, Nanjing, Jiangsu 210096, China (e-mail: lsh@seu.edu.cn; wxyu@seu.edu.cn).

L. Zhang is with the School of Marine Science and Technology, Northwestern Polytechnical University, Xi'an, Shanxi 710072, China (e-mail: zhanglj7385@nwpu.edu.cn).

Digital Object Identifier 10.1109/JOE.2014.2330958

obtain the translational velocities is via numerical differentiation of position measurements. However, this way is not feasible, since the position measurements are usually corrupted by noises. Being aware of this fact, to tackle the estimation problem of the translational velocities, several kinds of velocity observers have been developed [15]–[17]. In [15], an output feedback control scheme via observer backstepping was presented for the trajectory tracking control of AUVs which move in shallow-water areas and the translational velocity information was provided by a nonlinear observer based on the passivity approach. In [16], also by using backstepping control approach, a model-based output feedback control scheme was proposed for slender-body underactuated AUVs and the translational velocity information was generated from a nonlinear Luenberger observer. In [17], for the trajectory tracking control of AUVs, an adaptive output feedback controller based on dynamic recurrent fuzzy neural network (DRFNN) was proposed and the translational velocity information was generated from a linear observer.

Since most of the existing AUV controllers depend more or less on model information, a proper identification of the AUV model is desired. On this issue, there are several typical approaches, such as online adaptive identification [22], a least squares algorithm [23], identification based on support vector machines [24], neural network identification [25], and observer Kalman filter identification [26].

Trajectory tracking control is one of the most important issues in motion control for AUVs [9], [15], [17]. Note that for most of trajectory tracking control systems of AUVs in the literature, the Lipschitz continuity is satisfied. Therefore, the convergence rates of such systems are at best exponential with infinite time settling time, which implies that the states of such systems cannot be stabilized to their equilibria in finite time. To this end, tracking controllers which can provide finite-time convergence are more desirable. Nevertheless, finite-time convergence indicates that the closed-loop control system does not satisfy Lipschitz continuity, which is the main difference as well as difficulty for the analysis and synthesis problems of finite-time control.

The finite-time control systems are of interest because the systems with finite-time convergence usually demonstrate not only faster convergence rates, but also some other nice features, such as better disturbance rejection properties and better robustness against uncertainties [27]–[29]. Due to the above superiorities and the convenience of continuous controllers in actual operations, the continuous finite-time control technique has received increasing attention recently, such as finite-time state feedback control [28]–[37], finite-time convergent observer design [38]–[42], finite-time output feedback control [43]–[46], etc.

In this paper, the finite-time output feedback trajectory tracking control problem of AUVs in 6 DOFs is studied. The control design procedure is threefold.

First, based on adding a power integrator approach [33], two state feedback controllers with fractional powers are proposed to globally finite-time stabilize the vehicle translational and rotational tracking error subsystems, respectively. Similar to the conventional backstepping control technique, the adding of power integrator approach is also a recursive process composed of two steps. However, in each step, the designed (virtual) controller is a nonsmooth one with a fractional power, which is different from that in the backstepping design process. To avoid representation singularities that occur when using Euler angles, the vehicle attitude is described by quaternions. In this paper, the vehicle rotational control design is inspired by the set stabilization control method for the spacecraft attitude based on quaternion proposed in [28]. But different from [28], the vehicle rotational subsystem of AUVs is coupled with the translational velocities. In this paper, a corresponding output feedback controller for the rotational tracking error subsystem is also developed in the cases with inaccurate or without translational velocity measurements.

Second, to solve the estimation problem of the translational velocities, a global finite-time convergent observer is developed for the vehicle translational subsystem. There are two common obstacles in observer designs for AUVs. One obstacle is how to cope with the Coriolis and centripetal effects. In this paper, this obstacle is well overcome by exploiting some structural properties of the vehicle translational subsystem and using an ingenious coordinate transformation. The other obstacle lies in high nonlinearities of the translational subsystem. Based on the translated model and by using the homogeneous method [27], [32], the finite-time convergent observer design is achieved.

Finally, based on the finite-time state feedback controllers for the tracking error subsystems and the finite-time convergent observer, a global finite-time output feedback trajectory tracking control scheme for AUVs is derived. Rigorous stability analysis shows that the states of the tracking error subsystems will be globally stabilized to their equilibria in finite time under the output feedback controllers.

If the fractional powers of the proposed finite-time controllers are taken as 1, these controllers will reduce to the corresponding conventional backstepping controllers. Compared with these reduced controllers, the finite-time controllers provide faster convergence rates, better disturbance rejection properties, and better robustness for trajectory tracking control of AUVs (see Remarks 5 and 6). Moreover, compared with the output feedback backstepping control method presented in [15], the proposed finite-time output feedback control scheme also holds superiorities in the convergence rate, disturbance rejection capability, and robustness. Although some finite-time output feedback control results have been reported for other systems [43]–[46], no corresponding result for trajectory tracking control of AUVs has been available until now.

The remainder of this paper is organized as follows. In Section II, some useful notations and preliminaries are given. In Section III, system modeling and problem formulations are exhibited. In Section IV, the finite-time output feedback trajectory tracking control scheme for AUVs is presented. In Section V, the AUV model identification process is explicitly addressed, and several simulation comparisons between the proposed finite-time control scheme and the backstepping control scheme presented in [15] are performed. Finally, conclusions are drawn in Section VI.

II. Notations and Preliminaries

A. Notations

The following notations are used throughout this paper. Denote $\mathrm{sig}^\alpha(x) = \mathrm{sgn}(x)|x|^\alpha$, where $\alpha \geq 0, x \in \mathbb{R}$ and $\mathrm{sgn}(\cdot)$ is the standard sign function. For a vector $\boldsymbol{x} \in \mathbb{R}^n$, the Euclidean norm of $\boldsymbol{x}$ and the ith element of $\boldsymbol{x}$ are denoted as $\|\boldsymbol{x}\| = \sqrt{\boldsymbol{x}^T\boldsymbol{x}}$ and $[\boldsymbol{x}]_i$, respectively. For a matrix $\boldsymbol{P} \in \mathbb{R}^{n\times n}$, the maximum and minimum eigenvalues of matrix $\boldsymbol{P}$ are denoted as $\lambda_{\max}(\boldsymbol{P})$ and $\lambda_{\min}(\boldsymbol{P})$, respectively. For a matrix $\boldsymbol{A} \in \mathbb{R}^{m\times n}$, the standard notation

$$\|\boldsymbol{A}\| = \sqrt{\lambda_{\max}(\boldsymbol{A}^T\boldsymbol{A})}$$

is used to denote the induced 2-norm of $\boldsymbol{A}$. The $n \times n$ identity matrix is denoted as $\boldsymbol{I}_{n\times n}$ and the $m \times n$ zero matrix is denoted as $\boldsymbol{0}_{m\times n}$.

B. Preliminaries

In this section, some definitions and lemmas are reviewed, which will be useful for the subsequent analysis.

Consider the system

$$\dot{\boldsymbol{x}} = \boldsymbol{f}(\boldsymbol{x}), \quad \boldsymbol{f}(\boldsymbol{0}) = \boldsymbol{0}, \quad \boldsymbol{x} \in \mathbb{R}^n. \tag{1}$$

Definition 1 (Finite-Time Stability [27]): Consider system (1), where $\boldsymbol{f} : D \to \mathbb{R}^n$ is non-Lipschitz continuous on a neighborhood D of the origin $\boldsymbol{x} = \boldsymbol{0}$ in $\mathbb{R}^n$. The equilibrium $\boldsymbol{x} = \boldsymbol{0}$ of (1) is finite-time convergent if there are an open neighborhood U of the origin and a function $T : U \setminus \{\boldsymbol{0}\} \to (0, \infty)$, such that every solution trajectory $\boldsymbol{x}(t, \boldsymbol{x}_0)$ of (1) starting from the initial point $\boldsymbol{x}_0 \in U \setminus \{\boldsymbol{0}\}$ is well defined and unique in forward time for $t \in [0, T(\boldsymbol{x}_0))$, and $\lim_{t\to T(\boldsymbol{x}_0)} \boldsymbol{x}(t, \boldsymbol{x}_0) = \boldsymbol{0}$. Here $T(\boldsymbol{x}_0)$ is called the settling time (of the initial state $\boldsymbol{x}_0$). The equilibrium $\boldsymbol{x} = \boldsymbol{0}$ of (1) is finite-time stable if it is Lyapunov stable and finite-time convergent. If $U = D = \mathbb{R}^n$, the origin is a globally finite-time stable equilibrium.

Definition 2 (Finite-Time Set Stability [47], [48]): Suppose M is a nonempty set. System (1) is said to be finite-time stable with respect to M if there exists an open neighborhood $N \subset \mathbb{R}^n$ of the set M and a function $T : N \setminus M \to (0, \infty)$, called the settling-time function, such that the following conditions hold.

i) Finite-time convergence: For every $\boldsymbol{x}_0 \in N\setminus M, \boldsymbol{x}(t, \boldsymbol{x}_0)$ is defined on $[0, T(\boldsymbol{x}_0)), \boldsymbol{x}(t, \boldsymbol{x}_0) \in N \setminus M$ for all $t \in [0, T(\boldsymbol{x}_0))$, and $\lim_{t\to T(\boldsymbol{x}_0)} d(\boldsymbol{x}(t, \boldsymbol{x}_0), M) = 0$.

ii) Lyapunov stability: For every open neighborhood N_ε of M, there exists an open subset N_δ of N containing M, such that for every $\boldsymbol{x}_0 \in N_\delta \setminus M, \boldsymbol{x}(t, \boldsymbol{x}_0) \in N_\varepsilon$ for all $t \in [0, +\infty)$.

If $N = \mathbb{R}^n$, then system (1) is said to be globally finite-time stable with respect to M.

Definition 3 [50]: Suppose the set M is compact. A function $V(\boldsymbol{x}) : \mathbb{R}^n \to [0, +\infty)$ is said to be a positive–definite function with respect to M for system (1) if it is continuous and $\forall \boldsymbol{x} \in \mathbb{R}^n \setminus M, V(\boldsymbol{x}) > 0$ and $V(M) = 0$.

Definition 4 (Homogeneity [27]): Consider system (1), where $\boldsymbol{f} : D \to \mathbb{R}^n$ is continuous on a neighborhood D of the origin $\boldsymbol{x} = \boldsymbol{0}$ in $\mathbb{R}^n$. Let

$$[r_1, \ldots, r_n] \in \mathbb{R}^n, \qquad \text{with } r_i > 0, \quad i = 1, \ldots, n$$

Let

$$\boldsymbol{f}(\boldsymbol{x}) = [f_1(\boldsymbol{x}), \ldots, f_n(\boldsymbol{x})]^T$$

be a continuous vector field. $\boldsymbol{f}(\boldsymbol{x})$ is said to be homogeneous of degree $k \in \mathbb{R}$ with respect to $[r_1, \ldots, r_n]$ if, for any given $\varepsilon > 0$

$$f_i\left(\varepsilon^{r_1}x_1, \ldots, \varepsilon^{r_n}x_n\right) = \varepsilon^{k+r_i} f_i(\boldsymbol{x}), \qquad i = 1, \ldots, n, \forall \boldsymbol{x} \in \mathbb{R}^n$$

where $k \geq -\min\{r_i, i = 1, \ldots, n\}$. System (1) is said to be homogeneous if $\boldsymbol{f}(\boldsymbol{x})$ is homogeneous.

Lemma 1 [27]: Considering system (1), suppose there exists a continuous function $V(\boldsymbol{x}) : U \to \mathbb{R}$ such that the following conditions hold.

i) $V(\boldsymbol{x})$ is positive definite.

ii) There exist real numbers $c > 0$ and $\alpha \in (0, 1)$ and an open neighborhood $U_0 \subset U$ of the origin such that

$$\dot{V}(\boldsymbol{x}) + cV^\alpha(\boldsymbol{x}) \leq 0, \qquad \boldsymbol{x} \in U_0 \setminus \{\boldsymbol{0}\}.$$

Then, the origin is a finite-time stable equilibrium of system (1). If $U = U_0 = \mathbb{R}^n$, the origin is a globally finite-time stable equilibrium of system (1).

Lemma 2 [33]: For any real numbers $x_i, i = 1, \ldots, n$ and $0 < b \leq 1$, the following two inequalities hold:

$$\left(\sum_{i=1}^{n} |x_i|\right)^b \leq \sum_{i=1}^{n} |x_i|^b \tag{2}$$

$$\begin{aligned} |x + y|^{1/b} &\leq 2^{1/b-1}|x^{1/b} + y^{1/b}| \\ &\leq 2^{1/b-1}\left(|x|^{1/b} + |y|^{1/b}\right). \end{aligned} \tag{3}$$

When $b = p/q \leq 1$, where $p > 0$ and $q > 0$ are odd integers, another inequality holds

$$|x^b - y^b| \leq 2^{1-b}|x - y|^b. \tag{4}$$

Lemma 3 [33]: Let c, d be positive real numbers and $\gamma(x, y) > 0$ be a real-valued function with $x, y \in \mathbb{R}$. Then

$$|x|^c|y|^d \leq \frac{c\gamma(x, y)|x|^{c+d}}{c + d} + \frac{d\gamma^{-c/d}(x, y)|y|^{c+d}}{c + d}. \tag{5}$$

Lemma 4 [32]: Consider the following system:

$$\dot{\boldsymbol{x}} = \boldsymbol{f}(\boldsymbol{x}) + \hat{\boldsymbol{f}}(\boldsymbol{x}), \boldsymbol{f}(\boldsymbol{0}) = \boldsymbol{0}, \qquad \boldsymbol{x} \in \mathbb{R}^n \tag{6}$$

where $\boldsymbol{f}(\boldsymbol{x})$ is a continuous homogeneous vector field of degree $k < 0$ with respect to $[r_1, \ldots, r_n]$, and $\hat{\boldsymbol{f}}$ satisfies $\hat{\boldsymbol{f}}(\boldsymbol{0}) = \boldsymbol{0}$. Assume $\boldsymbol{x} = \boldsymbol{0}$ is an asymptotically stable equilibrium of the system $\dot{\boldsymbol{x}} = \boldsymbol{f}(\boldsymbol{x})$. Then, $\boldsymbol{x} = \boldsymbol{0}$ is a locally finite-time stable equilibrium of the system if

$$\lim_{\varepsilon\to 0} \frac{\hat{f}_i\left(\varepsilon^{r_1}x_1, \ldots, \varepsilon^{r_n}x_n\right)}{\varepsilon^{k+r_i}} = 0, \qquad i = 1, \ldots, n, \forall \boldsymbol{x} \neq \boldsymbol{0}.$$

III. System Modeling and Problem Formulation

In this section, the system modeling of AUVs, which consists of the vehicle kinematic and dynamic subsystems, is conducted. Then, based on the constructed system model, the main control problem considered in this paper is addressed.

A. Vehicle Kinematic Subsystem

The vehicle body-fixed and inertial reference frames are denoted as the B-frame (xyz) and the I-frame (XYZ), respectively. The I-frame position of the B-frame origin is denoted as $\boldsymbol{r} = [r_1, r_2, r_2]^T$.

It is well known that the use of minimal (i.e., three parameters) orientation descriptions, e.g., Euler angles, is subject to the occurrence of representation singularities. On the other hand, the quaternion uses the least possible number of parameters (i.e., four parameters) to globally represent orientation without representation singularities. Therefore, in this paper, the vehicle attitude is represented by the quaternion $\boldsymbol{q} = [\eta, \boldsymbol{\epsilon}^T]^T$ with $\boldsymbol{\epsilon} = [\epsilon_1, \epsilon_2, \epsilon_3]^T$. Actually, let Φ denote the principal angle and $\boldsymbol{n} = [n_1, n_2, n_3]^T$ denote the principal axis associated with Euler's theorem with $\|\boldsymbol{n}\| = 1$. Then, the quaternion is related to $\boldsymbol{n}$ and Φ by

$$\eta = \cos\left(\frac{\Phi}{2}\right), \quad \boldsymbol{\epsilon} = \boldsymbol{n}\sin\left(\frac{\Phi}{2}\right). \tag{7}$$

From (7), it can be obtained that

$$\eta^2 + \epsilon_1^2 + \epsilon_2^2 + \epsilon_3^2 = 1. \tag{8}$$

The vehicle translational and angular velocity vectors in the B-frame are denoted as

$$\boldsymbol{v} = [v_1, v_2, v_3]^T \quad \text{and} \quad \boldsymbol{\omega} = [\omega_1, \omega_2, \omega_3]^T$$

respectively.

For AUVs, the vehicle kinematics can be expressed as

$$\dot{\boldsymbol{r}} = \boldsymbol{R}(\boldsymbol{q})\boldsymbol{v} \tag{9}$$

$$\dot{\boldsymbol{q}} = \frac{1}{2}\boldsymbol{U}(\boldsymbol{q})\boldsymbol{\omega} \tag{10}$$

where

$$\boldsymbol{R}(\boldsymbol{q}) = \boldsymbol{I}_{3\times3} + 2\eta\boldsymbol{S}(\boldsymbol{\epsilon}) + 2\boldsymbol{S}^2(\boldsymbol{\epsilon})$$
$$\boldsymbol{U}(\boldsymbol{q}) = \begin{bmatrix} -\boldsymbol{\epsilon}^T \\ \eta\boldsymbol{I}_{3\times3} + \boldsymbol{S}(\boldsymbol{\epsilon}) \end{bmatrix}$$

with the skew-symmetric matrix

$$\boldsymbol{S}(\boldsymbol{a}) = -\boldsymbol{S}^T(\boldsymbol{a}), \quad \boldsymbol{a} = [a_1, a_2, a_3]^T \in \mathbb{R}^3$$

defined as follows:

$$\boldsymbol{S}(\boldsymbol{a}) = \begin{bmatrix} 0 & -a_3 & a_2 \\ a_3 & 0 & -a_1 \\ -a_2 & a_1 & 0 \end{bmatrix}.$$

Note that, $\forall \boldsymbol{a} \in \mathbb{R}^3$, the following equality holds:

$$\boldsymbol{S}^T(\boldsymbol{a})\boldsymbol{S}(\boldsymbol{a}) = \begin{bmatrix} a_2^2 + a_3^2 & -a_1a_2 & -a_1a_3 \\ -a_1a_2 & a_1^2 + a_3^2 & -a_2a_3 \\ -a_1a_3 & -a_2a_3 & a_1^2 + a_2^2 \end{bmatrix}.$$

Then, by using Gershgorin disk theorem [49], it can be obtained that

$$\begin{aligned}\lambda_{\max}(\boldsymbol{S}^T(\boldsymbol{a})\boldsymbol{S}(\boldsymbol{a})) \le \max\big\{&a_2^2 + a_3^2 + |a_1a_2| + |a_1a_3|,\\ &a_1^2 + a_3^2 + |a_1a_2| + |a_2a_3|,\\ &a_1^2 + a_2^2 + |a_1a_3| + |a_2a_3|\big\}.\end{aligned} \tag{11}$$

It follows from (11) that

$$\|\boldsymbol{S}(\boldsymbol{a})\| = \left[\lambda_{\max}(\boldsymbol{S}^T(\boldsymbol{a})\boldsymbol{S}(\boldsymbol{a}))\right]^{1/2} \le \frac{\sqrt{6}}{2}\|\boldsymbol{a}\| \qquad \forall \boldsymbol{a} \in \mathbb{R}^3. \tag{12}$$

In addition, for $\boldsymbol{R}(\boldsymbol{q})$, it holds that

$$\begin{aligned}&\boldsymbol{R}^T(\boldsymbol{q})\boldsymbol{R}(\boldsymbol{q}) = \boldsymbol{I}_{3\times3}\\ &\boldsymbol{R}(\boldsymbol{q}) = \boldsymbol{R}(-\boldsymbol{q}), \dot{\boldsymbol{R}}(\boldsymbol{q}) = \boldsymbol{R}(\boldsymbol{q})\boldsymbol{S}(\boldsymbol{\omega}).\end{aligned} \tag{13}$$

For $\boldsymbol{U}(\boldsymbol{q})$, it holds that

$$\boldsymbol{U}^T(\boldsymbol{q})\boldsymbol{U}(\boldsymbol{q}) = \boldsymbol{I}_{3\times3}, \quad \boldsymbol{U}^T(\boldsymbol{q})\boldsymbol{q} = \boldsymbol{0}_{3\times1}. \tag{14}$$

B. Vehicle Dynamic Subsystem

The vehicle dynamic model in the B-frame can be described as [10]

$$\boldsymbol{M}\dot{\boldsymbol{\nu}} + \boldsymbol{C}(\boldsymbol{\nu})\boldsymbol{\nu} + \boldsymbol{D}(\boldsymbol{\nu})\boldsymbol{\nu} + \boldsymbol{g}(\boldsymbol{q}) = \boldsymbol{\tau} + \boldsymbol{\tau}_d \tag{15}$$

where $\boldsymbol{\nu} = [\boldsymbol{v}^T, \boldsymbol{\omega}^T]^T$, $\boldsymbol{\tau} = [\boldsymbol{\tau}_1^T, \boldsymbol{\tau}_2^T]^T \in \mathbb{R}^6$ is the vector of actuator forces and moments with

$$\boldsymbol{\tau}_1 = [\tau_{11}, \tau_{12}, \tau_{13}]^T$$
$$\boldsymbol{\tau}_2 = [\tau_{21}, \tau_{22}, \tau_{23}]^T \in \mathbb{R}^3$$
$$\boldsymbol{\tau}_d = [\boldsymbol{\tau}_{d_1}^T, \boldsymbol{\tau}_{d_2}^T]^T \in \mathbb{R}^6$$

representing the vector of external disturbances affecting the control forces and moments with $\boldsymbol{\tau}_{d_1}, \boldsymbol{\tau}_{d_2} \in \mathbb{R}^3$. The system inertia matrix $\boldsymbol{M} \in \mathbb{R}^{6\times6}$ includes the rigid-body inertia matrix $\boldsymbol{M}_{RB}$ and the hydrodynamic added inertia matrix $\boldsymbol{M}_A$, i.e., $\boldsymbol{M} = \boldsymbol{M}_{RB} + \boldsymbol{M}_A$. Matrix $\boldsymbol{C}(\boldsymbol{\nu}) \in \mathbb{R}^{6\times6}$ is the matrix of Coriolis and centripetal effects. Matrix $\boldsymbol{D}(\boldsymbol{\nu}) \in \mathbb{R}^{6\times6}$ is the damping matrix. Vector $\boldsymbol{g}(\boldsymbol{q}) = [\boldsymbol{g}_1^T(\boldsymbol{q}), \boldsymbol{g}_2^T(\boldsymbol{q})]^T \in \mathbb{R}^6$ is the vector of restoring forces and moments with $\boldsymbol{g}_1(\boldsymbol{q}), \boldsymbol{g}_2(\boldsymbol{q}) \in \mathbb{R}^3$.

Matrix $\boldsymbol{M}$ can be written as

$$\boldsymbol{M} = \begin{bmatrix} \boldsymbol{M}_{11} & \boldsymbol{M}_{12} \\ \boldsymbol{M}_{21} & \boldsymbol{M}_{22} \end{bmatrix} = \boldsymbol{M}_{RB} + \boldsymbol{M}_A \tag{16}$$

where

$$\boldsymbol{M}_{RB} = \begin{bmatrix} m\boldsymbol{I}_{3\times3} & -m\boldsymbol{S}(\boldsymbol{r}_G) \\ m\boldsymbol{S}(\boldsymbol{r}_G) & \boldsymbol{I}_B \end{bmatrix}$$
$$\boldsymbol{M}_A = \begin{bmatrix} \boldsymbol{A}_{11} & \boldsymbol{A}_{12} \\ \boldsymbol{A}_{21} & \boldsymbol{A}_{22} \end{bmatrix}.$$

m is the vehicle mass, $\boldsymbol{I}_B$ is the inertia tensor of the vehicle with respect to B-frame origin, and $\boldsymbol{A}_{11} = \boldsymbol{A}_{11}^T, \boldsymbol{A}_{12} = \boldsymbol{A}_{21}^T, \boldsymbol{A}_{22} = \boldsymbol{A}_{22}^T$. Usually, $\boldsymbol{M}$ is assumed to contain only diagonal elements. It is easy to obtain that $\boldsymbol{M} = \boldsymbol{M}^T > \boldsymbol{0}_{6\times6}, \dot{\boldsymbol{M}} = \boldsymbol{0}_{6\times6}$.

Correspondingly, matrix $\boldsymbol{C}(\boldsymbol{\nu})$ can be expressed as

$$\boldsymbol{C}(\boldsymbol{\nu}) = \begin{bmatrix} \boldsymbol{0}_{3\times3} & -\boldsymbol{S}(\boldsymbol{M}_{11}\boldsymbol{v} + \boldsymbol{M}_{12}\boldsymbol{\omega}) \\ -\boldsymbol{S}(\boldsymbol{M}_{11}\boldsymbol{v} + \boldsymbol{M}_{12}\omega) & -\boldsymbol{S}(\boldsymbol{M}_{21}\boldsymbol{v} + \boldsymbol{M}_{22}\boldsymbol{\omega}) \end{bmatrix}. \tag{17}$$

Clearly, $\boldsymbol{C}(\boldsymbol{\nu})$ is skew-symmetric such that $\boldsymbol{C}(\boldsymbol{\nu}) = -\boldsymbol{C}^T(\boldsymbol{\nu})$.

Matrix $\boldsymbol{D}(\boldsymbol{\nu})$ can be expressed as

$$\boldsymbol{D}(\boldsymbol{\nu}) = \boldsymbol{D}_L(\boldsymbol{\nu}) + \boldsymbol{D}_Q(\boldsymbol{\nu}) \tag{18}$$

where

$$\begin{aligned}&\boldsymbol{D}_L(\boldsymbol{\nu})\\ &\quad= \mathbf{diag}\{d_{v_1}, d_{v_2}, d_{v_3}, d_{\omega_1}, d_{\omega_2}, d_{\omega_3}\}\\ &\boldsymbol{D}_Q(\boldsymbol{\nu})\\ &\quad= \mathbf{diag}\{d_{Q_1}|v_1|, d_{Q_2}|v_2|, d_{Q_3}|v_3|, d_{Q_4}|\omega_1|, d_{Q_5}|\omega_2|, d_{Q_6}|\omega_3|\}\end{aligned}$$

with $d_{v_i}, d_{\omega_i}, d_{Q_j} > 0, i = 1,2,3, j = 1,\ldots,6$. It is obvious that $\boldsymbol{D}(\boldsymbol{\nu}) > \mathbf{0}_{6\times 6}$.

The term $\boldsymbol{g}(\boldsymbol{q})$ can be written as (19), shown at the bottom of the page, where $W = mg$ and $B = \rho g \nabla$ denote the gravitational and buoyant forces of the AUV, respectively, where g is the acceleration of earth gravity, ρ is the water density, and ∇ is the AUV displacement volume. Moreover, W acts through the center of gravity $\boldsymbol{r}_G = [x_G, y_G, z_G]^T$ (in the B-frame) and B acts through the center of buoyancy $\boldsymbol{r}_B = [x_B, y_B, z_B]^T$ (in the B-frame), respectively.

C. Vehicle Complete Dynamics

For the sake of simplicity, the B-frame origin is located at the center of gravity such that $\boldsymbol{r}_G = [0,0,0]^T$. Since the AUVs considered in this paper are almost symmetric in all planes, M can be taken as [15]

$$\boldsymbol{M} = \mathbf{diag}\{m_{11}, m_{22}, m_{33}, m_{44}, m_{55}, m_{66}\} \tag{20}$$

where

$$\begin{aligned}\boldsymbol{M}_{11} &= \mathbf{diag}\{m_{11}, m_{22}, m_{33}\} > \mathbf{0}_{3\times 3}\\ \boldsymbol{M}_{22} &= \mathbf{diag}\{m_{44}, m_{55}, m_{66}\} > \mathbf{0}_{3\times 3}\end{aligned}$$

and

$$\boldsymbol{M}_{12} = \boldsymbol{M}_{21} = \mathbf{0}_{3\times 3}.$$

Hence, $\boldsymbol{C}(\boldsymbol{\nu})$ reduces to the following form:

$$\boldsymbol{C}(\boldsymbol{\nu}) = \begin{bmatrix} \mathbf{0}_{3\times 3} & -\boldsymbol{S}(\boldsymbol{M}_{11}\boldsymbol{v}) \\ -\boldsymbol{S}(\boldsymbol{M}_{11}\boldsymbol{v}) & -\boldsymbol{S}(\boldsymbol{M}_{22}\boldsymbol{\omega}) \end{bmatrix}. \tag{21}$$

Substituting (20) and (21) into (15) yields

$$\boldsymbol{M}_1\dot{\boldsymbol{v}} + \boldsymbol{C}_1(\boldsymbol{v})\boldsymbol{\omega} + \boldsymbol{D}_1(\boldsymbol{v})\boldsymbol{v} + \boldsymbol{g}_1(\boldsymbol{q}) = \boldsymbol{\tau}_1 + \boldsymbol{\tau}_{d_1} \tag{22}$$

and

$$\boldsymbol{M}_2\dot{\boldsymbol{\omega}} + \boldsymbol{C}_1(\boldsymbol{v})\boldsymbol{v} + \boldsymbol{C}_2(\boldsymbol{\omega})\boldsymbol{\omega} + \boldsymbol{D}_2(\boldsymbol{\omega})\boldsymbol{\omega} + \boldsymbol{g}_2(\boldsymbol{q}) = \boldsymbol{\tau}_2 + \boldsymbol{\tau}_{d_2} \tag{23}$$

where

$$\begin{aligned}\boldsymbol{M}_1 &= \boldsymbol{M}_{11}\\ \boldsymbol{C}_1(\boldsymbol{v}) &= -\boldsymbol{S}(\boldsymbol{M}_{11}\boldsymbol{v})\\ \boldsymbol{D}_1(\boldsymbol{v}) &= \mathbf{diag}\{d_{v_1} + d_{Q_1}|v_1|, d_{v_2} + d_{Q_2}|v_2|, d_{v_3} + d_{Q_3}|v_3|\}\\ \boldsymbol{M}_2 &= \boldsymbol{M}_{22}\\ \boldsymbol{C}_2(\boldsymbol{\omega}) &= -\boldsymbol{S}(\boldsymbol{M}_{22}\boldsymbol{\omega})\\ \boldsymbol{D}_2(\boldsymbol{\omega}) &= \mathbf{diag}\{d_{\omega_1} + d_{Q_4}|\omega_1|, d_{\omega_2} + d_{Q_5}|\omega_2|, d_{\omega_3} + d_{Q_6}|\omega_3|\}.\end{aligned}$$

Then, the vehicle complete dynamics can be divided into the following two parts, i.e., the translational subsystem

$$\begin{cases} \dot{\boldsymbol{r}} = \boldsymbol{R}(\boldsymbol{q})\boldsymbol{v} \\ \dot{\boldsymbol{v}} = \boldsymbol{M}_1^{-1}[-\boldsymbol{C}_1(\boldsymbol{v})\boldsymbol{\omega} - \boldsymbol{D}_1(\boldsymbol{v})\boldsymbol{v} - \boldsymbol{g}_1(\boldsymbol{q}) + \boldsymbol{\tau}_1 + \boldsymbol{\tau}_{d_1}] \end{cases} \tag{24}$$

and the rotational subsystem

$$\begin{cases} \dot{\boldsymbol{q}} = \dfrac{1}{2}\boldsymbol{U}(\boldsymbol{q})\boldsymbol{\omega} \\ \dot{\boldsymbol{\omega}} = \boldsymbol{M}_2^{-1}[-\boldsymbol{C}_1(\boldsymbol{v})\boldsymbol{v} - \boldsymbol{C}_2(\boldsymbol{\omega})\boldsymbol{\omega} - \boldsymbol{D}_2(\boldsymbol{\omega})\boldsymbol{\omega} - \boldsymbol{g}_2(\boldsymbol{q}) + \boldsymbol{\tau}_2 + \boldsymbol{\tau}_{d_2}]. \end{cases} \tag{25}$$

D. Vehicle Tracking Error Dynamics

The desired position and attitude are denoted as

$$\boldsymbol{r}_d(t) = [x_d(t), y_d(t), z_d(t)]^T \quad \text{and} \quad \boldsymbol{q}_d(t) = \left[\eta_d(t), \boldsymbol{\epsilon}_d^T(t)\right]^T$$

in the I-frame, respectively. Actually, the desired attitude can also be represented by $-\boldsymbol{q}_d(t)$, since $\boldsymbol{R}(\boldsymbol{q}_d) = \boldsymbol{R}(-\boldsymbol{q}_d)$ holds.

The desired translational and angular velocities are denoted as

$$\boldsymbol{v}_d(t) = [v_{1d}(t), v_{2d}(t), v_{3d}(t)]^T$$

and

$$\boldsymbol{\omega}_d(t) = [\omega_{1d}(t), \omega_{2d}(t), \omega_{3d}(t)]^T$$

in the B-frame, respectively. In fact, $\boldsymbol{v}_d$ and $\boldsymbol{\omega}_d$ can be obtained by the following numerical computation [2]:

$$\boldsymbol{v}_d = \boldsymbol{R}^T(\boldsymbol{q})\dot{\boldsymbol{r}}_d, \quad \boldsymbol{\omega}_d = 2\boldsymbol{R}^T(\boldsymbol{e}_q)\boldsymbol{U}^T(\boldsymbol{q}_d)\dot{\boldsymbol{q}}_d \tag{26}$$

where $\boldsymbol{e}_q$ represents the attitude tracking error and its detailed expression will be given later.

For $\boldsymbol{v}_d(t)$ and $\dot{\boldsymbol{v}}_d(t)$, the following assumption is made.

$$\boldsymbol{g}(\boldsymbol{q}) = \begin{bmatrix} 2(\eta\epsilon_2 - \epsilon_1\epsilon_3)(W - B) \\ -2(\eta\epsilon_1 + \epsilon_2\epsilon_3)(W - B) \\ \left(-\eta^2 + \epsilon_1^2 + \epsilon_2^2 - \epsilon_3^2\right)(W - B) \\ \left(-\eta^2 + \epsilon_1^2 + \epsilon_2^2 - \epsilon_3^2\right)(y_G W - y_B B) + 2(\eta\epsilon_1 + \epsilon_2\epsilon_3)(z_G W - z_B B) \\ -\left(-\eta^2 + \epsilon_1^2 + \epsilon_2^2 - \epsilon_3^2\right)(x_G W - x_B B) + 2(\eta\epsilon_2 - \epsilon_1\epsilon_3)(z_G W - z_B B) \\ -2(\eta\epsilon_1 + \epsilon_2\epsilon_3)(x_G W - x_B B) - 2(\eta\epsilon_2 - \epsilon_1\epsilon_3)(y_G W - y_B B) \end{bmatrix} \tag{19}$$

Assumption 1: $\boldsymbol{v}_d(t)$ and $\dot{\boldsymbol{v}}_d(t)$ are bounded, that is, there exist $v_{\max}, a_{\max} > 0$ such that

$$|\boldsymbol{v}_d(t)| \leq v_{\max}, |\dot{\boldsymbol{v}}_d(t)| \leq a_{\max} \qquad \forall t \in [0, \infty). \tag{27}$$

This assumption is reasonable due to the limitations in practical implementation.

The position tracking error vector is denoted as

$$\boldsymbol{e_r} = [e_{r_1}, e_{r_2}, e_{r_3}]^T = \boldsymbol{r} - \boldsymbol{r}_d.$$

The attitude tracking error vector is denoted as

$$\boldsymbol{e_q} = \left[e_\eta, \boldsymbol{e}_{\boldsymbol{\epsilon}}^T\right]^T = \bar{\boldsymbol{q}}_d \otimes \boldsymbol{q}$$

where $\boldsymbol{e}_{\boldsymbol{\epsilon}} = [e_{\epsilon_1}, e_{\epsilon_2}, e_{\epsilon_3}]^T, \bar{\boldsymbol{q}}_d = [\eta_d, -\boldsymbol{\epsilon}_d^T]^T$, and $\otimes$ represents the following calculation rule:

$$\boldsymbol{q}_a \otimes \boldsymbol{q}_b = \begin{bmatrix} \eta_a & -\boldsymbol{\epsilon}_a^T \\ \boldsymbol{\epsilon}_a & \eta_a \boldsymbol{I}_{3\times3} + \boldsymbol{S}(\boldsymbol{\epsilon}_a) \end{bmatrix} \begin{bmatrix} \eta_b \\ \boldsymbol{\epsilon}_b \end{bmatrix} \tag{28}$$

for any two quaternions $\boldsymbol{q}_a = [\eta_a, \boldsymbol{\epsilon}_a^T]^T$ and $\boldsymbol{q}_b = [\eta_b, \boldsymbol{\epsilon}_b^T]^T$. From (28), it is easy to verify that

$$\begin{aligned} \boldsymbol{q} = \boldsymbol{q}_d &\Leftrightarrow \boldsymbol{e_q} = [1, 0, 0, 0]^T \\ \boldsymbol{q} = -\boldsymbol{q}_d &\Leftrightarrow \boldsymbol{e_q} = [-1, 0, 0, 0]^T. \end{aligned}$$

Therefore, the desired attitude tracking error vector can be represented by either $\boldsymbol{e_q} = [1, 0, 0, 0]^T$ or $\boldsymbol{e_q} = [-1, 0, 0, 0]^T$.

The translational and angular velocity tracking errors are denoted as

$$\boldsymbol{e_v} = [e_{v_1}, e_{v_2}, e_{v_3}]^T = \boldsymbol{v} - \boldsymbol{v}_d$$

and

$$\boldsymbol{e_\omega} = [e_{\omega_1}, e_{\omega_2}, e_{\omega_3}]^T = \boldsymbol{\omega} - \boldsymbol{\omega}_d$$

respectively. Note that

$$\dot{\boldsymbol{r}}_d = \boldsymbol{R}(\boldsymbol{q})\boldsymbol{v}_d \quad \text{and} \quad \dot{\boldsymbol{q}}_d = \frac{1}{2}\boldsymbol{U}(\boldsymbol{q}_d)\boldsymbol{R}(\boldsymbol{e_q})\boldsymbol{\omega}_d.$$

Then, from (24) and (25), the translational tracking error dynamics can be written as

$$\begin{cases} \dot{\boldsymbol{e}}_{\boldsymbol{r}} = \boldsymbol{R}(\boldsymbol{q})\boldsymbol{e_v} \\ \dot{\boldsymbol{e}}_{\boldsymbol{v}} = \boldsymbol{M}_1^{-1}[-\boldsymbol{C}_1(\boldsymbol{v})\boldsymbol{\omega} - \boldsymbol{D}_1(\boldsymbol{v})\boldsymbol{v} - \boldsymbol{g}_1(\boldsymbol{q}) + \boldsymbol{\tau}_1 + \boldsymbol{\tau}_{d_1}] - \dot{\boldsymbol{v}}_d \end{cases} \tag{29}$$

an the rotational tracking error dynamics can be written as

$$\begin{cases} \dot{\boldsymbol{e}}_{\boldsymbol{q}} = \frac{1}{2}\boldsymbol{U}(\boldsymbol{e_q})\boldsymbol{e_\omega} \\ \dot{\boldsymbol{e}}_{\boldsymbol{\omega}} = \boldsymbol{M}_2^{-1}[-\boldsymbol{C}_1(\boldsymbol{v})\boldsymbol{v} - \boldsymbol{C}_2(\boldsymbol{\omega})\boldsymbol{\omega} \\ \qquad\qquad -\boldsymbol{D}_2(\boldsymbol{\omega})\boldsymbol{\omega} - \boldsymbol{g}_2(\boldsymbol{q}) + \boldsymbol{\tau}_2 + \boldsymbol{\tau}_{d_2}] - \dot{\boldsymbol{\omega}}_d \end{cases} \tag{30}$$

where

$$\begin{aligned} \dot{\boldsymbol{v}}_d &= \boldsymbol{R}^T(\boldsymbol{q})\ddot{\boldsymbol{r}}_d - \boldsymbol{S}(\boldsymbol{\omega})\boldsymbol{R}^T(\boldsymbol{q})\dot{\boldsymbol{r}}_d \\ \dot{\boldsymbol{\omega}}_d &= 2\boldsymbol{R}^T(\boldsymbol{e_q})\boldsymbol{U}^T(\boldsymbol{q}_d)\ddot{\boldsymbol{q}}_d - 2\boldsymbol{S}(\boldsymbol{e_\omega})\boldsymbol{R}^T(\boldsymbol{e_q})\boldsymbol{U}^T(\boldsymbol{q}_d)\dot{\boldsymbol{q}}_d. \end{aligned} \tag{31}$$

In this paper, to achieve a global control result, both equilibria $[\boldsymbol{e}_{\boldsymbol{q}}^T, \boldsymbol{e}_{\boldsymbol{\omega}}^T]^T = [[\pm1, \boldsymbol{0}_{1\times3}], \boldsymbol{0}_{1\times3}]^T$ of rotational tracking error subsystem (30) will be made stable. Then, the stabilization of subsystem (30) can be regarded as a set stabilization problem (see Definition 1).

The control objective in this paper is to design controllers $\boldsymbol{\tau}_1$ and $\boldsymbol{\tau}_2$ such that, in the absence of disturbances $\boldsymbol{\tau}_d$, tracking error subsystems (29) and (30) are both globally finite-time stable with respect to the equilibrium set

$$Q_1 = \left\{[\boldsymbol{e}_{\boldsymbol{r}}^T, \boldsymbol{e}_{\boldsymbol{q}}^T, \boldsymbol{e}_{\boldsymbol{v}}^T, \boldsymbol{e}_{\boldsymbol{\omega}}^T]^T | \boldsymbol{e_r} = \boldsymbol{e_v} = \boldsymbol{e_\omega} = \boldsymbol{0}_{3\times1}, \\ \boldsymbol{e_q} = [\pm1, \boldsymbol{0}_{1\times3}]^T\right\}.$$

IV. Control Design

The control design is composed of three parts, i.e., the finite-time state feedback control design, the finite-time convergent observer design, and the finite-time output feedback control design. First, state feedback controllers $\boldsymbol{\tau}_1$ and $\boldsymbol{\tau}_2$ are proposed to provide global finite-time (set) stability for tracking error subsystems (29) and (30), respectively. Then, to solve the estimation problem of translational velocity vector $\boldsymbol{v}$, a finite-time convergent observer is developed to provide an estimate of $\boldsymbol{v}$ for feedback. At last, a finite-time output feedback control scheme, involving two output feedback controllers and the developed finite-time convergent observer, is presented. It will be shown that the output feedback controllers also guarantee global finite-time (set) stability for the tracking error subsystems. Rigorous stability analysis will be given.

A. Design of State Feedback Control

In this section, assume that $\boldsymbol{r}, \boldsymbol{q}, \boldsymbol{v}$, and $\boldsymbol{\omega}$ are all measurable. Based on this assumption and finite-time control technique, controllers $\boldsymbol{\tau}_1$ and $\boldsymbol{\tau}_2$ are explicitly designed to globally finite-time stabilize translational and rotational tracking error subsystems (29) and (30), respectively.

1) Stabilization of the Translational Tracking Error Subsystem: In this section, controller $\boldsymbol{\tau}_1$ is designed to globally finite-time stabilize translational tracking error subsystem (29).

Before proceeding, a coordinate transformation on $\boldsymbol{r}$ and $\boldsymbol{v}$ is introduced

$$\begin{aligned} \boldsymbol{z}_1 &= [z_{11}, z_{12}, z_{13}]^T = \boldsymbol{r} \\ \boldsymbol{z}_2 &= [z_{21}, z_{22}, z_{23}]^T = \boldsymbol{R}(\boldsymbol{q})\boldsymbol{M}_1\boldsymbol{v} \end{aligned} \tag{32}$$

which will be very helpful for control design, especially for the observer design, in the following parts. Clearly, this coordinate transformation is invertible. Substituting (32) into (24) yields

$$\begin{cases} \dot{\boldsymbol{z}}_1 = \boldsymbol{R}(\boldsymbol{q})\boldsymbol{M}_1^{-1}\boldsymbol{R}^T(\boldsymbol{q})\boldsymbol{z}_2 \\ \dot{\boldsymbol{z}}_2 = \boldsymbol{R}(\boldsymbol{q})[-\boldsymbol{D}_1\left(\boldsymbol{M}_1^{-1}\boldsymbol{R}^T(\boldsymbol{q})\boldsymbol{z}_2\right)\boldsymbol{M}_1^{-1}\boldsymbol{R}^T(\boldsymbol{q})\boldsymbol{z}_2 \\ \qquad\qquad -\boldsymbol{g}_1(\boldsymbol{q}) + \boldsymbol{\tau}_1 + \boldsymbol{\tau}_{d_1}] \end{cases} \tag{33}$$

where Coriolis term $\boldsymbol{C}_1(\boldsymbol{v})\boldsymbol{\omega}$ in system (24) has been canceled.

The desired values of $\boldsymbol{z}_1(t)$ and $\boldsymbol{z}_2(t)$ are denoted as $\boldsymbol{z}_{1d}(t)$ and $\boldsymbol{z}_{2d}(t)$, respectively. Then, from (32), it can be obtained that $\boldsymbol{z}_{1d} = \boldsymbol{r}_d, \boldsymbol{z}_{2d} = \boldsymbol{R}(\boldsymbol{q})\boldsymbol{M}_1\boldsymbol{v}_d$. New tracking errors are denoted as

$$\begin{aligned} \boldsymbol{e}_{\boldsymbol{z}_1} &= [e_{z_{11}}, e_{z_{12}}, e_{z_{13}}]^T = \boldsymbol{z}_1 - \boldsymbol{z}_{1d} \\ \boldsymbol{e}_{\boldsymbol{z}_2} &= [e_{z_{21}}, e_{z_{22}}, e_{z_{23}}]^T = \boldsymbol{z}_2 - \boldsymbol{z}_{2d}. \end{aligned}$$

Then, from (33), translational tracking error subsystem (29) can be rewritten as

$$\begin{cases} \dot{\boldsymbol{e}}_{\boldsymbol{z}_1} = \boldsymbol{R}(\boldsymbol{q})\boldsymbol{M}_1^{-1}\boldsymbol{R}^T(\boldsymbol{q})\boldsymbol{e}_{\boldsymbol{z}_2} \\ \dot{\boldsymbol{e}}_{\boldsymbol{z}_2} = \boldsymbol{R}(\boldsymbol{q})[-\boldsymbol{D}_1(\boldsymbol{M}_1^{-1}\boldsymbol{R}^T(\boldsymbol{q})\boldsymbol{z}_2)\boldsymbol{M}_1^{-1}\boldsymbol{R}^T(\boldsymbol{q})\boldsymbol{z}_2 \\ \qquad -\boldsymbol{g}_1(\boldsymbol{q}) + \boldsymbol{\tau}_1 + \boldsymbol{\tau}_{d_1}] - \dot{\boldsymbol{z}}_{2d}. \end{cases} \tag{34}$$

Now, the following result is ready to be given.

Theorem 1: In the absence of disturbances $\boldsymbol{\tau}_{d_1}$, if controller $\boldsymbol{\tau}_1$ is chosen as

$$\begin{aligned} \boldsymbol{\tau}_1 = &-k_2\boldsymbol{M}_1\boldsymbol{R}^T(\boldsymbol{q})\left[\varphi_1^{2p_1-1}, \varphi_2^{2p_1-1}, \varphi_3^{2p_1-1}\right]^T \\ &- \boldsymbol{M}_1\left[\boldsymbol{S}(\boldsymbol{\omega})\boldsymbol{M}_1^{-1}\boldsymbol{R}^T(\boldsymbol{q}) - \boldsymbol{M}_1^{-1}\boldsymbol{S}(\boldsymbol{\omega})\boldsymbol{R}^T(\boldsymbol{q})\right]\boldsymbol{e}_{\boldsymbol{z}_2} \\ &+ \boldsymbol{D}_1(\boldsymbol{M}_1^{-1}\boldsymbol{R}^T(\boldsymbol{q})\boldsymbol{z}_2)\boldsymbol{M}_1^{-1}\boldsymbol{R}^T(\boldsymbol{q})\boldsymbol{z}_2 + \boldsymbol{g}_1(\boldsymbol{q}) \\ &+ \boldsymbol{R}^T(\boldsymbol{q})\dot{\boldsymbol{z}}_{2d} \end{aligned} \tag{35}$$

where

$$\varphi_i = [\boldsymbol{R}(\boldsymbol{q})\boldsymbol{M}_1^{-1}\boldsymbol{R}^T(\boldsymbol{q})\boldsymbol{e}_{\boldsymbol{z}_2}]_i^{1/p_1} + k_1^{1/p_1}e_{z_{1i}}, \qquad i = 1, 2, 3$$

and $1 < p_1 = p_{11}/p_{12} < 1, p_{11}, p_{12}$ are positive odd integers, and

$$\begin{aligned} &k_1 \geq 2^{1-p_1}/(1+p_1) + 2p_1/(1+p_1) + c_1 \\ &k_2 \geq (2-p_1)2^{-p_1}k_1^{1+1/p_1} \\ &\quad \times [2^{1-p_1}p_1/(1+p_1) + 2/(1+p_1) + 2^{2-p_1}/k_1 + c_1], \\ &\qquad c_1 > 0 \end{aligned}$$

then, system (34) is globally finite-time stable with respect to the equilibrium $[\boldsymbol{e}_{\boldsymbol{z}_1}^T, \boldsymbol{e}_{\boldsymbol{z}_2}^T]^T = \boldsymbol{0}_{6\times 1}$, namely, tracking errors $\boldsymbol{e_r}$ and $\boldsymbol{e_v}$ of system (29) will globally converge to the equilibrium $[\boldsymbol{e_r}^T, \boldsymbol{e_v}^T]^T = \boldsymbol{0}_{6\times 1}$ in finite time.

Proof: First, an invertible coordinate transformation for system (34) is introduced

$$\begin{aligned} \boldsymbol{\beta}_1 &= [\beta_{11}, \beta_{12}, \beta_{13}]^T = \boldsymbol{e}_{\boldsymbol{z}_1} \\ \boldsymbol{\beta}_2 &= [\beta_{21}, \beta_{22}, \beta_{23}]^T = \boldsymbol{R}(\boldsymbol{q})\boldsymbol{M}_1^{-1}\boldsymbol{R}^T(\boldsymbol{q})\boldsymbol{e}_{\boldsymbol{z}_2}. \end{aligned} \tag{36}$$

Then, in the absence of disturbances $\boldsymbol{\tau}_{d_1}$, system (34) is equivalent to the following system:

$$\dot{\boldsymbol{\beta}}_1 = \boldsymbol{\beta}_2, \dot{\boldsymbol{\beta}}_2 = \boldsymbol{u}_1 \tag{37}$$

where

$$\begin{aligned} &\boldsymbol{u}_1 \\ &= [u_{11}, u_{12}, u_{13}]^T \\ &= \boldsymbol{R}(\boldsymbol{q})\left[\boldsymbol{S}(\boldsymbol{\omega})\boldsymbol{M}_1^{-1}\boldsymbol{R}^T(\boldsymbol{q}) - \boldsymbol{M}_1^{-1}\boldsymbol{S}(\boldsymbol{\omega})\boldsymbol{R}^T(\boldsymbol{q})\right]\boldsymbol{e}_{\boldsymbol{z}_2} \\ &\quad + \boldsymbol{R}(\boldsymbol{q})\boldsymbol{M}_1^{-1}\left[\boldsymbol{\tau}_1 - \boldsymbol{D}_1\left(\boldsymbol{M}_1^{-1}\boldsymbol{R}^T(\boldsymbol{q})\boldsymbol{z}_2\right)\boldsymbol{M}_1^{-1}\boldsymbol{R}^T(\boldsymbol{q})\boldsymbol{z}_2 - \boldsymbol{g}_1(\boldsymbol{q})\right] \\ &\quad - \boldsymbol{R}(\boldsymbol{q})\boldsymbol{M}_1^{-1}\boldsymbol{R}^T(\boldsymbol{q})\dot{\boldsymbol{z}}_{2d}. \end{aligned} \tag{38}$$

The following proof is based on adding the power integrator approach [33] (similar to backstepping but nonsmooth) and it can be divided into two steps. First, by regarding $\boldsymbol{\beta}_2$ as the input of the first-order subsystem $\dot{\boldsymbol{\beta}}_1 = \boldsymbol{\beta}_2$, a virtual controller $\boldsymbol{\beta}_2^*$ is presented to globally finite-time stabilize the above subsystem. Second, controller $\boldsymbol{u}_1$ is developed to force $\boldsymbol{\beta}_2$ to track $\boldsymbol{\beta}_2^*$ in finite time. It will be shown that the developed controller $\boldsymbol{u}_1$ is equal to the one obtained by substituting (35) into (38) and $\boldsymbol{u}_1$ guarantees global finite-time stability for system (37). Thus, due to the equivalence among systems (29), (34), and (37), controller $\boldsymbol{\tau}_1$ given in (35) guarantees global finite-time stability for systems (34) and (29).

The detailed proof can be found in Appendix A. ■

2) Stabilization of the Rotational Tracking Error Subsystem: In this section, controller $\boldsymbol{\tau}_2$ is designed to provide global finite-time set stability for rotational tracking error subsystem (30).

For subsystem (30), the following result is ready to be given.

Theorem 2: In the absence of disturbances $\boldsymbol{\tau}_{d_2}$, if controller $\boldsymbol{\tau}_2$ is chosen as

$$\begin{aligned} \boldsymbol{\tau}_2 = &-k_4\boldsymbol{M}_2\left[\xi_1^{2p_2-1}, \xi_2^{2p_2-1}, \xi_3^{2p_2-1}\right]^T \\ &+ \boldsymbol{C}_1(\boldsymbol{v})\boldsymbol{v} + \boldsymbol{C}_2(\boldsymbol{\omega})\boldsymbol{\omega} + \boldsymbol{D}_2(\boldsymbol{\omega})\boldsymbol{\omega} + \boldsymbol{g}_2(\boldsymbol{q}) + \boldsymbol{M}_2\dot{\boldsymbol{\omega}}_d \end{aligned} \tag{39}$$

where

$$\xi_i = e_{\omega_i}^{1/p_2} + \operatorname{sgn}(e_\eta(0))k_3^{1/p_2}e_{\epsilon_i}, \qquad i = 1, 2, 3$$

$1/2 < p_2 = p_{21}/p_{22} < 1, p_{21}$, and p_{22} are positive odd integers, and

$$\begin{aligned} &k_3 \geq 2^{1-p_2}/(1+p_2) + 3p_2/(1+p_2) + c_2 \\ &k_4 \geq k_3^{1+1/p_2}(2-p_2)2^{-p_2} \\ &\quad \times [2^{1-p_2}(p_2/(1+p_2) + 3/k_3) + 3/(1+p_2) + c_2], \\ &\qquad c_2 > 0 \end{aligned}$$

and $e_\eta(0)$ represents the initial value of $e_\eta(t)$, then, rotational tracking error subsystem (30) is globally finite-time stable with respect to the equilibrium set

$$Q_2 = \{[\boldsymbol{e}_{\boldsymbol{q}}^T, \boldsymbol{e}_{\boldsymbol{\omega}}^T]^T | \boldsymbol{e}_{\boldsymbol{q}} = [\pm 1, \boldsymbol{0}_{1\times 3}]^T, \boldsymbol{e}_{\boldsymbol{\omega}} = \boldsymbol{0}_{3\times 1}\}.$$

Proof: First, let

$$\begin{aligned} \boldsymbol{u}_2 &= [u_{21}, u_{22}, u_{23}]^T \\ &= \boldsymbol{M}_2^{-1}[-\boldsymbol{C}_1(\boldsymbol{v})\boldsymbol{v} - \boldsymbol{C}_2(\boldsymbol{\omega})\boldsymbol{\omega} - \boldsymbol{D}_2(\boldsymbol{\omega})\boldsymbol{\omega} - \boldsymbol{g}_2(\boldsymbol{q}) + \boldsymbol{\tau}_2] - \dot{\boldsymbol{\omega}}_d. \end{aligned} \tag{40}$$

Then, in the absence of disturbances $\boldsymbol{\tau}_{d_2}$, system (30) can be rewritten as

$$\dot{\boldsymbol{e}}_{\boldsymbol{q}} = \frac{1}{2}\boldsymbol{U}(\boldsymbol{e}_{\boldsymbol{q}})\boldsymbol{e}_{\boldsymbol{\omega}}, \dot{\boldsymbol{e}}_{\boldsymbol{\omega}} = \boldsymbol{u}_2. \tag{41}$$

Similar to the proof of Theorem 1, the following proof consists of two steps. The first step is to design a global finite-time stabilizing virtual controller $\boldsymbol{e}_{\boldsymbol{\omega}}^*$ for the first-order subsystem $\dot{\boldsymbol{e}}_{\boldsymbol{q}} = (1/2)\boldsymbol{U}(\boldsymbol{e}_{\boldsymbol{q}})\boldsymbol{e}_{\boldsymbol{\omega}}$. The second step is to design controller $\boldsymbol{u}_2$ such that $\boldsymbol{e}_{\boldsymbol{\omega}}$ can track $\boldsymbol{e}_{\boldsymbol{\omega}}^*$ in finite time. It will be shown that the developed controller $\boldsymbol{u}_2$ is equal to the one obtained by substituting (39) into (40) and $\boldsymbol{u}_2$ guarantees global finite-time set stability for system (41) with respect to the aforementioned equilibrium set Q_2. Therefore, controller $\boldsymbol{\tau}_2$ given in (39) guarantees global finite-time set stability for rotational tracking error subsystem (30) with respect to the equilibrium set Q_2.

The detailed proof can be found in Appendix B. ■

Remark 1: The reasons to design a global finite-time set stabilization controller for subsystem (30) are twofold. On the one hand, since subsystem (30) has two equilibria as

$$\left[\boldsymbol{e}_{\boldsymbol{q}}^T, \boldsymbol{e}_{\boldsymbol{\omega}}^T\right]^T = [[\pm 1, \boldsymbol{0}_{1\times 3}], \boldsymbol{0}_{1\times 3}]^T$$

both equilibria should be made stable to obtain a global control stabilization result. On the other hand, under the set stabilization controller, the states of subsystem (30) can converge to the equilibrium which is closer to them in finite time, and thus the control method is more power efficient.

B. Design of Finite-Time Convergent Observer

To handle the estimation problem of translational velocities in the cases with inaccurate measurements or without measurements, in this section, a global finite-time convergent observer is developed to obtain the real information of $\boldsymbol{v}$. Due to the invertibility of coordinate transformation (32) between $\boldsymbol{r}, \boldsymbol{v}$ and $\boldsymbol{z}_1, \boldsymbol{z}_2$, it is equivalent to construct an observer for system (33) to estimate $\boldsymbol{z}_1$ and $\boldsymbol{z}_2$.

For system (33) and neglecting disturbances $\boldsymbol{\tau}_{d_1}$, a nonlinear observer is designed as

$$\begin{cases} \dot{\hat{\boldsymbol{z}}}_1 = \boldsymbol{R}(\boldsymbol{q})\boldsymbol{M}_1^{-1}\boldsymbol{R}^T(\boldsymbol{q})\hat{\boldsymbol{z}}_2 + \boldsymbol{f}_1(\tilde{\boldsymbol{z}}_1) \\ \dot{\hat{\boldsymbol{z}}}_2 = \boldsymbol{R}(\boldsymbol{q})[\boldsymbol{\tau}_1 - \boldsymbol{D}_1\left(\boldsymbol{M}_1^{-1}\boldsymbol{R}^T(\boldsymbol{q})\hat{\boldsymbol{z}}_2\right)\boldsymbol{M}_1^{-1}\boldsymbol{R}^T(\boldsymbol{q})\hat{\boldsymbol{z}}_2 \\ \qquad -\boldsymbol{g}_1(\boldsymbol{q})] + \boldsymbol{f}_2(\tilde{\boldsymbol{z}}_1) \end{cases} \tag{42}$$

where $\hat{\boldsymbol{z}}_1$ and $\hat{\boldsymbol{z}}_2$ represent the estimates of $\boldsymbol{z}_1$ and $\boldsymbol{z}_2$, $\tilde{\boldsymbol{z}}_1 = [\tilde{z}_{11}, \tilde{z}_{12}, \tilde{z}_{13}]^T = \boldsymbol{z}_1 - \hat{\boldsymbol{z}}_1$ denotes the observation error of $\boldsymbol{z}_1$, and

$$\boldsymbol{f}_1(\tilde{\boldsymbol{z}}_1) = l_1\left[\mathrm{sig}^{\alpha_1}(\tilde{z}_{11}), \mathrm{sig}^{\alpha_1}(\tilde{z}_{12}), \mathrm{sig}^{\alpha_1}(\tilde{z}_{13})\right]^T \tag{43}$$

$$\begin{aligned} \boldsymbol{f}_2(\tilde{\boldsymbol{z}}_1) = {} & l_2\boldsymbol{R}(\boldsymbol{q})\boldsymbol{M}_1^{-1}\boldsymbol{R}^T(\boldsymbol{q}) \\ & \times\left[\mathrm{sig}^{\alpha_2}(\tilde{z}_{11}), \mathrm{sig}^{\alpha_2}(\tilde{z}_{12}), \mathrm{sig}^{\alpha_2}(\tilde{z}_{13})\right]^T \end{aligned} \tag{44}$$

with $l_1, l_2 > 0, 1/2 < \alpha_1 < 1, \alpha_2 = 2\alpha_1 - 1$. Let

$$\tilde{\boldsymbol{z}}_2 = [\tilde{z}_{21}, \tilde{z}_{22}, \tilde{z}_{23}]^T = \boldsymbol{z}_2 - \hat{\boldsymbol{z}}_2$$

denote the observation error of $\boldsymbol{z}_2$. Then, from systems (33) and (42), the observation error system can be described as

$$\begin{cases} \dot{\tilde{\boldsymbol{z}}}_1 = \boldsymbol{R}(\boldsymbol{q})\boldsymbol{M}_1^{-1}\boldsymbol{R}^T(\boldsymbol{q})\tilde{\boldsymbol{z}}_2 - \boldsymbol{f}_1(\tilde{\boldsymbol{z}}_1) \\ \dot{\tilde{\boldsymbol{z}}}_2 = -\boldsymbol{R}(\boldsymbol{q})[\boldsymbol{D}_1\left(\boldsymbol{M}_1^{-1}\boldsymbol{R}^T(\boldsymbol{q})\boldsymbol{z}_2\right)\boldsymbol{M}_1^{-1}\boldsymbol{R}^T(\boldsymbol{q})\boldsymbol{z}_2 \\ \qquad -\boldsymbol{D}_1\left(\boldsymbol{M}_1^{-1}\boldsymbol{R}^T(\boldsymbol{q})\hat{\boldsymbol{z}}_2\right)\boldsymbol{M}_1^{-1}\boldsymbol{R}^T(\boldsymbol{q})\hat{\boldsymbol{z}}_2] \\ \quad -\boldsymbol{f}_2(\tilde{\boldsymbol{z}}_1). \end{cases} \tag{45}$$

Correspondingly, the estimates of $\boldsymbol{r}$ and $\boldsymbol{v}$ are denoted as $\hat{\boldsymbol{r}}$ and $\hat{\boldsymbol{v}}$, respectively. The position and translational velocity observation errors are denoted as $\tilde{\boldsymbol{r}} = [\tilde{r}_1, \tilde{r}_2, \tilde{r}_3]^T = \boldsymbol{r} - \hat{\boldsymbol{r}}$ and $\tilde{\boldsymbol{v}} = [\tilde{\boldsymbol{v}}_1, \tilde{\boldsymbol{v}}_2, \tilde{\boldsymbol{v}}_3]^T = \boldsymbol{v} - \hat{\boldsymbol{v}}$, respectively.

The following result will show that observation error system (45) is globally finite-time stable.

Theorem 3: Assume that $\boldsymbol{z}_2(t)$ and $\hat{\boldsymbol{z}}_2(t)$ are bounded, $\forall t \in [0, \infty)$. Then, observation error system (45) is globally finite-time stable. In other words, observer (42) is globally finite-time convergent.

Proof: The proof consists of two steps, i.e., proof on global asymptotical stability and local finite-time stability of system (45). Then, these two points imply global finite-time stability of system (45). The detailed proof can be found in Appendix C. ■

C. Design of Output Feedback Control

In this section, with the help of finite-time convergent observer (42), two modified controllers $\boldsymbol{\tau}_1$ and $\boldsymbol{\tau}_2$ based on output feedback are proposed to globally finite-time stabilize translational and rotational tracking error subsystems (29) and (30), respectively. Then, a finite-time output feedback trajectory tracking control scheme for AUVs is derived.

The main result of this paper is given as the following theorem.

Theorem 4: For translational and rotational tracking error subsystems (29) and (30), in the absence of external disturbances $\boldsymbol{\tau}_d$, the states of tracking error subsystems (29) and (30) will be globally stabilized to the following equilibrium set:

$$\begin{aligned} Q_1 = \Big\{ \left[\boldsymbol{e}_{\boldsymbol{r}}^T, \boldsymbol{e}_{\boldsymbol{q}}^T, \boldsymbol{e}_{\boldsymbol{v}}^T, \boldsymbol{e}_{\boldsymbol{\omega}}^T\right]^T | \boldsymbol{e}_{\boldsymbol{r}} = \boldsymbol{e}_{\boldsymbol{v}} = \boldsymbol{e}_{\boldsymbol{\omega}} = \boldsymbol{0}_{3\times 1}, \\ \boldsymbol{e}_{\boldsymbol{q}} = [\pm 1, \boldsymbol{0}_{1\times 3}]^T \Big\} \end{aligned}$$

in finite time, if the following conditions hold.

i) For observer (42), the restrictions of control parameters are $l_1, l_2 > 0, p_1 \le \alpha_1 < 1, \alpha_2 = 2\alpha_1 - 1$, where $1/2 < p_1 = p_{11}/p_{12} < 1$, and p_1 and p_2 are positive odd integers.

ii) For equivalent translational tracking error subsystem (34), controller $\boldsymbol{\tau}_1$ is chosen as

$$\begin{aligned} \boldsymbol{\tau}_1 = {} & -k_2\boldsymbol{M}_1\boldsymbol{R}^T(\boldsymbol{q})\left[\hat{\varphi}_1^{2p_1-1}, \hat{\varphi}_2^{2p_1-1}, \hat{\varphi}_3^{2p_1-1}\right]^T \\ & - \boldsymbol{M}_1\left[\boldsymbol{S}(\boldsymbol{\omega})\boldsymbol{M}_1^{-1}\boldsymbol{R}^T(\boldsymbol{q}) - \boldsymbol{M}_1^{-1}\boldsymbol{S}(\boldsymbol{\omega})\boldsymbol{R}^T(\boldsymbol{q})\right]\hat{\boldsymbol{e}}_{\boldsymbol{z}_2} \\ & + \boldsymbol{D}_1\left(\boldsymbol{M}_1^{-1}\boldsymbol{R}^T(\boldsymbol{q})\hat{\boldsymbol{z}}_2\right)\boldsymbol{M}_1^{-1}\boldsymbol{R}^T(\boldsymbol{q})\hat{\boldsymbol{z}}_2 \\ & + \boldsymbol{g}_1(\boldsymbol{q}) + \boldsymbol{R}^T(\boldsymbol{q})\dot{\boldsymbol{z}}_{2d} \end{aligned} \tag{46}$$

where

$$\begin{aligned} \hat{\varphi}_i &= [\boldsymbol{R}(\boldsymbol{q})\boldsymbol{M}_1^{-1}\boldsymbol{R}^T(\boldsymbol{q})\hat{\boldsymbol{e}}_{\boldsymbol{z}_2}]_i^{1/p_1} + k_1^{1/p_1}\hat{e}_{z_{1i}}, \\ & \qquad i = 1, 2, 3 \\ \hat{\boldsymbol{e}}_{\boldsymbol{z}_1} &= [\hat{e}_{z_{11}}, \hat{e}_{z_{12}}, \hat{e}_{z_{13}}]^T = \hat{\boldsymbol{z}}_1 - \boldsymbol{z}_{1d} \\ \hat{\boldsymbol{e}}_{\boldsymbol{z}_2} &= [\hat{e}_{z_{21}}, \hat{e}_{z_{22}}, \hat{e}_{z_{23}}]^T = \hat{\boldsymbol{z}}_2 - \boldsymbol{z}_{2d} \end{aligned}$$

$\hat{\boldsymbol{z}}_1$ and $\hat{\boldsymbol{z}}_2$ are the estimates of $\boldsymbol{z}_1$ and $\boldsymbol{z}_2$ generated from observer (42), and

$$\begin{aligned} k_2 &\ge (2 - p_1)2^{-p_1}k_1^{1+1/p_1}(h_1 + c_1) \\ k_1 &\ge (2^{1-p_1})/(1 + p_1) \\ & \quad + (2p_1 + l_1\phi_1^{\alpha_1 - p_1})/(1 + p_1) + c_1 \\ h_1 &= (2^{1-p_1}p_1 + 2)/(1 + p_1) \\ & \quad + (2^{2-p_1})/(k_1) \\ & \quad + (3b_1 l_2\phi_1^{2(\alpha_1 - p_1)})/((1 + p_1)2^{-p_1}k_1^{1+1/p_1}) \\ \phi_1 &= \left(\sum_{i=1}^{3}|\tilde{z}_{1i}(0)|^{2\alpha_1} + (\alpha_1)/(l_2)\tilde{\boldsymbol{z}}_2^T(0)\tilde{\boldsymbol{z}}_2(0)\right)^{1/(2\alpha_1)} \\ c_1 &> 0 \\ b_1 &= \|\boldsymbol{M}_1^{-2}\| \end{aligned}$$

and $\tilde{\boldsymbol{z}}_1(0)$ and $\tilde{\boldsymbol{z}}_2(0)$ represent the initial values of observation errors $\tilde{\boldsymbol{z}}_1(t)$ and $\tilde{\boldsymbol{z}}_2(t)$, respectively.

iii) For rotational tracking error subsystem (30), controller $\boldsymbol{\tau}_2$ is chosen as

$$\begin{aligned} \boldsymbol{\tau}_2 = {} & -k_4\boldsymbol{M}_2\left[\xi_1^{2p_2-1}, \xi_2^{2p_2-1}, \xi_3^{2p_2-1}\right]^T \\ & + \boldsymbol{C}_1(\hat{\boldsymbol{v}})\hat{\boldsymbol{v}} + \boldsymbol{C}_2(\boldsymbol{\omega})\boldsymbol{\omega} \\ & + \boldsymbol{D}_2(\boldsymbol{\omega})\boldsymbol{\omega} + \boldsymbol{g}_2(\boldsymbol{q}) + \boldsymbol{M}_2\dot{\boldsymbol{\omega}}_d \end{aligned} \tag{47}$$

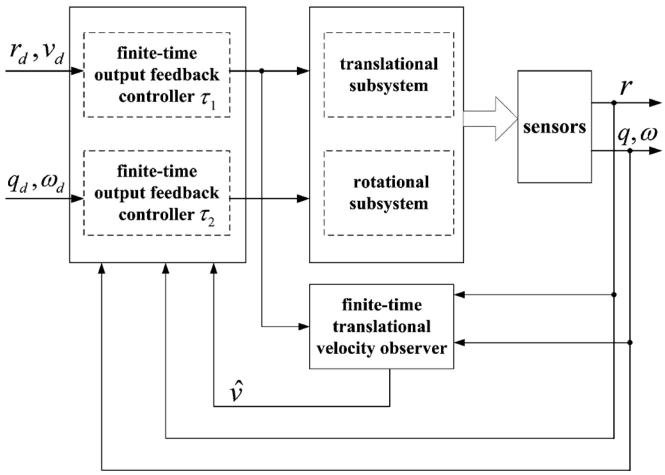

Fig. 1. Block diagram of the closed-loop system (24), (25), (42), (46), and (47).

where

$$\xi_i = e_{\omega_i}^{1/p_2} + \mathrm{sgn}(e_\eta(0))k_3^{1/p_2}e_{\epsilon_i}, \qquad i = 1,2,3$$

$\hat{\boldsymbol{v}}$ is the estimate of $\boldsymbol{v}$ generated from observer (42), and the definitions of control parameters are the same as those in Theorem 2.

Proof: The proof consists of three steps. The first step is to prove boundedness of $\boldsymbol{e_r}(t), \boldsymbol{e_v}(t)$ in $t \in [0,\infty)$ and global finite-time convergence of observer (42). The second step is to prove boundedness of $\boldsymbol{e_q}(t), \boldsymbol{e_\omega}(t)$ in $t \in [0,\infty)$. Based on these two steps, states of both systems (29) and (30) are shown to be bounded for $t \in [0, T_{ob})$, where T_{ob} is the finite settling time of observer (42). Then, after T_{ob}, output feedback controllers (46) and (47) reduce to their state feedback counterparts (35) and (39), respectively. Finally, by utilizing Theorems 1 and 2 directly, in the absence of disturbances $\boldsymbol{\tau}_d$, global finite-time (set) stability of tracking error subsystems (29) and (30) is achieved under controllers (46) and (47).

The detailed proof can be found in Appendix D. ■

The block diagram of the closed-loop system (24), (25), (42), (46), and (47) is shown in Fig. 1.

Remark 2: For tracking error subsystems (29) and (30), based on the observer backstepping technique, output feedback controllers were proposed in [15]. In detail, these controllers can be written as

$$\boldsymbol{\tau}_1 = -\boldsymbol{M}_1\boldsymbol{R}^T(\boldsymbol{q})[\boldsymbol{\Lambda}_1 + (\boldsymbol{E}_2+\boldsymbol{F}_2)\boldsymbol{\mu}_2 + \boldsymbol{\mu}_1] \tag{48}$$

$$\boldsymbol{\tau}_2 = -\boldsymbol{M}_2\boldsymbol{U}^T(\boldsymbol{q})(\boldsymbol{\Lambda}_2 + \boldsymbol{E}_4\boldsymbol{\mu}_4 + \boldsymbol{\mu}_3) + \boldsymbol{C}_1(\hat{\boldsymbol{v}})\hat{\boldsymbol{v}} \tag{49}$$

where

$$\begin{aligned}
\boldsymbol{\mu}_1 &= \hat{\boldsymbol{z}}_1 - \boldsymbol{r}_d + \boldsymbol{K}_1\int_0^t (\hat{\boldsymbol{z}}_1(s) - \boldsymbol{r}_d(s))\,ds\\
\boldsymbol{\mu}_2 &= (\boldsymbol{E}_1+\boldsymbol{F}_1)\boldsymbol{\mu}_1 - \dot{\boldsymbol{r}}_d + \boldsymbol{K}_1(\hat{\boldsymbol{z}}_1 - \boldsymbol{r}_d) + \boldsymbol{R}(\boldsymbol{q})\boldsymbol{M}_1^{-1}\boldsymbol{R}^T(\boldsymbol{q})\hat{\boldsymbol{z}}_1\\
\boldsymbol{\Lambda}_1 &= \boldsymbol{R}(\boldsymbol{q})\boldsymbol{S}(\boldsymbol{\omega})\boldsymbol{M}_1^{-1}\boldsymbol{R}^T(\boldsymbol{q})\hat{\boldsymbol{z}}_2 + \boldsymbol{R}(\boldsymbol{q})\boldsymbol{M}_1^{-1}\boldsymbol{S}^T(\boldsymbol{\omega})\boldsymbol{R}^T(\boldsymbol{q})\hat{\boldsymbol{z}}_2\\
&\quad + \boldsymbol{R}(\boldsymbol{q})\boldsymbol{M}_1^{-1}\left[-\boldsymbol{D}_1(\hat{\boldsymbol{v}})\hat{\boldsymbol{v}} - \boldsymbol{g}_1(\boldsymbol{q}) + \boldsymbol{M}_1^{-1}\boldsymbol{R}^T(\boldsymbol{q})\boldsymbol{K}_4\tilde{\boldsymbol{z}}_1\right]\\
&\quad + (\boldsymbol{E}_1+\boldsymbol{F}_1)[-(\boldsymbol{E}_1+\boldsymbol{F}_1)\boldsymbol{\mu}_1 + \boldsymbol{\mu}_2]\\
&\quad - \ddot{\boldsymbol{r}}_d + \boldsymbol{K}_1\left[\boldsymbol{R}(\boldsymbol{q})\boldsymbol{M}_1^{-1}\boldsymbol{R}^T(\boldsymbol{q})\hat{\boldsymbol{z}}_2 - \dot{\boldsymbol{r}}_d\right]
\end{aligned}$$

TABLE I
CONTROL PARAMETERS FOR THE PROPOSED FINITE-TIME OUTPUT FEEDBACK CONTROL SCHEME

Controller $\boldsymbol{\tau}_1$ (46)	$p_1 = 15/17, c_1 = 3, k_1 = 7.8759, k_2 = 240.0121$
Controller $\boldsymbol{\tau}_2$ (47)	$p_2 = 11/13, c_2 = 2, k_3 = 4.3754, k_4 = 86.5760$
Observer (42)	$l_1 = 5, l_2 = 2, \alpha_1 = 12/13, \alpha_2 = 11/13$

$$\begin{aligned}
\boldsymbol{\mu}_3 &= \boldsymbol{q} - \boldsymbol{q}_d + K_2\int_0^t (\boldsymbol{q}(s) - \boldsymbol{q}_d(s))\,ds\\
\boldsymbol{\mu}_4 &= \boldsymbol{E}_3\boldsymbol{z}_3 - \dot{\boldsymbol{q}}_d + \boldsymbol{K}_2(\boldsymbol{q}-\boldsymbol{q}_d) + \boldsymbol{U}(\boldsymbol{q})\boldsymbol{\omega}\\
\boldsymbol{\Lambda}_2 &= \dot{\boldsymbol{U}}(\boldsymbol{q})\boldsymbol{\omega} + \boldsymbol{U}(\boldsymbol{q})\boldsymbol{M}_2^{-1}\left[-\boldsymbol{C}_2(\boldsymbol{\omega})\boldsymbol{\omega} - \boldsymbol{D}_2(\boldsymbol{\omega})\boldsymbol{\omega} - \boldsymbol{g}_2(\boldsymbol{q})\right]\\
&\quad + \boldsymbol{E}_3(-\boldsymbol{E}_3\boldsymbol{\mu}_3 + \boldsymbol{\mu}_4) - \ddot{\boldsymbol{q}}_d + \boldsymbol{K}_2(\boldsymbol{U}(\boldsymbol{q})\boldsymbol{\omega} - \dot{\boldsymbol{q}}_d).
\end{aligned}$$

$\boldsymbol{K}_1, \boldsymbol{K}_2, \boldsymbol{K}_3, \boldsymbol{K}_4, \boldsymbol{E}_1, \boldsymbol{E}_2, \boldsymbol{E}_3, \boldsymbol{E}_4, \boldsymbol{F}_1$, and $\boldsymbol{F}_2$ are all strictly positive diagonal matrices, the definitions of $\boldsymbol{z}_1$ and $\boldsymbol{z}_2$ have been given in (32), and the estimates $\hat{\boldsymbol{z}}_1$ and $\hat{\boldsymbol{z}}_2$ are generated from the following nonlinear observer based on the passivity approach:

$$\begin{cases} \dot{\hat{\boldsymbol{z}}}_1 = \boldsymbol{R}(\boldsymbol{q})\boldsymbol{M}_1^{-1}\boldsymbol{R}^T(\boldsymbol{q})\hat{\boldsymbol{z}}_2 + \boldsymbol{K}_3\tilde{\boldsymbol{z}}_1\\ \dot{\hat{\boldsymbol{z}}}_2 = \boldsymbol{R}(\boldsymbol{q})\left[-\boldsymbol{D}_1(\hat{\boldsymbol{v}})\hat{\boldsymbol{v}} - \boldsymbol{g}_1(\boldsymbol{q}) + \boldsymbol{\tau}_1 + \boldsymbol{M}_1^{-1}\boldsymbol{R}^T(\boldsymbol{q})\boldsymbol{K}_4\tilde{\boldsymbol{z}}_1\right]. \end{cases} \tag{50}$$

Through Lyapunov stability theory, it has been proved in [15] that observer (50) is globally exponentially convergent. Furthermore, system (29) under controller (48) and system (30) under controller (49) are both globally exponentially stable in the absence of external disturbances.

V. NUMERICAL SIMULATIONS

In this section, some simulations are performed on the AUV model called Kambara [11] to illustrate the effectiveness of the proposed finite-time output feedback control scheme.

Before proceeding, the model identification process of Kambara is introduced here. The rigid-body inertia matrix $\boldsymbol{M}_{RB}$ is obtained through solid modeling of Kambara with the Pro Engineer software by Parametric Technology Corporation. With this solid model, mass m, inertia tensor $\boldsymbol{I}_B$, and center of gravity $\boldsymbol{r}_G$ can be estimated accurately. The hydrodynamic added mass matrix $\boldsymbol{M}_A$ is obtained empirically by fitting data obtained from experiments. Then, the matrix of Coriolis and centripetal effects $\boldsymbol{C}(\boldsymbol{\nu})$ can be obtained directly from $\boldsymbol{M}_{RB}$ and $\boldsymbol{M}_A$ [see (16) and (17)]. The damping matrix $\boldsymbol{D}(\boldsymbol{\nu})$ is obtained empirically through observation of the real system in the same way as estimating the hydrodynamic added mass matrix. The displacement volume ∇ and center of buoyancy $\boldsymbol{r}_B$ are determined by replacing all the material in the Kambara solid model with a uniform material which has the density equal to that of water.

In simulations, the vehicle translational velocities are regarded to be unmeasurable. The estimated (nominal) values of model parameters of Kambara [in the sense of (24) and (25)] are [11]

$$\begin{aligned}
\bar{\boldsymbol{M}}_1 &= \mathbf{diag}\{175.4, 140.8, 140.8\}\\
\bar{\boldsymbol{M}}_2 &= \mathbf{diag}\{14.08, 12.98, 16.07\}\\
\bar{\boldsymbol{D}}_1(\boldsymbol{v}) &= \mathbf{diag}\{120 + 90|v_1|, 90 + 90|v_2|, 150 + 120|v_3|\}\\
\bar{\boldsymbol{D}}_2(\boldsymbol{\omega}) &= \mathbf{diag}\{15 + 10|\omega_1|, 15 + 12|\omega_2|, 18 + 15|\omega_3|\}.
\end{aligned}$$

TABLE II
CONTROL PARAMETERS FOR THE OUTPUT FEEDBACK BACKSTEPPING CONTROL SCHEME

Controller $\boldsymbol{\tau}_1$ (48)	$\boldsymbol{K}_1 = \boldsymbol{I}_{3\times 3}, \boldsymbol{E}_1 = 0.02\boldsymbol{I}_{3\times 3}, \boldsymbol{F}_1 = 0.02\boldsymbol{I}_{3\times 3}, \boldsymbol{E}_2 = 0.2\boldsymbol{I}_{3\times 3}, \boldsymbol{F}_2 = 151.6\boldsymbol{I}_{3\times 3}$
Controller $\boldsymbol{\tau}_2$ (49)	$\boldsymbol{K}_2 = \boldsymbol{I}_{4\times 4}, \boldsymbol{E}_3 = 0.4\boldsymbol{I}_{4\times 4}, \boldsymbol{E}_4 = 1.6\boldsymbol{I}_{4\times 4}$
Observer (50)	$\boldsymbol{K}_3 = 5\boldsymbol{I}_{3\times 3}, \boldsymbol{K}_4 = \boldsymbol{I}_{3\times 3}$

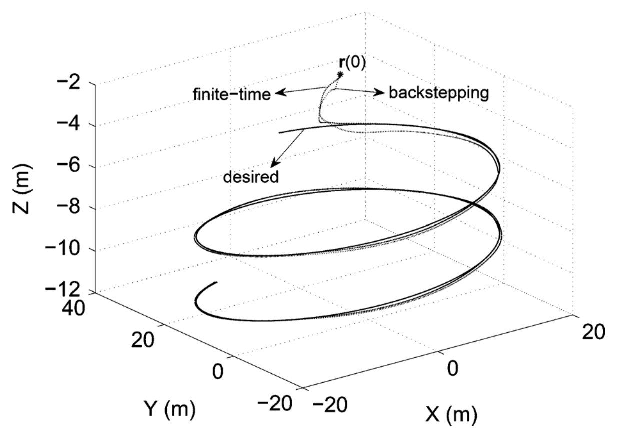

Fig. 2. Three-dimensional phase plot for the AUV in the absence of external disturbances.

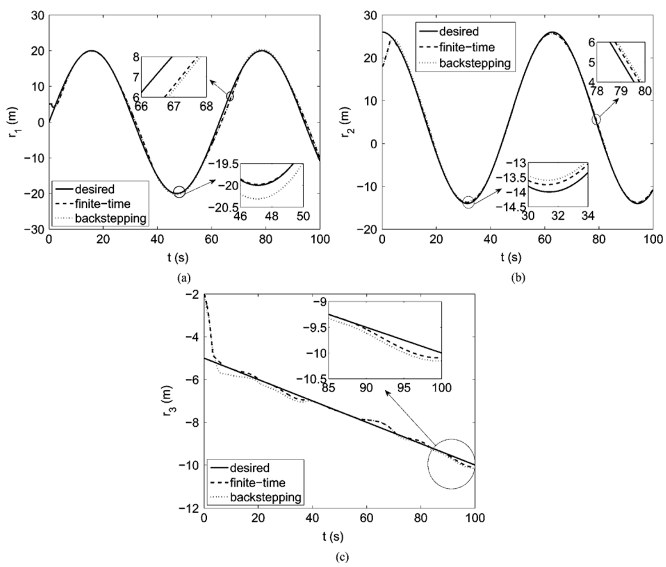

Fig. 3. Response curves of position vector $\boldsymbol{r}$ in the absence of external disturbances: (a) r_1, (b) r_2, and (c) r_3.

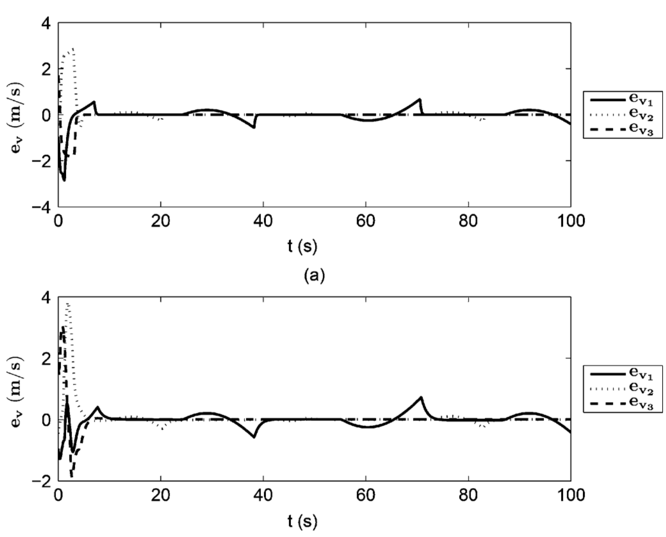

Fig. 4. Response curves of translational velocity tracking errors $\boldsymbol{e_v}$ in the absence of external disturbances. (a) $\boldsymbol{e_v}$ under the finite-time control scheme. (b) $\boldsymbol{e_v}$ under the backstepping control scheme.

$\bar{\boldsymbol{C}}_1(\boldsymbol{v})$ and $\bar{\boldsymbol{C}}_2(\boldsymbol{\omega})$ can be obtained directly from $\bar{\boldsymbol{M}}_1$ and $\bar{\boldsymbol{M}}_2$ by (16) and (17). The gravitational force is $\bar{W} = 1148$ N and the buoyant force is $\bar{B} = 1108$ N. The center of gravity is set as $\boldsymbol{r}_G = [0, 0, 0]^T$ and the center of buoyancy relative to the center of gravity is $\bar{\boldsymbol{r}}_B = [-0.017, 0, -0.115]^T$ in the B-frame. Assume that all the model parameters have 3% uncertainties with respect to their nominal values.

The initial conditions of the AUV are set as $\boldsymbol{r}(0) = [5, 18, -2]^T$, $\boldsymbol{v}(0) = [0, 0, 0]^T$, $\boldsymbol{q}(0) = [-0.5000, -0.6928, 0.1732, 0.4899]^T$ (the initial principal angle Φ is equal to $2\pi/3$), and $\boldsymbol{\omega}(0) = [2.1, -1.3, 1.6]^T$. For observer systems (42) and (50), the initial conditions are set as $\hat{\boldsymbol{r}}(0) = [-1, 11, 6]^T, \hat{\boldsymbol{v}}(0) = [0.9, -1.8, 0.5]^T$.

Here, comparisons of dynamic performances are made between the finite-time output feedback control scheme [controllers (46) and (47) and observer (42)] proposed in this paper and the output feedback backstepping control scheme [controllers (48) and (49) and observer (50)] presented in [15]. To be fair, the control forces $\boldsymbol{\tau}_1$ are limited not to exceed 500 N, and the control moments $\boldsymbol{\tau}_2$ are limited not to exceed 200 Nm. Under these restrictions, the control parameters for each control scheme are appropriately selected. Moreover, time has also been spent on regulating the control parameters for controllers (48) and (49) and observer (50) to make the performance of their closed-loop system as good as possible.

By Theorem 4, for the proposed finite-time output feedback control scheme consisting of controllers (46) and (47) and observer (42), the control parameter values are given in Table I.

By Remark 2, for the output feedback backstepping control scheme involving controllers (48) and (49) and observer (50), the control parameter values are exhibited in Table II.

A. Simulations in the Absence of External Disturbances

In this section, in the absence of external disturbances, simulations of a spiral trajectory tracking example are exhibited. The desired spiral trajectory (which is circular in the X-Y plane) and attitude (the desired principal angle Φ is equal to $\pi/9$) for the AUV are

$$\begin{aligned}\boldsymbol{r}_d(t) &= [20\sin(0.1t), 6 + 20\cos(0.1t), -5 - 0.05t]^T \\ \boldsymbol{q}_d &= [0.9848, 0.1042, 0.0868, 0.1084]^T. \end{aligned} \tag{51}$$

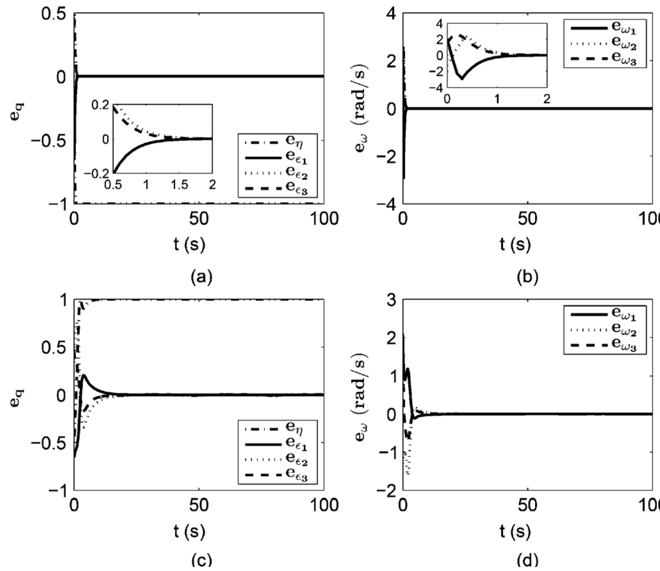

Fig. 5. Response curves of attitude and angular velocity tracking errors $\boldsymbol{e_q}$ and $\boldsymbol{e_\omega}$ in the absence of external disturbances. (a) $\boldsymbol{e_q}$ under the finite-time control scheme. (b) $\boldsymbol{e_\omega}$ under the finite-time control scheme. (c) $\boldsymbol{e_q}$ under the backstepping control scheme. (d) $\boldsymbol{e_\omega}$ under the backstepping control scheme.

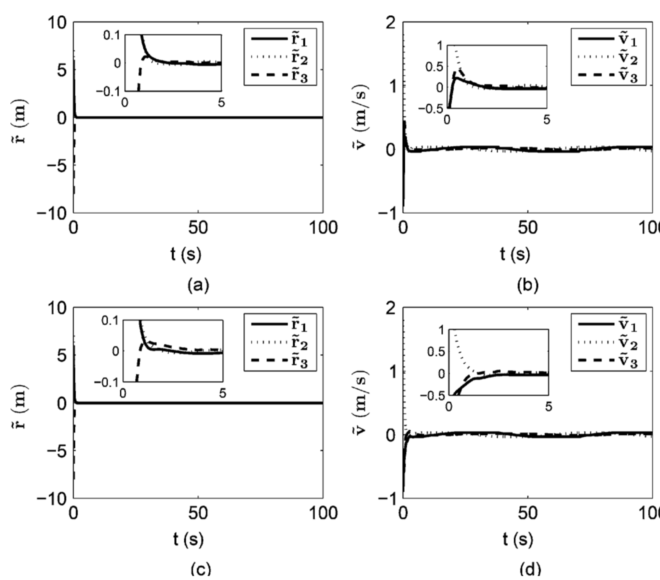

Fig. 6. Response curves of position and translational velocity observation errors $\tilde{\boldsymbol{r}}$ and $\tilde{\boldsymbol{v}}$ in the absence of external disturbances. (a) $\tilde{\boldsymbol{r}}$ of observer (42). (b) $\tilde{\boldsymbol{v}}$ of observer (42). (c) $\tilde{\boldsymbol{r}}$ of observer (50). (d) $\tilde{\boldsymbol{v}}$ of observer (50).

The response curves of the closed-loop systems under both control schemes are shown in Figs. 2–7. As analyzed in Remark 4, due to the presence of model parameter uncertainties, the tracking errors $\boldsymbol{e_r}, \boldsymbol{e_v}, \boldsymbol{e_q}, \boldsymbol{e_\omega}$ are stabilized to small regions around their equilibria under both control schemes. From Figs. 2–5, it can be seen that the finite-time output feedback control scheme offers faster convergence rates for the tracking errors and better robustness than the output feedback backstepping control scheme.

B. Simulations in the Presence of External Disturbances

In this section, a comparison is made on the disturbance rejection properties of the closed-loop systems under the two control schemes. A simulation example of tracking spiral trajectory

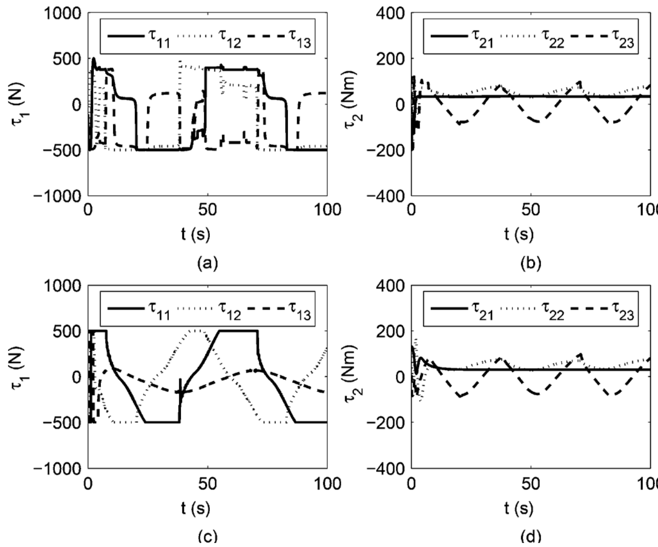

Fig. 7. Response curves of control forces $\boldsymbol{\tau}_1$ and moments $\boldsymbol{\tau}_2$ in the absence of external disturbances. (a) $\boldsymbol{\tau}_1$ under the finite-time control scheme. (b) $\boldsymbol{\tau}_2$ under the finite-time control scheme. (c) $\boldsymbol{\tau}_1$ under the backstepping control scheme. (d) $\boldsymbol{\tau}_2$ under the backstepping control scheme.

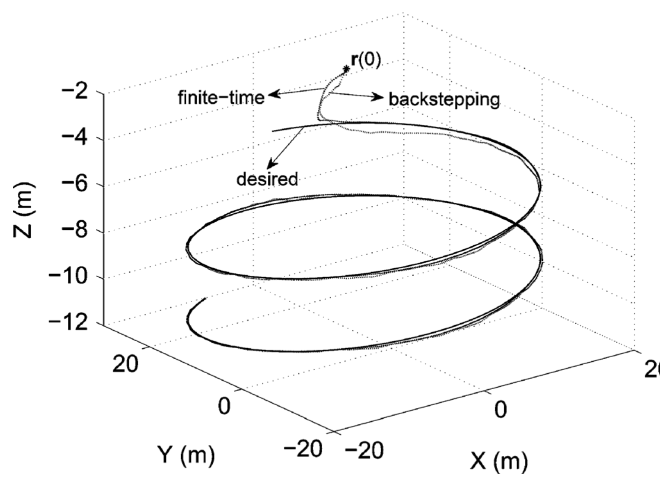

Fig. 8. Three-dimensional phase plot for the AUV in the presence of external disturbances.

(51) is conducted in the presence of external disturbances. The external disturbances on control inputs $\boldsymbol{\tau}_1$ and $\boldsymbol{\tau}_2$ are

$$\boldsymbol{\tau}_{d_1} = [50\sin(6t), 60\sin(5t), 30\sin(4t) + 18\cos(2t)]^T$$
$$\boldsymbol{\tau}_{d_2} = [11\cos(2t+1), 3\sin(3t) + 5\cos(3t), 6\sin(t)]^T.$$

The simulation results are given in Figs. 8–14. It can be seen from Figs. 8–12 that in the presence of external disturbances, the tracking errors will be stabilized to bounded regions around the equilibria under both control schemes. This is mainly because both control schemes are continuous such that the external disturbances cannot be suppressed completely. The bounds of the steady tracking errors under the finite-time control scheme are much smaller than those under the backstepping control scheme, which implies that the finite-time control scheme provides a better disturbance rejection property for the AUV dynamics.

Note that it is difficult that the experiments can produce the same results as simulations, due to model parameter variation and noisy measurements of the sensors in experiments. But as

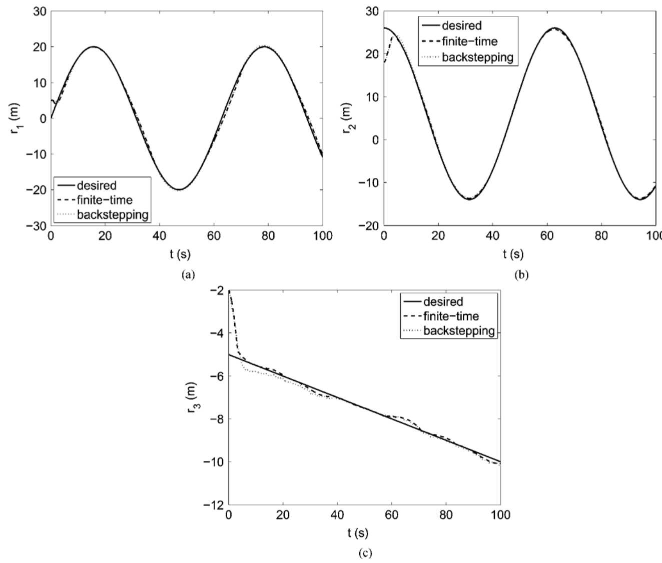

Fig. 9. Response curves of position vector $\boldsymbol{r}$ in the presence of external disturbances: (a) r_1, (b) r_2, and (c) r_3.

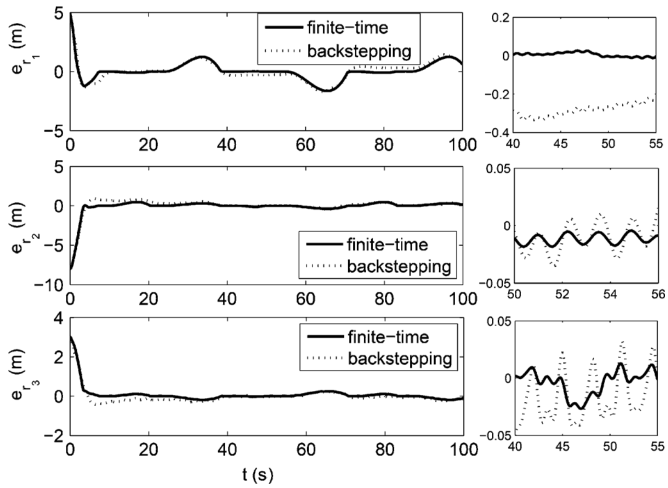

Fig. 10. Response curves of position tracking errors $\boldsymbol{e_r}$ in the presence of external disturbances.

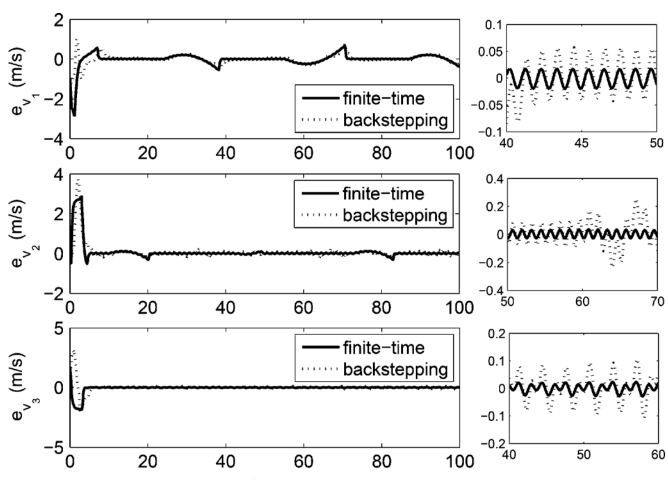

Fig. 11. Response curves of translational velocity tracking errors $\boldsymbol{e_v}$ in the presence of external disturbances.

a future work, the proposed control scheme can be validated through real experiments.

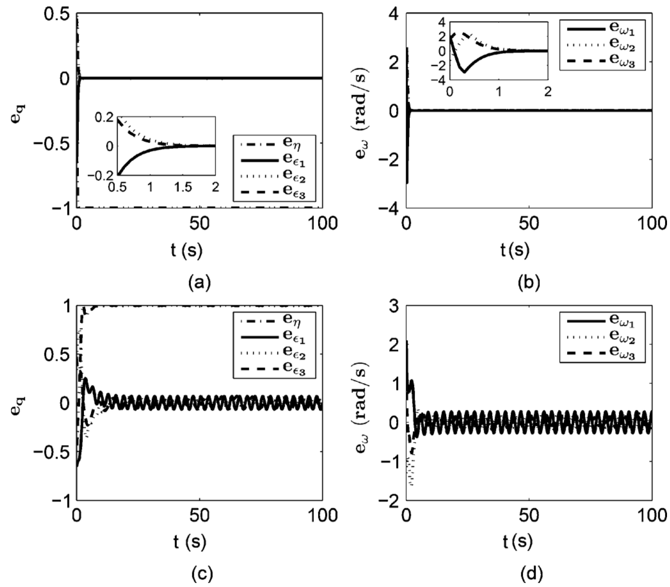

Fig. 12. Response curves of attitude and angular velocity tracking errors $\boldsymbol{e_q}$ and $\boldsymbol{e_\omega}$ in the presence of external disturbances. (a) $\boldsymbol{e_q}$ under the finite-time control scheme. (b) $\boldsymbol{e_\omega}$ under the finite-time control scheme. (c) $\boldsymbol{e_q}$ under the backstepping control scheme. (d) $\boldsymbol{e_\omega}$ under the backstepping control scheme.

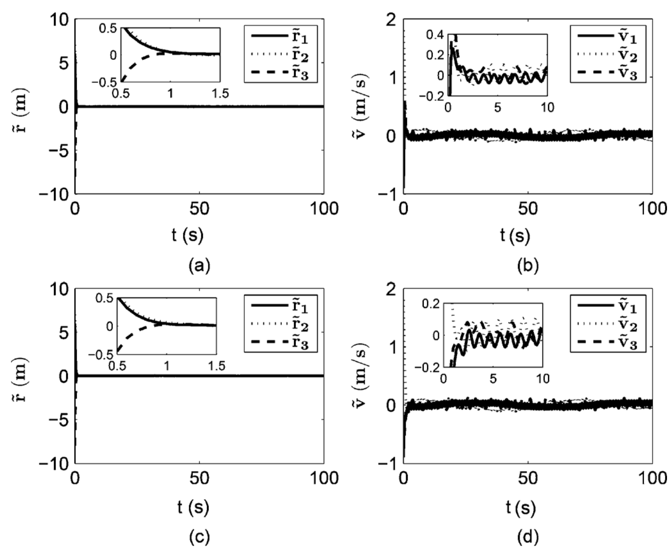

Fig. 13. Response curves of position and translational velocity observation errors $\tilde{\boldsymbol{r}}$ and $\tilde{\boldsymbol{v}}$ in the presence of external disturbances. (a) $\tilde{\boldsymbol{r}}$ of observer (42). (b) $\tilde{\boldsymbol{v}}$ of observer (42). (c) $\tilde{\boldsymbol{r}}$ of observer (50). (d) $\tilde{\boldsymbol{v}}$ of observer (50).

VI. Conclusion

In this paper, the finite-time trajectory tracking problem for AUVs without translational velocity measurements has been studied. By making a proper coordinate transformation and using finite-time control technique, a finite-time state feedback controller has been proposed for the vehicle translational subsystem. Meanwhile, a finite-time state feedback controller has also been designed for the vehicle rotational subsystem. To obtain the vehicle translational velocity information for feedback, a global finite-time convergent observer has been developed. Then, a finite-time output feedback control scheme has been derived by combining the corresponding output feedback controllers and the finite-time convergent observer together. In the absence of external disturbances, the proposed finite-time control scheme offers a faster convergence rate for the tracking errors than the conventional backstepping control scheme. Furthermore, in the presence of external disturbances or model parameter uncertainties, the proposed finite-time control scheme provides a higher tracking accuracy for AUVs than the conventional backstepping control scheme.

APPENDIX A
PROOF OF THEOREM 1

Step 1 (Design of Virtual Controller $\boldsymbol{\beta}_2^*$): Choose a Lyapunov function $V_1(\boldsymbol{\beta}_1) = (1/2)\boldsymbol{\beta}_1^T\boldsymbol{\beta}_1$. The derivative of V_1 along system (37) satisfies

$$\dot{V}_1 = \boldsymbol{\beta}_1^T\boldsymbol{\beta}_2 = \boldsymbol{\beta}_1^T(\boldsymbol{\beta}_2 - \boldsymbol{\beta}_2^*) + \boldsymbol{\beta}_1^T\boldsymbol{\beta}_2^* \tag{A.1}$$

where $\boldsymbol{\beta}_2^* = [\beta_{21}^*, \beta_{22}^*, \beta_{23}^*]^T \in \mathbb{R}^3$ is a continuous virtual controller. Here, $\boldsymbol{\beta}_2^*$ is taken as

$$\boldsymbol{\beta}_2^* = -k_1 \left[\beta_{11}^{p_1}, \beta_{12}^{p_1}, \beta_{13}^{p_1}\right]^T \tag{A.2}$$

where $k_1 > 0, 1/2 < p_1 = p_{11}/p_{12} < 1$, and p_{11} and p_{12} are positive odd integers. Substituting (A.2) into (A.1) yields

$$\dot{V}_1 = -k_1\left(\beta_{11}^{1+p_1} + \beta_{12}^{1+p_1} + \beta_{13}^{1+p_1}\right) + \boldsymbol{\beta}_1^T(\boldsymbol{\beta}_2 - \boldsymbol{\beta}_2^*). \tag{A.3}$$

Step 2 (Design of Controller $\boldsymbol{u}_1$): Denote

$$\varphi_i = \beta_{2i}^{1/p_1} - \beta_{2i}^{*1/p_1}, \qquad i = 1, 2, 3.$$

Choose the following Lyapunov function for system (37):

$$V_{tr}(\boldsymbol{\beta}_1, \boldsymbol{\beta}_2) = V_1(\boldsymbol{\beta}_1) + \sum_{i=1}^{3} V_{2i}(\beta_{1i}, \beta_{2i}) \tag{A.4}$$

where

$$V_{2i}(\beta_{1i}, \beta_{2i}) = \frac{1}{(2-p_1)2^{-p_1}k_1^{1+1/p_1}} \times \int_{\beta_{2i}^*}^{\beta_{2i}} \left(s^{1/p_1} - \beta_{2i}^{*1/p_1}\right)^{2-p_1} ds, \qquad i = 1, 2, 3. \tag{A.5}$$

The following task is to prove that $V_{tr}(\boldsymbol{\beta}_1, \boldsymbol{\beta}_2)$ satisfies both sufficient conditions in Lemma 1.

i) From Propositions B1 and B2 in [33], it can be obtained that $\int_{\beta_{2i}^*}^{\beta_{2i}}(s^{1/p_1} - \beta_{2i}^{*1/p_1})^{2-p_1} ds, i = 1, 2, 3$, are differentiable, positive definite, and proper. Hence, $V_{tr}(\boldsymbol{\beta}_1, \boldsymbol{\beta}_2)$ is positive definite.

ii) It will be shown that $V_{tr}(\boldsymbol{\beta}_1, \boldsymbol{\beta}_2)$ also satisfies the second sufficient condition in Lemma 1.

According to Lemma 2, it can be obtained that

$$\boldsymbol{\beta}_1^T(\boldsymbol{\beta}_2 - \boldsymbol{\beta}_2^*) \le \sum_{i=1}^{3} |\beta_{1i}|\left|(\beta_{2i}^{1/p_1})^{p_1} - (\beta_{2i}^{*1/p_1})^{p_1}\right| \le \sum_{i=1}^{3} 2^{1-p_1}|\beta_{1i}||\varphi_i|^{p_1}. \tag{A.6}$$

By Lemma 3, the following inequality holds:

$$2^{1-p_1}|\beta_{1i}||\varphi_i|^{p_1} \le \frac{2^{1-p_1}}{1+p_1}\beta_{1i}^{1+p_1} + \frac{2^{1-p_1}p_1}{1+p_1}\varphi_i^{1+p_1}, \qquad i = 1, 2, 3. \tag{A.7}$$

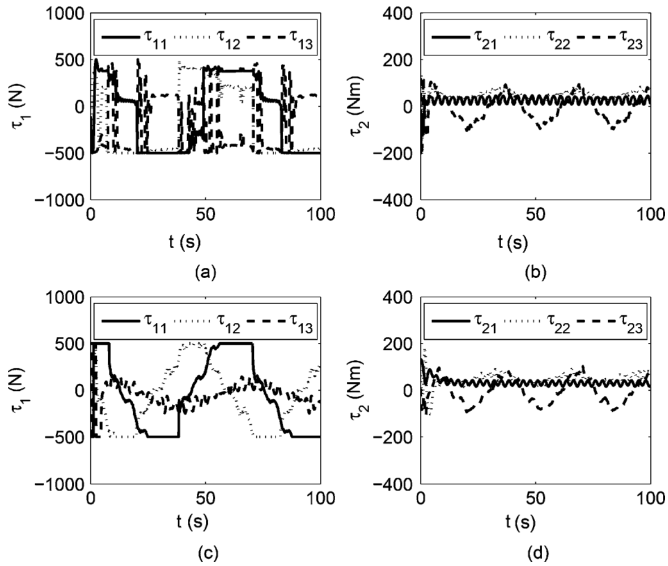

Fig. 14. Response curves of control forces $\boldsymbol{\tau}_1$ and moments $\boldsymbol{\tau}_2$ in the presence of external disturbances. (a) $\boldsymbol{\tau}_1$ under the finite-time control scheme. (b) $\boldsymbol{\tau}_2$ under the finite-time control scheme. (c) $\boldsymbol{\tau}_1$ under the backstepping control scheme. (d) $\boldsymbol{\tau}_2$ under the backstepping control scheme.

Substituting (A.6) and (A.7) into (A.3) yields

$$\dot{V}_1 \le -\left(k_1 - \frac{2^{1-p_1}}{1+p_1}\right)\sum_{i=1}^{3}\beta_{1i}^{1+p_1} + \sum_{i=1}^{3}\frac{2^{1-p_1}p_1}{1+p_1}\varphi_i^{1+p_1}. \tag{A.8}$$

The derivative of $V_{2i}(\beta_{1i}, \beta_{2i}), i = 1, 2, 3$, along system (37) is

$$\dot{V}_{2i} = -\frac{1}{2^{-p_1}k_1^{1+1/p_1}}\frac{d\beta_{2i}^{*1/p_1}}{dt}\int_{\beta_{2i}^*}^{\beta_{2i}}\left(s^{1/p_1} - \beta_{2i}^{*1/p_1}\right)^{1-p_1} ds + \frac{1}{(2-p_1)2^{-p_1}k_1^{1+1/p_1}}\varphi_i^{2-p_1}\dot{\beta}_{2i}. \tag{A.9}$$

Note that $(d\beta_{2i}^{*1/p_1})/dt = -k_1^{1/p_1}\beta_{2i}$. By Lemma 2, it can be verified that

$$|\beta_{2i}| \le |\beta_{2i}^*| + |\beta_{2i} - \beta_{2i}^*| \le k_1|\beta_{1i}|^{p_1} + 2^{1-p_1}|\varphi_i|^{p_1}, \qquad i = 1, 2, 3. \tag{A.10}$$

In addition, still by Lemma 2, the following inequality holds:

$$\int_{\beta_{2i}^*}^{\beta_{2i}}\left(s^{1/p_1} - \beta_{2i}^{*1/p_1}\right)^{1-p_1} ds \le |\beta_{2i} - \beta_{2i}^*||\varphi_i|^{1-p_1} \le 2^{1-p_1}|\varphi_i|, \qquad i = 1, 2, 3. \tag{A.11}$$

Substituting (A.10) and (A.11) into (A.9) yields

$$\dot{V}_{2i} \le 2|\beta_{1i}|^{p_1}|\varphi_i| + \frac{2^{2-p_1}}{k_1}\varphi_i^{1+p_1} + \frac{1}{(2-p_1)2^{-p_1}k_1^{1+1/p_1}}\varphi_i^{2-p_1}\dot{\beta}_{2i}, \qquad i = 1, 2, 3. \tag{A.12}$$

From Lemma 3, it holds that

$$2|\beta_{1i}|^{p_1}|\varphi_i| \le \frac{2p_1}{1+p_1}\beta_{1i}^{1+p_1} + \frac{2}{1+p_1}\varphi_i^{1+p_1}, \qquad i = 1, 2, 3.$$

Then, it follows from (A.12) that

$$\dot{V}_{2i} \leq \frac{2p_1}{1+p_1}\beta_{1i}^{1+p_1} + \left(\frac{2}{1+p_1} + \frac{2^{2-p_1}}{k_1}\right)\varphi_i^{1+p_1} + \frac{1}{(2-p_1)2^{-p_1}k_1^{1+1/p_1}}\varphi_i^{2-p_1}\dot{\beta}_{2i}, \qquad i = 1,2,3. \quad \text{(A.13)}$$

Hence, it follows from (A.4), (A.8), and (A.13) that

$$\begin{aligned}\dot{V}_{tr} &= \dot{V}_1 + \sum_{i=1}^{3}\dot{V}_{2i} \\ &\leq -\left(k_1 - \frac{2^{1-p_1}}{1+p_1} - \frac{2p_1}{1+p_1}\right)\sum_{i=1}^{3}\beta_{1i}^{1+p_1} \\ &\quad + \left(\frac{2^{1-p_1}p_1}{1+p_1} + \frac{2}{1+p_1} + \frac{2^{2-p_1}}{k_1}\right)\sum_{i=1}^{3}\varphi_i^{1+p_1} \\ &\quad + \frac{1}{(2-p_1)2^{-p_1}k_1^{1+1/p_1}}\sum_{i=1}^{3}\varphi_i^{2-p_1}\dot{\beta}_{2i}. \end{aligned} \quad \text{(A.14)}$$

Note that $\dot{\beta}_{2i} = u_{1i}, i = 1,2,3$. Controller u_{1i} is taken as

$$u_{1i} = -k_2\varphi_i^{2p_1-1}, \qquad i = 1,2,3 \quad \text{(A.15)}$$

where

$$\begin{aligned} &k_1 \geq 2^{1-p_1}/(1+p_1) + 2p_1/(1+p_1) + c_1 \\ &k_2 \geq (2-p_1)2^{-p_1}k_1^{1+1/p_1}[2^{1-p_1}p_1/(1+p_1) + 2/(1+p_1) \\ &\qquad\qquad + 2^{2-p_1}/k_1 + c_1], \qquad c_1 > 0. \end{aligned}$$

Substituting controller (A.15) into (A.14) yields

$$\dot{V}_{tr} \leq -c_1\sum_{i=1}^{3}\beta_{1i}^{1+p_1} - c_1\sum_{i=1}^{3}\varphi_i^{1+p_1}. \quad \text{(A.16)}$$

On the other hand, by utilizing Lemma 2, it can be obtained from (A.4) that

$$\begin{aligned} V_{tr}(\boldsymbol{\beta}_1, \boldsymbol{\beta}_2) &\leq \frac{1}{2}\sum_{i=1}^{3}\beta_{1i}^2 + \frac{2}{(2-p_1)k_1^{1+1/p_1}}\sum_{i=1}^{3}\varphi_i^2 \\ &\leq \lambda\left(\sum_{i=1}^{3}\beta_{1i}^2 + \sum_{i=1}^{3}\varphi_i^2\right) \end{aligned} \quad \text{(A.17)}$$

where

$$\lambda = \max\left\{1/2, 2/\left[(2-p_1)k_1^{1+1/p_1}\right]\right\}.$$

Let

$$c = \frac{c_1}{\lambda^{(1+p_1)/2}} > 0.$$

Then, still by Lemma 2, it can be obtained that

$$\dot{V}_{tr} + cV_{tr}^{(1+p_1)/2} \leq 0. \quad \text{(A.18)}$$

Note that $0 < (1+p_1)/2 < 1$. Hence, from Lemma 1, it can be concluded that system (37) is globally finite-time stable under controller $\boldsymbol{u}_1$ designed as (A.15) with respect to the equilibrium $[\boldsymbol{\beta}_1^T, \boldsymbol{\beta}_2^T]^T = \mathbf{0}_{6\times1}$. From (38) and (A.15), controller $\boldsymbol{\tau}_1$ can be written as (35). Note that coordinate transformations (32) and (36) are both invertible. Therefore, systems (34) and (29) are both globally finite-time stable under controller $\boldsymbol{\tau}_1$ (35). This completes the proof.

Appendix B
Proof of Theorem 2

Step 1 (Design of Virtual Controller $\boldsymbol{e}_{\boldsymbol{\omega}}^*$): Choose the following Lyapunov function:

$$V_3(\boldsymbol{e_q}) = (e_\eta - \text{sgn}(e_\eta(0)))^2 + \boldsymbol{e}_{\boldsymbol{\epsilon}}^T\boldsymbol{e}_{\boldsymbol{\epsilon}}. \quad \text{(B.1)}$$

By using the property $\boldsymbol{e}_{\boldsymbol{\epsilon}}^T\boldsymbol{S}(\boldsymbol{e}_{\boldsymbol{\epsilon}}) = \mathbf{0}_{1\times3}$, the derivative of V_3 along system (41) satisfies

$$\begin{aligned}\dot{V}_3 &= 2(e_\eta - \text{sgn}(e_\eta(0)))\dot{e}_\eta + 2\boldsymbol{e}_{\boldsymbol{\epsilon}}^T\dot{\boldsymbol{e}}_{\boldsymbol{\epsilon}} \\ &= \text{sgn}(e_\eta(0))\boldsymbol{e}_{\boldsymbol{\epsilon}}^T\boldsymbol{e}_{\boldsymbol{\omega}} \\ &= \text{sgn}(e_\eta(0))\boldsymbol{e}_{\boldsymbol{\epsilon}}^T\boldsymbol{e}_{\boldsymbol{\omega}}^* + \text{sgn}(e_\eta(0))\boldsymbol{e}_{\boldsymbol{\epsilon}}^T(\boldsymbol{e}_{\boldsymbol{\omega}} - \boldsymbol{e}_{\boldsymbol{\omega}}^*) \end{aligned} \quad \text{(B.2)}$$

where $\boldsymbol{e}_{\boldsymbol{\omega}}^* = [e_{\omega_1}^*, e_{\omega_2}^*, e_{\omega_3}^*]^T \in \mathbb{R}^3$ is a virtual controller to be designed. Here $\boldsymbol{e}_{\boldsymbol{\omega}}^*$ is deigned as

$$e_{\omega_i}^* = -\text{sgn}(e_\eta(0))k_3e_{\epsilon_i}^{p_2}, \qquad i = 1,2,3 \quad \text{(B.3)}$$

where $k_3 > 0, 1/2 < p_2 = p_{21}/p_{22} < 1$, and p_{21} and p_{22} are positive odd integers. Substituting (B.3) into (B.2) yields

$$\dot{V}_3 = -k_3\sum_{i=1}^{3}e_{\epsilon_i}^{1+p_2} + \text{sgn}(e_\eta(0))\boldsymbol{e}_{\boldsymbol{\epsilon}}^T(\boldsymbol{e}_{\boldsymbol{\omega}} - \boldsymbol{e}_{\boldsymbol{\omega}}^*). \quad \text{(B.4)}$$

Step 2 (Design of Controller $\boldsymbol{u}_2$): Denote

$$\xi_i = e_{\omega_i}^{1/p_2} - e_{\omega_i}^{*1/p_2}, \qquad i = 1,2,3.$$

Choose a Lyapunov function for system (41) as

$$V_{ro}(\boldsymbol{e_q}, \boldsymbol{e_\omega}) = V_3(\boldsymbol{e_q}) + \sum_{i=1}^{3}V_{4i}(\boldsymbol{e_q}, \boldsymbol{e_\omega}) \quad \text{(B.5)}$$

where

$$V_{4i}(\boldsymbol{e_q}, \boldsymbol{e_\omega}) = \frac{1}{(2-p_2)2^{-p_2}k_3^{1+1/p_2}} \times \int_{e_{\omega_i}^*}^{e_{\omega_i}}(s^{1/p_2} - e_{\omega_i}^{*1/p_2})^{2-p_2}\,ds, \qquad i = 1,2,3. \quad \text{(B.6)}$$

From Propositions B1 and B2 in [33], it can be obtained that $V_{ro}(\boldsymbol{e_q}, \boldsymbol{e_\omega})$ is positive definite with respect to the equilibrium set

$$Q_2 = \left\{\left[\boldsymbol{e}_{\boldsymbol{q}}^T, \boldsymbol{e}_{\boldsymbol{\omega}}^T\right]^T | \boldsymbol{e_q} = [\pm1, \mathbf{0}_{1\times3}]^T, \boldsymbol{e_\omega} = \mathbf{0}_{3\times1}\right\}.$$

The following task is to prove that $V_{ro}(\boldsymbol{e_q}, \boldsymbol{e_\omega})$ also satisfies the second sufficient condition in Lemma 1.

By Lemma 2, it can be verified that

$$\begin{aligned}\text{sgn}(e_\eta(0))\boldsymbol{e}_{\boldsymbol{\epsilon}}^T(\boldsymbol{e}_{\boldsymbol{\omega}} - \boldsymbol{e}_{\boldsymbol{\omega}}^*) &\leq \sum_{i=1}^{3}|e_{\epsilon_i}|\left|\left(e_{\omega_i}^{1/p_2}\right)^{p_2} - \left(e_{\omega_i}^{*1/p_2}\right)^{p_2}\right| \\ &\leq \sum_{i=1}^{3}2^{1-p_2}|e_{\epsilon_i}||\xi_i|^{p_2}. \end{aligned} \quad \text{(B.7)}$$

In addition, by Lemma 3, it can be obtained that

$$2^{1-p_2}|e_{\epsilon_i}||\xi_i|^{p_2} \leq \frac{2^{1-p_2}}{1+p_2}e_{\epsilon_i}^{1+p_2} + \frac{2^{1-p_2}p_2}{1+p_2}\xi_i^{1+p_2}, \qquad i = 1,2,3. \quad \text{(B.8)}$$

Substituting (B.7) and (B.8) into (B.4) yields

$$\dot{V}_3 \leq -\left(k_3 - \frac{2^{1-p_2}}{1+p_2}\right)\sum_{i=1}^{3} e_{\epsilon_i}^{1+p_2} + \frac{2^{1-p_2}p_2}{1+p_2}\sum_{i=1}^{3}\xi_i^{1+p_2}. \tag{B.9}$$

The derivative of $V_{4i}(\boldsymbol{e_q}, \boldsymbol{e_\omega})$, $i = 1, 2, 3$, along system (41) is

$$\dot{V}_{4i} = -\frac{1}{2^{-p_2}k_3^{1+1/p_2}}\frac{de_{\omega_i}^{*1/p_2}}{dt}\int_{e_{\omega_i}^*}^{e_{\omega_i}}\left(s^{1/p_2} - e_{\omega_i}^{*1/p_2}\right)^{1-p_2} ds + \frac{1}{(2-p_2)2^{-p_2}k_3^{1+1/p_2}}\xi_i^{2-p_2}u_{2i}. \tag{B.10}$$

Note that

$$(de_{\omega_i}^{*1/p_2})/dt = -\mathrm{sgn}(e_\eta(0))k_3^{1/p_2}\dot{e}_{\epsilon_i}, \qquad i = 1, 2, 3$$

and

$$\dot{\boldsymbol{e}}_{\boldsymbol{\epsilon}} = \frac{1}{2}(e_\eta \boldsymbol{I}_{3\times 3} + \boldsymbol{S}(\boldsymbol{e_\epsilon}))\boldsymbol{e_\omega}.$$

According to (8), $e_\eta, e_{\epsilon_i} \leq 1, i = 1, 2, 3$, which implies that

$$|\dot{e}_{\epsilon_i}| \leq \frac{1}{2}\sum_{j=1}^{3}|e_{\omega_j}|, \qquad i = 1, 2, 3. \tag{B.11}$$

By Lemma 2, it can be verified that

$$|e_{\omega_j}| \leq |e_{\omega_j}^*| + |e_{\omega_j} - e_{\omega_j}^*| \leq k_3|e_{\epsilon_j}|^{p_2} + 2^{1-p_2}|\xi_j|^{p_2}, \qquad j = 1, 2, 3. \tag{B.12}$$

On the other hand, still by Lemma 2, the following inequality holds:

$$\int_{e_{\omega_i}^*}^{e_{\omega_i}}(s^{1/p_2} - e_{\omega_i}^{*1/p_2})^{1-p_2} \leq |e_{\omega_i} - e_{\omega_i}^*||\xi_i|^{1-p_2} \leq 2^{1-p_2}|\xi_i|, \qquad i = 1, 2, 3. \tag{B.13}$$

Substituting (B.11)–(B.13) into (B.10) yields

$$\dot{V}_{4i} \leq \sum_{j=1}^{3}|e_{\epsilon_j}|^{p_2}|\xi_i| + \frac{2^{1-p_2}}{k_3}\sum_{j=1}^{3}|\xi_j|^{p_2}|\xi_i| + \frac{1}{(2-p_2)2^{-p_2}k_3^{1+1/p_2}}\xi_i^{2-p_2}u_{2i}, \qquad i = 1, 2, 3. \tag{B.14}$$

By Lemma 3, it can be obtained that

$$|e_{\epsilon_j}|^{p_2}|\xi_i| \leq \frac{p_2}{1+p_2}e_{\epsilon_j}^{1+p_2} + \frac{1}{1+p_2}\xi_i^{1+p_2} \tag{B.15}$$

$$|\xi_j|^{p_2}|\xi_i| \leq \frac{p_2}{1+p_2}\xi_j^{1+p_2} + \frac{1}{1+p_2}\xi_i^{1+p_2}, \qquad j = 1, 2, 3. \tag{B.16}$$

Substituting (B.15) and (B.16) into (B.14) yields

$$\begin{aligned}\dot{V}_{4i} \leq{}& \left(\frac{2^{1-p_2}}{k_3} + 1\right)\frac{3}{1+p_2}\xi_i^{1+p_2} + \frac{p_2}{1+p_2}\sum_{j=1}^{3}e_{\epsilon_j}^{1+p_2} \\ &+ \frac{2^{1-p_2}p_2}{k_3(1+p_2)}\sum_{j=1}^{3}\xi_j^{1+p_2} \\ &+ \frac{1}{(2-p_2)2^{-p_2}k_3^{1+1/p_2}}\xi_i^{2-p_2}u_{2i}, \qquad i = 1, 2, 3.\end{aligned} \tag{B.17}$$

Subsequently, it follows from (B.5), (B.9), and (B.17) that

$$\begin{aligned}\dot{V}_{ro} ={}& \dot{V}_3 + \sum_{i=1}^{3}\dot{V}_{4i} \\ \leq{}& -\left(k_3 - \frac{2^{1-p_2}}{1+p_2} - \frac{3p_2}{1+p_2}\right)\sum_{i=1}^{3}e_{\epsilon_i}^{1+p_2} \\ &+ \left[2^{1-p_2}\left(\frac{p_2}{1+p_2} + \frac{3}{k_2}\right) + \frac{3}{1+p_2}\right]\xi_i^{1+p_2} \\ &+ \frac{1}{(2-p_2)2^{-p_2}k_3^{1+1/p_2}}\sum_{i=1}^{3}\xi_i^{2-p_2}u_{2i}.\end{aligned} \tag{B.18}$$

Controller u_{2i} is designed as

$$u_{2i} = k_4\xi_i^{2p_2-1}, \qquad i = 1, 2, 3 \tag{B.19}$$

where

$$\begin{aligned}&k_3 \geq 2^{1-p_2}/(1+p_2) + 3p_2/(1+p_2) + c_2 \\ &k_4 \geq k_3^{1+1/p_2}(2-p_2)2^{-p_2}[2^{1-p_2}(p_2/(1+p_2) + 3/k_3) \\ &\qquad + 3/(1+p_2) + c_2], \qquad c_2 > 0.\end{aligned}$$

Substituting controller (B.19) into (B.18) yields

$$\dot{V}_{ro} \leq -c_2\sum_{i=1}^{3}e_{\epsilon_i}^{1+p_2} - c_2\sum_{i=1}^{3}\xi_i^{1+p_2}. \tag{B.20}$$

On the other hand, from (B.5) and (B.6), it can be obtained that

$$V_{ro}(\boldsymbol{e_q}, \boldsymbol{e_\omega}) \leq 2(1 - \mathrm{sgn}(e_\eta(0))e_\eta) + \frac{1}{(2-p_2)2^{-p_2}k_3^{1+1/p_2}}\sum_{i=1}^{3}|e_{\omega_i} - e_{\omega_i}^*||\xi_i|^{2-p_2}. \tag{B.21}$$

By Lemma 2, it can be verified that

$$|e_{\omega_i} - e_{\omega_i}^*||\xi_i|^{2-p_2} \leq 2^{1-p_2}|\xi_i|^{p_2}|\xi_i|^{2-p_2} = 2^{1-p_2}|\xi_i|^2.$$

Then, it follows from (B.21) that

$$\begin{aligned}V_{ro}(\boldsymbol{e_q}, \boldsymbol{e_\omega}) \leq{}& 2(1 - \mathrm{sgn}(e_\eta(0))e_\eta) + \frac{2}{(2-p_2)k_3^{1+1/p_2}}\sum_{i=1}^{3}|\xi_i|^2 \\ \leq{}& \bar{\lambda}(1 - \mathrm{sgn}(e_\eta(0))e_\eta) + \bar{\lambda}\sum_{i=1}^{3}|\xi_i|^2\end{aligned} \tag{B.22}$$

where

$$\bar{\lambda} = \max\left\{2, 2/\left[(2-p_2)k_3^{1+1/p_2}\right]\right\}.$$

Let

$$\bar{c} = \frac{c_2}{2\bar{\lambda}^{(1+p_2)/2}}.$$

Then, from (B.20) and (B.22), and Lemma 2, it can be obtained that

$$\begin{aligned}
&\dot{V}_{ro} + \bar{c}V_{ro}^{(1+p_2)/2}\\
&\quad\le -\frac{c_2}{2}\sum_{i=1}^{3}\xi_i^{1+p_2} - c_2\sum_{i=1}^{3}e_{\epsilon_i}^{1+p_2}\\
&\qquad + \frac{c_2}{2}(1-\mathrm{sgn}(e_\eta(0))e_\eta)^{(1+p_2)/2}\\
&\quad\le -\frac{c_2}{2}\sum_{i=1}^{3}\xi_i^{1+p_2} - c_2(1-e_\eta^2)^{(1+p_2)/2}\\
&\qquad + \frac{c_2}{2}(1-\mathrm{sgn}(e_\eta(0))e_\eta)^{(1+p_2)/2}\\
&\quad= -\frac{c_2}{2}\sum_{i=1}^{3}\xi_i^{1+p_2} - c_2(1-\mathrm{sgn}(e_\eta(0))e_\eta)^{(1+p_2)/2}\\
&\qquad\times[(1+\mathrm{sgn}(e_\eta(0))e_\eta)^{(1+p_2)/2} - 1/2] \qquad \text{(B.23)}
\end{aligned}$$

where $0 < (1+p_2)/2 < 1$. For the case of $e_\eta(0) \ge 0$, from (B.5) and (B.20), it can be concluded that the states will be stabilized to the region

$$R_{e_\eta \ge 0} = \{[\boldsymbol{e}_{\boldsymbol{q}}^T, \boldsymbol{e}_{\boldsymbol{\omega}}^T]^T | e_\eta \ge 0\}$$

in a finite time t^* and satisfy

$$[\boldsymbol{e}_{\boldsymbol{q}}^T, \boldsymbol{e}_{\boldsymbol{\omega}}^T]^T \in R_{e_\eta \ge 0} \qquad \forall t \in [t^*, \infty).$$

Thus, it holds that

$$(1+e_\eta)^{(1+p_2)/2} - 1/2 > 0 \qquad \forall t \in [t^*, \infty)$$

which, together with (B.23), implies that

$$\dot{V}_{ro} + \bar{c}V_{ro}^{(1+p_2)/2} \le 0 \qquad \forall t \in [t^*, \infty). \qquad \text{(B.24)}$$

For the case of $e_\eta(0) < 0$, the proof is similar, thus being omitted here. Based on the above proof, from Lemma 1, it can be obtained that system (41) under controller $\boldsymbol{u}_2$ (B.19) is globally finite-time stable with respect to the equilibrium set Q_2. Actually, from (40) and (B.19), the controller $\boldsymbol{\tau}_2$ can be written as (39). Due to equivalence between systems (30) and (41), it can also be concluded that system (30) under controller $\boldsymbol{\tau}_2$ (39) is globally finite-time stable with respect to the equilibrium set Q_2. This completes the proof.

Appendix C
Proof of Theorem 3

Step 1 [Global Asymptotical Stability of System (45)]: Choose the following Lyapunov function:

$$V_{ob}(\tilde{\boldsymbol{z}}) = \frac{l_2}{1+\alpha_2}\sum_{i=1}^{3}|\tilde{z}_{1i}|^{1+\alpha_2} + \frac{1}{2}\tilde{\boldsymbol{z}}_2^T\tilde{\boldsymbol{z}}_2 \qquad \text{(C.1)}$$

where $\tilde{\boldsymbol{z}} = [\tilde{\boldsymbol{z}}_1^T, \tilde{\boldsymbol{z}}_2^T]^T$. Clearly, V_{ob} is positive definite with respect to $[\tilde{\boldsymbol{z}}_1^T, \tilde{\boldsymbol{z}}_2^T]^T$. Note that $\tilde{\boldsymbol{z}}_2 = \boldsymbol{R}(\boldsymbol{q})\boldsymbol{M}_1\tilde{\boldsymbol{v}}$. Then, the derivative of V_{ob} along system (45) is

$$\begin{aligned}
&\dot{V}_{ob}\\
&= l_2\sum_{i=1}^{3}\mathrm{sig}^{\alpha_2}(\tilde{z}_{1i})\dot{\tilde{z}}_{1i} + \tilde{\boldsymbol{z}}_2^T\dot{\tilde{\boldsymbol{z}}}_2\\
&= l_2\sum_{i=1}^{3}\mathrm{sig}^{\alpha_2}(\tilde{z}_{1i})\left([\boldsymbol{R}(\boldsymbol{q})\boldsymbol{M}_1^{-1}\boldsymbol{R}^T(\boldsymbol{q})\tilde{\boldsymbol{z}}_2]_i - l_1\mathrm{sig}^{\alpha_1}(\tilde{z}_{1i})\right)\\
&\quad - \tilde{\boldsymbol{z}}_2^T\boldsymbol{R}(\boldsymbol{q})[\boldsymbol{D}_1(\boldsymbol{v})\boldsymbol{v} - \boldsymbol{D}_1(\hat{\boldsymbol{v}})\hat{\boldsymbol{v}}]\\
&\quad - l_2\tilde{\boldsymbol{z}}_2^T\boldsymbol{R}(\boldsymbol{q})\boldsymbol{M}_1^{-1}\boldsymbol{R}^T(\boldsymbol{q})[\mathrm{sig}^{\alpha_2}(\tilde{z}_{11}), \mathrm{sig}^{\alpha_2}(\tilde{z}_{12}), \mathrm{sig}^{\alpha_2}(\tilde{z}_{13})]^T.
\end{aligned} \qquad \text{(C.2)}$$

In addition, it can be verified that

$$\begin{aligned}
&l_2\sum_{i=1}^{3}\mathrm{sig}^{\alpha_2}(\tilde{z}_{1i})[\boldsymbol{R}(\boldsymbol{q})\boldsymbol{M}_1^{-1}\boldsymbol{R}^T(\boldsymbol{q})\tilde{\boldsymbol{z}}_2]_i\\
&\quad= l_2\tilde{\boldsymbol{z}}_2^T\boldsymbol{R}(\boldsymbol{q})\boldsymbol{M}_1^{-1}\boldsymbol{R}^T(\boldsymbol{q})\\
&\qquad\times[\mathrm{sig}^{\alpha_2}(\tilde{z}_{11}), \mathrm{sig}^{\alpha_2}(\tilde{z}_{12}), \mathrm{sig}^{\alpha_2}(\tilde{z}_{13})]^T. \qquad \text{(C.3)}
\end{aligned}$$

Then, it follows from (C.2) and (C.3) that

$$\begin{aligned}
\dot{V}_{ob} &\le -l_1l_2\sum_{i=1}^{3}|\tilde{z}_{1i}|^{\alpha_1+\alpha_2} - \tilde{\boldsymbol{v}}^T\boldsymbol{M}_1[\boldsymbol{D}_1(\boldsymbol{v})\boldsymbol{v} - \boldsymbol{D}_1(\hat{\boldsymbol{v}})\hat{\boldsymbol{v}}]\\
&\le -l_1l_2\sum_{i=1}^{3}|\tilde{z}_{1i}|^{\alpha_1+\alpha_2} - \tilde{\boldsymbol{v}}^T\boldsymbol{M}_1\boldsymbol{D}_1\tilde{\boldsymbol{v}}\\
&\quad - \sum_{i=1}^{3}m_{ii}d_{Q_i}(v_i - \hat{v}_i)(|v_i|v_i - |\hat{v}_i|\hat{v}_i)\\
&\le 0
\end{aligned} \qquad \text{(C.4)}$$

where $\boldsymbol{D}_1 = \mathbf{diag}\{d_{v_1}, d_{v_2}, d_{v_3}\}$ and $d_{v_i}, d_{Q_i}, i = 1, 2, 3$ are defined below (18). Here, the nondecreasing property of function $g(x) = |x|x, x \in \mathbb{R}$ has been utilized.

Note that $\dot{V}_{ob} \equiv 0$ implies $\tilde{\boldsymbol{z}}_1 \equiv 0$, which, in turn, implies $\tilde{\boldsymbol{z}}_2 \equiv 0$ from system (45). By Lasalle's invariance principle, system (45) is globally asymptotically stable with respect to the equilibrium $[\tilde{\boldsymbol{z}}_1^T, \tilde{\boldsymbol{z}}_2^T]^T = \boldsymbol{0}_{6\times 1}$.

Step 2 [Local Finite-Time Stability of System (45)]: Consider the following system:

$$\begin{cases}\dot{\tilde{\boldsymbol{z}}}_1 = \boldsymbol{R}(\boldsymbol{q})\boldsymbol{M}_1^{-1}\boldsymbol{R}^T(\boldsymbol{q})\tilde{\boldsymbol{z}}_2 - \boldsymbol{f}_1(\tilde{\boldsymbol{z}}_1)\\ \dot{\tilde{\boldsymbol{z}}}_2 = -\boldsymbol{f}_2(\tilde{\boldsymbol{z}}_1).\end{cases} \qquad \text{(C.5)}$$

According to Definition 4, system (C.5) is homogeneous of degree $k = \alpha_1 - 1 < 0$ with respect to the dilation $[r_1, r_1, r_1, r_2, r_2, r_2] = [1, 1, 1, \alpha_1, \alpha_1, \alpha_1]$. By a proof similar to that of Step 1, it can be verified that system (C.5) is also globally asymptotically stable.

Let

$$\begin{aligned}
\hat{\boldsymbol{f}}(\tilde{\boldsymbol{z}}_2) = -\boldsymbol{R}(\boldsymbol{q})[&\boldsymbol{D}_1(\boldsymbol{R}^T(\boldsymbol{q})\boldsymbol{M}_1^{-1}\boldsymbol{z}_2)\boldsymbol{R}^T(\boldsymbol{q})\boldsymbol{M}_1^{-1}\boldsymbol{z}_2\\
&-\boldsymbol{D}_1(\boldsymbol{R}^T(\boldsymbol{q})\boldsymbol{M}_1^{-1}\hat{\boldsymbol{z}}_2)\boldsymbol{R}^T(\boldsymbol{q})\boldsymbol{M}_1^{-1}\hat{\boldsymbol{z}}_2].
\end{aligned}$$

Then

$$\hat{\boldsymbol{f}}(\tilde{\boldsymbol{z}}_2) = -\boldsymbol{R}(\boldsymbol{q})\boldsymbol{D}_1\boldsymbol{R}^T(\boldsymbol{q})\boldsymbol{M}_1^{-1}\tilde{\boldsymbol{z}}_2 - \boldsymbol{R}(\boldsymbol{q})\boldsymbol{\delta}(\tilde{\boldsymbol{z}}_2) \qquad \text{(C.6)}$$

where

$$\begin{aligned}
\boldsymbol{\delta}(\tilde{\boldsymbol{z}}_2) = [&d_{Q_1}(|v_1|v_1 - |\hat{v}_1|\hat{v}_1), d_{Q_2}(|v_2|v_2 - |\hat{v}_2|\hat{v}_2),\\
&d_{Q_3}(|v_3|v_3 - |\hat{v}_3|\hat{v}_3)]^T.
\end{aligned} \qquad \text{(C.7)}$$

It can be verified that $\hat{\boldsymbol{f}}(\mathbf{0}_{3\times1}) = \mathbf{0}_{3\times1}$, since $\tilde{\boldsymbol{z}}_2 = \mathbf{0}_{3\times1}$ implies $\boldsymbol{z}_2 = \hat{\boldsymbol{z}}_2$ and then $\boldsymbol{v} = \hat{\boldsymbol{v}}$. For $|v_i|v_i - |\hat{v}_i|\hat{v}_i$, it holds that

$$\begin{aligned}|(|v_i|v_i - |\hat{v}_i|\hat{v}_i)| &= ||v_i|\tilde{v}_i + (|v_i| - |\hat{v}_i|)\hat{v}_i| \\ &\le |v_i||\tilde{v}_i| + |v_i - \hat{v}_i||\hat{v}_i| \le L_i|\tilde{v}_i|, \\ &\qquad i = 1,2,3 \quad \text{(C.8)}\end{aligned}$$

where $L_i > 0, i = 1,2,3$. Due to the assumption on boundedness of $\boldsymbol{z}_2$ and $\hat{\boldsymbol{z}}_2$, and the relationships $\boldsymbol{v} = \boldsymbol{M}_1^{-1}\boldsymbol{R}^T(\boldsymbol{q})\boldsymbol{z}_2$ and $\hat{\boldsymbol{v}} = \boldsymbol{M}_1^{-1}\boldsymbol{R}^T(\boldsymbol{q})\hat{\boldsymbol{z}}_2$, the existence of $L_i, i = 1,2,3$ is guaranteed. Note that

$$\hat{\boldsymbol{f}}(\varepsilon^{r_2}\tilde{\boldsymbol{z}}_2) = -\varepsilon^{r_2}\boldsymbol{R}(\boldsymbol{q})\boldsymbol{D}_1\boldsymbol{R}^T(\boldsymbol{q})\boldsymbol{M}_1^{-1}\tilde{\boldsymbol{z}}_2 - \boldsymbol{R}(\boldsymbol{q})\boldsymbol{\delta}(\varepsilon^{r_2}\tilde{\boldsymbol{z}}_2).$$

Then

$$\begin{aligned}\lim_{\varepsilon\to0}\frac{\hat{\boldsymbol{f}}(\varepsilon^{r_2}\tilde{\boldsymbol{z}}_2)}{\varepsilon^{r_2+k}} &= -\boldsymbol{R}(\boldsymbol{q})\boldsymbol{D}_1\boldsymbol{R}^T(\boldsymbol{q})\boldsymbol{M}_1^{-1}\tilde{\boldsymbol{z}}_2\lim_{\varepsilon\to0}\varepsilon^{-k} \\ &\quad - \lim_{\varepsilon\to0}\frac{\boldsymbol{R}(\boldsymbol{q})\boldsymbol{\delta}(\varepsilon^{r_2}\tilde{\boldsymbol{z}}_2)}{\varepsilon^{r_2+k}} \\ &= -\lim_{\varepsilon\to0}\frac{\boldsymbol{R}(\boldsymbol{q})\boldsymbol{\delta}(\varepsilon^{r_2}\tilde{\boldsymbol{z}}_2)}{\varepsilon^{r_2+k}}. \qquad \text{(C.9)}\end{aligned}$$

In addition, it follows from (C.7) and (C.8) that

$$\begin{aligned}&\lim_{\varepsilon\to0}\frac{|[\boldsymbol{R}(\boldsymbol{q})\boldsymbol{\delta}(\varepsilon^{r_2}\tilde{\boldsymbol{z}}_2)]_i|}{\varepsilon^{r_2+k}} \\ &\le \lim_{\varepsilon\to0}\frac{\|\boldsymbol{R}(\boldsymbol{q})\boldsymbol{\delta}(\varepsilon^{r_2}\tilde{\boldsymbol{z}}_2)\|}{\varepsilon^{r_2+k}} \le \lim_{\varepsilon\to0}\frac{\|\boldsymbol{\delta}(\varepsilon^{r_2}\tilde{\boldsymbol{z}}_2)\|}{\varepsilon^{r_2+k}} \\ &\le \lim_{\varepsilon\to0}\frac{L\|\varepsilon^{r_2}\tilde{\boldsymbol{z}}_2\|}{\varepsilon^{r_2+k}} \le L\|\tilde{\boldsymbol{z}}_2\|\lim_{\varepsilon\to0}\varepsilon^{-k} = 0, \qquad i = 1,2,3 \\ &\qquad \text{(C.10)}\end{aligned}$$

where

$$L = \sqrt{3}\max_{1\le i\le3}(d_{Q_i}L_i)\|\boldsymbol{M}_1^{-1}\| > 0.$$

Actually, L results from the following computation:

$$\begin{aligned}\|\boldsymbol{\delta}(\tilde{\boldsymbol{z}}_2)\| &\le \sum_{i=1}^{3}d_{Q_i}L_i|\tilde{v}_i| = \max_{1\le i\le3}(d_{Q_i}L_i)\sum_{i=1}^{3}|\tilde{v}_i| \\ &\le \sqrt{3}\max_{1\le i\le3}(d_{Q_i}L_i)\|\tilde{\boldsymbol{v}}\| \\ &= \sqrt{3}\max_{1\le i\le3}(d_{Q_i}L_i)\|\boldsymbol{M}_1^{-1}\boldsymbol{R}^T(\boldsymbol{q})\tilde{\boldsymbol{z}}_2\| \\ &\le \sqrt{3}\max_{1\le i\le3}(d_{Q_i}L_i)\|\boldsymbol{M}_1^{-1}\|\|\tilde{\boldsymbol{z}}_2\| = L\|\tilde{\boldsymbol{z}}_2\| \quad \text{(C.11)}\end{aligned}$$

where

$$\|\boldsymbol{R}(\boldsymbol{q})\| = \|\boldsymbol{R}^T(\boldsymbol{q})\| = \sqrt{\lambda_{\max}(\boldsymbol{R}^T(\boldsymbol{q})\boldsymbol{R}(\boldsymbol{q}))} = 1$$

has been utilized.

Then, it follows from (C.9) and (C.10) that

$$\lim_{\varepsilon\to0}\frac{\hat{\boldsymbol{f}}(\varepsilon^{r_2}\tilde{\boldsymbol{z}}_2)}{\varepsilon^{r_2+k}} = -\lim_{\varepsilon\to0}\frac{\boldsymbol{R}(\boldsymbol{q})\boldsymbol{\delta}(\varepsilon^{r_2}\tilde{\boldsymbol{z}}_2)}{\varepsilon^{r_2+k}} = \mathbf{0}_{3\times1}. \qquad \text{(C.12)}$$

Therefore, from Lemma 4, it can be concluded that system (45) is locally finite-time stable with respect to the equilibrium $[\tilde{\boldsymbol{z}}_1^T, \tilde{\boldsymbol{z}}_2^T]^T = \mathbf{0}_{6\times1}$.

From the proof of the above two steps, system (45) is both globally asymptotically stable and locally finite-time stable. Thus, system (45) is globally finite-time stable, namely, observer (42) is globally finite-time convergent. This completes the proof.

Appendix D
Proof of Theorem 4

Step 1 [Boundedness of $\boldsymbol{e_r}(t), \boldsymbol{e_v}(t), \forall t \in [0,\infty)$ and Global Finite-Time Convergence of Observer (42)]: Denote the following tracking errors based on the estimated states from observer (42):

$$\begin{aligned}\hat{\boldsymbol{e}}_{\boldsymbol{r}} &= [\hat{e}_{r_1}, \hat{e}_{r_2}, \hat{e}_{r_3}]^T = \hat{\boldsymbol{r}} - \boldsymbol{r}_d \\ \hat{\boldsymbol{e}}_{\boldsymbol{v}} &= [\hat{e}_{v_1}, \hat{e}_{v_2}, \hat{e}_{v_3}]^T = \hat{\boldsymbol{v}} - \boldsymbol{v}_d \\ \hat{\boldsymbol{e}}_{\boldsymbol{z}_1} &= [\hat{e}_{z_{11}}, \hat{e}_{z_{12}}, \hat{e}_{z_{13}}]^T = \hat{\boldsymbol{z}}_1 - \boldsymbol{z}_{1d} \\ \hat{\boldsymbol{e}}_{\boldsymbol{z}_2} &= [\hat{e}_{z_{21}}, \hat{e}_{z_{22}}, \hat{e}_{z_{23}}]^T = \hat{\boldsymbol{z}}_2 - \boldsymbol{z}_{2d}.\end{aligned}$$

Make the following invertible coordinate transformation:

$$\begin{aligned}\hat{\boldsymbol{\beta}}_1 &= [\hat{\beta}_{11}, \hat{\beta}_{12}, \hat{\beta}_{13}]^T = \hat{\boldsymbol{e}}_{\boldsymbol{z}_1} \\ \hat{\boldsymbol{\beta}}_2 &= [\hat{\beta}_{21}, \hat{\beta}_{22}, \hat{\beta}_{23}]^T = \boldsymbol{R}(\boldsymbol{q})\boldsymbol{M}_1^{-1}\boldsymbol{R}^T(\boldsymbol{q})\hat{\boldsymbol{e}}_{\boldsymbol{z}_2}. \qquad \text{(D.1)}\end{aligned}$$

Note that $\dot{\boldsymbol{z}}_{1d} = \boldsymbol{R}(\boldsymbol{q})\boldsymbol{M}_1^{-1}\boldsymbol{R}^T(\boldsymbol{q})\boldsymbol{z}_{2d}$. Then, it follows from (42) that

$$\begin{cases}\dot{\hat{\boldsymbol{\beta}}}_1 = \hat{\boldsymbol{\beta}}_2 + \boldsymbol{f}_1(\tilde{\boldsymbol{z}}_1) \\ \dot{\hat{\boldsymbol{\beta}}}_2 = \boldsymbol{u}_2 + \boldsymbol{R}(\boldsymbol{q})\boldsymbol{M}_1^{-1}\boldsymbol{R}^T(\boldsymbol{q})\boldsymbol{f}_2(\tilde{\boldsymbol{z}}_1)\end{cases} \qquad \text{(D.2)}$$

where

$$\begin{aligned}\boldsymbol{u}_2 &= [u_{21}, u_{22}, u_{23}]^T \\ &= \boldsymbol{R}(\boldsymbol{q})\left[\boldsymbol{S}(\boldsymbol{\omega})\boldsymbol{M}_1^{-1}\boldsymbol{R}^T(\boldsymbol{q}) - \boldsymbol{M}_1^{-1}\boldsymbol{S}(\boldsymbol{\omega})\boldsymbol{R}^T(\boldsymbol{q})\right]\hat{\boldsymbol{e}}_{\boldsymbol{z}_2} \\ &\quad + \boldsymbol{R}(\boldsymbol{q})\boldsymbol{M}_1^{-1}\left[\boldsymbol{\tau}_1 - \boldsymbol{D}_1(\boldsymbol{M}_1^{-1}\boldsymbol{R}^T(\boldsymbol{q})\hat{\boldsymbol{z}}_2)\right. \\ &\qquad \left.\times\ \boldsymbol{M}_1^{-1}\boldsymbol{R}^T(\boldsymbol{q})\hat{\boldsymbol{z}}_2 - \boldsymbol{g}_1(\boldsymbol{q})\right] \\ &\quad - \boldsymbol{R}(\boldsymbol{q})\boldsymbol{M}_1^{-1}\boldsymbol{R}^T(\boldsymbol{q})\dot{\boldsymbol{z}}_{2d}. \qquad \text{(D.3)}\end{aligned}$$

Choose the following Lyapunov function:

$$\begin{aligned}V_{tr}(\hat{\boldsymbol{\beta}}_1, \hat{\boldsymbol{\beta}}_2) &= \frac{1}{2}\hat{\boldsymbol{\beta}}_1^T\hat{\boldsymbol{\beta}}_1 \\ &+ \frac{1}{(2-p_1)2^{-p_1}k_1^{1+1/p_1}}\sum_{i=1}^{3}\int_{\hat{\beta}_{2i}^*}^{\hat{\beta}_{2i}}(s^{1/p_1} - \hat{\beta}_{2i}^{*1/p_1})\,ds \qquad \text{(D.4)}\end{aligned}$$

where $\hat{\beta}_{2i}^* = -k_1\hat{\beta}_{1i}^{p_1}, i = 1,2,3, k_1 > 0, 1/2 < p_1 = p_{11}/p_{12} < 1$, and p_{11} and p_{12} are positive odd integers. Clearly, $V_{tr}(\hat{\boldsymbol{\beta}}_1, \hat{\boldsymbol{\beta}}_2)$ is positive definite with respect to $[\hat{\boldsymbol{\beta}}_1^T, \hat{\boldsymbol{\beta}}_2^T]^T$.

By a proof similar to that of Theorem 1, the derivative of V_{tr} along system (D.2) satisfies

$$\begin{aligned}\dot{V}_{tr} &\le -\left(k_1 - \frac{2^{1-p_1}}{1+p_1} - \frac{2p_1}{1+p_1}\right)\sum_{i=1}^{3}\hat{\beta}_{1i}^{1+p_1} \\ &\quad + \left(\frac{2^{1-p_1}p_1}{1+p_1} + \frac{2}{1+p_1} + \frac{2^{2-p_1}}{k_1}\right)\sum_{i=1}^{3}\hat{\varphi}_i^{1+p_1} \\ &\quad + \frac{1}{(2-p_1)2^{-p_1}k_1^{1+1/p_1}}\sum_{i=1}^{3}\hat{\varphi}_i^{2-p_1}u_{2i} \\ &\quad + \frac{1}{(2-p_1)2^{-p_1}k_1^{1+1/p_1}}\left[\hat{\varphi}_1^{2-p_1}, \hat{\varphi}_2^{2-p_1}, \hat{\varphi}_3^{2-p_1}\right] \\ &\quad \times \boldsymbol{R}(\boldsymbol{q})\boldsymbol{M}_1^{-1}\boldsymbol{R}^T(\boldsymbol{q})\boldsymbol{f}_2(\tilde{\boldsymbol{z}}_1) + \hat{\boldsymbol{\beta}}_1^T\boldsymbol{f}_1(\tilde{\boldsymbol{z}}_1) \qquad \text{(D.5)}\end{aligned}$$

where

$$\hat{\varphi}_i = \hat{\beta}_{2i}^{1/p_1} - \hat{\beta}_{2i}^{*1/p_1}, \qquad i = 1,2,3.$$

Consider the term $\hat{\boldsymbol{\beta}}_1^T \boldsymbol{f}_1(\tilde{z}_1)$ in (D.5). By noting that $\alpha_1 \geq p_1$ and the definition of $\boldsymbol{f}_1(\cdot)$ in (43), it can be obtained that

$$\hat{\boldsymbol{\beta}}_1^T \boldsymbol{f}_1(\tilde{z}_1) = l_1 \sum_{i=1}^{3} \hat{\beta}_{1i} \mathrm{sig}^{p_1}(\tilde{z}_{1i}) |\tilde{z}_{1i}|^{\alpha_1 - p_1}. \quad \text{(D.6)}$$

By Lemma 3

$$\hat{\beta}_{1i} \mathrm{sig}^{p_1}(\tilde{z}_{1i}) \leq \frac{1}{1+p_1} \hat{\beta}_{1i}^{1+p_1} + \frac{p_1}{1+p_1} \tilde{z}_{1i}^{1+p_1}$$

holds. Then, it follows from (D.6) that

$$\hat{\boldsymbol{\beta}}_1^T \boldsymbol{f}_1(\tilde{z}_1) \leq \frac{l_1}{1+p_1} \sum_{i=1}^{3} \hat{\beta}_{1i}^{1+p_1} |\tilde{z}_{1i}|^{\alpha_1 - p_1} + \frac{l_1 p_1}{1+p_1} \sum_{i=1}^{3} |\tilde{z}_{1i}|^{1+\alpha_1}. \quad \text{(D.7)}$$

On the other hand, by noting the definition of $\boldsymbol{f}_2(\cdot)$ in (44), it can be obtained that

$$\begin{aligned} &\left[\hat{\varphi}_1^{2-p_1}, \hat{\varphi}_2^{2-p_1}, \hat{\varphi}_3^{2-p_1}\right] \boldsymbol{R}(\boldsymbol{q}) \boldsymbol{M}_1^{-1} \boldsymbol{R}^T(\boldsymbol{q}) \boldsymbol{f}_2(\tilde{z}_1) \\ &\quad \leq l_2 \left\| \boldsymbol{R}(\boldsymbol{q}) \boldsymbol{M}_1^{-2} \boldsymbol{R}^T(\boldsymbol{q}) \right\| \left\| \left[\hat{\varphi}_1^{2-p_1}, \hat{\varphi}_2^{2-p_1}, \hat{\varphi}_3^{2-p_1}\right] \right\| \\ &\quad \times \left\| \left[\mathrm{sig}^{2\alpha_1 - 1}(\tilde{z}_{11}), \mathrm{sig}^{2\alpha_1 - 1}(\tilde{z}_{12}), \mathrm{sig}^{2\alpha_1 - 1}(\tilde{z}_{13})\right]^T \right\|. \end{aligned} \quad \text{(D.8)}$$

From Lemma 2, it can be verified that

$$\left\| \left[\hat{\varphi}_1^{2-p_1}, \hat{\varphi}_2^{2-p_1}, \hat{\varphi}_3^{2-p_1}\right] \right\| \leq \sum_{i=1}^{3} |\hat{\varphi}_i|^{2-p_1} \quad \text{(D.9)}$$

$$\left\| \left[\mathrm{sig}^{2\alpha_1 - 1}(\tilde{z}_{11}), \mathrm{sig}^{2\alpha_1 - 1}(\tilde{z}_{12}), \mathrm{sig}^{2\alpha_1 - 1}(\tilde{z}_{13})\right]^T \right\| \leq \sum_{i=1}^{3} |\tilde{z}_{1i}|^{2\alpha_1 - 1}. \quad \text{(D.10)}$$

By Lemma 3, it can be obtained that

$$|\hat{\varphi}_i|^{2-p_1} |\tilde{z}_{1j}|^{2p_1 - 1} \leq \frac{2-p_1}{1+p_1} \hat{\varphi}_i^{1+p_1} + \frac{2p_1 - 1}{1+p_1} \tilde{z}_{1j}^{1+p_1}, \quad i, j = 1, 2, 3. \quad \text{(D.11)}$$

Then, it follows from (D.9), (D.10), and (D.11) that

$$\begin{aligned} &\left\| \left[\hat{\varphi}_1^{2-p_1}, \hat{\varphi}_2^{2-p_1}, \hat{\varphi}_3^{2-p_1}\right] \right\| \\ &\quad \times \left\| \left[\mathrm{sig}^{2\alpha_1 - 1}(\tilde{z}_{11}), \mathrm{sig}^{2\alpha_1 - 1}(\tilde{z}_{12}), \mathrm{sig}^{2\alpha_1 - 1}(\tilde{z}_{13})\right]^T \right\| \\ &\quad \leq \frac{3(2-p_1)}{1+p_1} \sum_{i=1}^{3} \hat{\varphi}_i^{1+p_1} |\tilde{z}_{1i}|^{2(\alpha_1 - p_1)} \\ &\quad + \frac{3(2p_1 - 1)}{1+p_1} \sum_{i=1}^{3} |\tilde{z}_{1i}|^{1+2\alpha_1 - p_1}. \end{aligned} \quad \text{(D.12)}$$

Note that

$$\|\boldsymbol{R}(\boldsymbol{q})\| = 1 \quad \text{and} \quad \|\boldsymbol{M}_1^{-2}\| = \sqrt{\lambda_{\max}(\mathbf{M}_1^{-4})} = b_1$$

where $b_1 = \max\left\{m_{11}^{-2}, m_{22}^{-2}, m_{33}^{-2}\right\}$. Then, it holds that

$$\left\| \boldsymbol{R}(\boldsymbol{q}) \boldsymbol{M}_1^{-2} \boldsymbol{R}^T(\boldsymbol{q}) \right\| \leq \|\boldsymbol{R}(\boldsymbol{q})\| \left\| \boldsymbol{M}_1^{-2} \right\| \left\| \boldsymbol{R}^T(\boldsymbol{q}) \right\| = b_1. \quad \text{(D.13)}$$

Substituting (D.12) and (D.13) into (D.8) yields

$$\begin{aligned} &\left[\hat{\varphi}_1^{2-p_1}, \hat{\varphi}_2^{2-p_1}, \hat{\varphi}_3^{2-p_1}\right] \boldsymbol{R}(\boldsymbol{q}) \boldsymbol{M}_1^{-1} \boldsymbol{R}^T(\boldsymbol{q}) \boldsymbol{f}_2(\tilde{z}_1) \\ &\quad \leq \frac{3b_1 l_2 (2-p_1)}{1+p_1} \sum_{i=1}^{3} \hat{\varphi}_i^{1+p_1} |\tilde{z}_{1i}|^{2(\alpha_1 - p_1)} \\ &\quad + \frac{3b_1 l_2 (2p_1 - 1)}{1+p_1} \sum_{i=1}^{3} |\tilde{z}_{1i}|^{1+2\alpha_1 - p_1}. \end{aligned} \quad \text{(D.14)}$$

Similar to Step 1 in the proof of Theorem 3, it can be verified that observer (42) is globally asymptotically stable and $\dot{V}_{ob}(\tilde{\boldsymbol{z}}(t)) \leq 0, \forall t \in [0, \infty)$ with $V_{ob}(\tilde{\boldsymbol{z}})$ defined as (C.1). Then

$$\begin{aligned} V_{ob}(\tilde{\boldsymbol{z}}(t)) \leq V_{ob}(\tilde{\boldsymbol{z}}(0)) = \frac{l_2}{2\alpha_1} \sum_{i=1}^{3} |\tilde{z}_{1i}(0)|^{2\alpha_1} \\ + \frac{1}{2} \tilde{\boldsymbol{z}}_2^T(0) \tilde{\boldsymbol{z}}_2(0) \qquad \forall t \in [0, \infty). \end{aligned} \quad \text{(D.15)}$$

Thus, the following estimate for bound of $\tilde{z}_{1i}$ holds:

$$|\tilde{z}_{1i}(t)| \leq \phi_1 \qquad \forall t \in [0, +\infty), \qquad i = 1, 2, 3 \quad \text{(D.16)}$$

where

$$\phi_1 = \left(\sum_{i=1}^{3} |\tilde{z}_{1i}(0)|^{2\alpha_1} + (\alpha_1)/(l_2) \tilde{\boldsymbol{z}}_2^T(0) \tilde{\boldsymbol{z}}_2(0) \right)^{1/(2\alpha_1)}.$$

Then, substituting (D.7), (D.14), and (D.16) into (D.5) yields

$$\begin{aligned} \dot{V}_{tr} \leq &- \left(k_1 - \frac{2^{1-p_1}}{1+p_1} - \frac{2p_1 + l_1 \phi_1^{\alpha_1 - p_1}}{1+p_1} \right) \\ &\times \sum_{i=1}^{3} \hat{\beta}_{1i}^{1+p_1} + h_1 \sum_{i=1}^{3} \hat{\varphi}_i^{1+p_1} \\ &+ \frac{1}{(2-p_1) 2^{-p_1} k_1^{1+1/p_1}} \sum_{i=1}^{3} \hat{\varphi}_i^{2-p_1} u_{2i} \\ &+ h_2 \sum_{i=1}^{3} |\tilde{z}_{1i}|^{1+\alpha_1} + h_3 \sum_{i=1}^{3} |\tilde{z}_{1i}|^{1+2\alpha_1 - p_1} \end{aligned} \quad \text{(D.17)}$$

where

$$\begin{aligned} h_1 &= \frac{2^{1-p_1} p_1 + 2}{1+p_1} + \frac{2^{2-p_1}}{k_1} + \frac{3b_1 l_2 \phi_1^{2(\alpha_1 - p_1)}}{(1+p_1) 2^{-p_1} k_1^{1+1/p_1}} \\ h_2 &= \frac{l_1 \alpha_1}{1+\alpha_1} \\ h_3 &= \frac{3b_1 l_2 (2p_1 - 1)}{(1+p_1)(2-p_1) 2^{-p_1} k_1^{1+1/p_1}}. \end{aligned}$$

Controller u_{2i} is designed as

$$u_{2i} = -k_2 \hat{\varphi}_i^{2p_1 - 1}, \qquad i = 1, 2, 3 \quad \text{(D.18)}$$

where

$$\begin{aligned} k_2 &\geq (2-p_1) 2^{-p_1} k_1^{1+1/p_1} (h_1 + c_1) \\ k_1 &\geq \frac{2^{1-p_1}}{1+p_1} + \frac{2p_1 + l_1 \phi_1^{\alpha_1 - p_1}}{1+p_1} + c_1, \\ &c_1 > 0, \qquad l_1 > 0, \qquad l_2 > 0. \end{aligned}$$

Substituting (D.16) and controller (D.18) into (D.17) yields

$$\dot{V}_{tr} \le -c_1 \sum_{i=1}^{3} \left(\hat{\beta}_{1i}^{1+p_1} + \hat{\varphi}_i^{1+p_1}\right) + 3h_2\phi_1^{1+\alpha_1} + 3h_3\phi_1^{1+2\alpha_1-p_1}. \quad \text{(D.19)}$$

Denote

$$\phi_2 = \left((3h_2\phi_1^{1+\alpha_1} + 3h_3\phi_1^{1+2\alpha_1-p_1})/(c_1\gamma)\right)^{1/(1+p_1)}, \quad 0 < \gamma < 1$$

$$\Omega_1 = \left\{ \left[\hat{\boldsymbol{\beta}}_1^T, \hat{\boldsymbol{\beta}}_2^T\right]^T \Big| \left\| \left[\hat{\boldsymbol{\beta}}_1^T, \hat{\boldsymbol{\varphi}}^T\right]^T \right\| \le \phi_2 \right\}$$

where $\hat{\boldsymbol{\varphi}} = [\hat{\varphi}_1, \hat{\varphi}_2, \hat{\varphi}_3]^T$. If

$$\left[\hat{\boldsymbol{\beta}}_1^T, \hat{\boldsymbol{\beta}}_2^T\right]^T \bar{\in} \Omega_1$$

it can be obtained from Lemma 2 that $(0 < (1+p_1)/2 < 1)$

$$3h_2\phi_1^{1+\alpha_1} + 3h_3\phi_1^{1+2\alpha_1-p_1} \le c_1\gamma \left[\sum_{i=1}^{3} (\hat{\beta}_{1i}^2 + \hat{\varphi}_i^2)\right]^{(1+p_1)/2} \le c_1\gamma \sum_{i=1}^{3} (\hat{\beta}_{1i}^{1+p_1} + \hat{\varphi}_i^{1+p_1}). \quad \text{(D.20)}$$

In this case, it follows from (D.19) and (D.20) that

$$\dot{V}_{tr} \le -(1-\gamma)c_1 \sum_{i=1}^{3} (\hat{\beta}_{1i}^{1+p_1} + \hat{\varphi}_i^{1+p_1}) < 0. \quad \text{(D.21)}$$

Therefore, $[\hat{\boldsymbol{\beta}}_1^T(t), \hat{\boldsymbol{\beta}}_2^T(t)]^T$ will converge to region Ω_1 in finite time. Based on the fact that

$$\hat{\varphi}_i = \hat{\beta}_{2i}^{1/p_1} + k_1^{1/p_1}\hat{\beta}_{1i}, \qquad i = 1, 2, 3$$

and the above proof, it can be concluded that $\hat{\boldsymbol{\beta}}_1(t)$ and $\hat{\boldsymbol{\beta}}_2(t)$ are bounded under controller (D.18), $\forall t \in [0, \infty)$.

Due to the invertible coordinate transformation between $\hat{\boldsymbol{e}}_{\boldsymbol{r}}, \hat{\boldsymbol{e}}_{\boldsymbol{v}}$ and $\hat{\boldsymbol{\beta}}_1, \hat{\boldsymbol{\beta}}_2$, it can be obtained that $\hat{\boldsymbol{e}}_{\boldsymbol{r}}$ and $\hat{\boldsymbol{e}}_{\boldsymbol{v}}$ are also bounded. In addition, $\tilde{\boldsymbol{r}}$ and $\tilde{\boldsymbol{v}}$ are bounded, since observer (42) is globally asymptotically convergent. Therefore, $\boldsymbol{e}_{\boldsymbol{r}}$ and $\boldsymbol{e}_{\boldsymbol{v}}$ are bounded. This, together with Assumption 1, i.e., $\boldsymbol{v}_d$ is bounded [see (27)], gives that $\boldsymbol{v}$ and $\hat{\boldsymbol{v}}$ are bounded under controller (D.18).

Since $\boldsymbol{z}_2 = \boldsymbol{R}(\boldsymbol{q})\boldsymbol{M}_1\boldsymbol{v}$ and $\hat{\boldsymbol{z}}_2 = \boldsymbol{R}(\boldsymbol{q})\boldsymbol{M}_1\hat{\boldsymbol{v}}$, $\boldsymbol{z}_2(t)$ and $\hat{\boldsymbol{z}}_2(t)$ are also bounded under controller (D.18), $\forall t \in [0, \infty)$. Then, by Theorem 3, the global finite-time convergence of observer (42) is guaranteed. Thus, there is a finite settling time T_{ob} of observer (42) such that

$$\boldsymbol{r}(t) = \hat{\boldsymbol{r}}(t), \boldsymbol{v}(t) = \hat{\boldsymbol{v}}(t), \forall t \in [T_{ob}, \infty).$$

Step 2 [Boundedness of $\boldsymbol{e}_{\boldsymbol{q}}(t), \boldsymbol{e}_{\boldsymbol{\omega}}(t), \forall t \in [0,\infty)$*]:* Actually, $\boldsymbol{e}_{\boldsymbol{q}}(t)$ is naturally bounded, since it follows from (8) that $\|\boldsymbol{e}_{\boldsymbol{q}}(t)\| \equiv 1, \forall t \in [0, +\infty)$. Therefore, the main task in this step is to prove that $\boldsymbol{e}_{\boldsymbol{\omega}}(t)$ is bounded $\forall t \in [0, \infty)$. For rotational tracking error subsystem (30), $\boldsymbol{\tau}_2$ is designed as

$$\boldsymbol{\tau}_2 = -k_4\boldsymbol{M}_2\left[\xi_1^{2p_2-1}, \xi_2^{2p_2-1}, \xi_3^{2p_2-1}\right]^T + \boldsymbol{C}_1(\hat{\boldsymbol{v}})\hat{\boldsymbol{v}} + \boldsymbol{C}_2(\boldsymbol{\omega})\boldsymbol{\omega} + \boldsymbol{D}_2(\boldsymbol{\omega})\boldsymbol{\omega} + \boldsymbol{g}_2(\boldsymbol{q}) + \boldsymbol{M}_2\dot{\boldsymbol{\omega}}_d \quad \text{(D.22)}$$

where

$$\xi_i = e_{\omega_i}^{1/p_2} + \mathrm{sgn}(e_\eta(0))k_3^{1/p_2}e_{\epsilon_i}, \qquad i = 1, 2, 3$$

and $\hat{\boldsymbol{v}}$ is the estimated value of $\boldsymbol{v}$ from observer (42), and the definitions of control parameters are still the same as those in Theorem 2.

Substituting (D.22) into system (30) yields

$$\begin{cases} \dot{\boldsymbol{e}}_{\boldsymbol{q}} = \dfrac{1}{2}\boldsymbol{U}(\boldsymbol{e}_{\boldsymbol{q}})\boldsymbol{e}_{\boldsymbol{\omega}} \\ \dot{\boldsymbol{e}}_{\boldsymbol{\omega}} = -k_4\left[\xi_1^{2p_2-1}, \xi_2^{2p_2-1}, \xi_3^{2p_2-1}\right]^T \\ \qquad + \boldsymbol{M}_2^{-1}\left[\boldsymbol{C}_1(\hat{\boldsymbol{v}})\hat{\boldsymbol{v}} - \boldsymbol{C}_1(\boldsymbol{v})\boldsymbol{v}\right]. \end{cases} \quad \text{(D.23)}$$

For system (D.23), let

$$\rho(\boldsymbol{e}_{\boldsymbol{q}}, \boldsymbol{e}_{\boldsymbol{\omega}}) = \frac{3}{2}\boldsymbol{e}_{\boldsymbol{q}}^T\boldsymbol{e}_{\boldsymbol{q}} + \frac{1}{2}\boldsymbol{e}_{\boldsymbol{\omega}}^T\boldsymbol{e}_{\boldsymbol{\omega}} = \frac{3}{2} + \frac{1}{2}\sum_{i=1}^{3} e_{\omega_i}^2. \quad \text{(D.24)}$$

The derivative of $\rho(\boldsymbol{e}_{\boldsymbol{q}}, \boldsymbol{e}_{\boldsymbol{\omega}})$ along system (D.23) is

$$\dot{\rho} = \boldsymbol{e}_{\boldsymbol{\omega}}^T\dot{\boldsymbol{e}}_{\boldsymbol{\omega}} = -k_4\sum_{i=1}^{3} e_{\omega_i}\xi_i^{2p_2-1} + \boldsymbol{e}_{\boldsymbol{\omega}}^T\boldsymbol{M}_2^{-1}[\boldsymbol{C}_1(\hat{\boldsymbol{v}})\hat{\boldsymbol{v}} - \boldsymbol{C}_1(\boldsymbol{v})\boldsymbol{v}]. \quad \text{(D.25)}$$

By noting that $|e_{\epsilon_i}| \le 1, i = 1, 2, 3$ and $0 < 2p_2 - 1 < 1$, from Lemma 2, it holds that

$$\xi_i^{2p_2-1} = \left[e_{\omega_i}^{1/p_2} + \mathrm{sgn}(e_\eta(0))k_3^{1/p_2}e_{\epsilon_i}\right]^{2p_2-1} \le |e_{\omega_i}|^{2-1/p_2} + k_3^{2-1/p_2}, \qquad i = 1, 2, 3. \quad \text{(D.26)}$$

It follows from (D.26) that

$$-k_4\sum_{i=1}^{3} e_{\omega_i}\xi_i^{2p_2-1} \le k_4\sum_{i=1}^{3} |e_{\omega_i}|^{3-1/p_2} + k_4k_3^{2-1/p_2}\sum_{i=1}^{3} |e_{\omega_i}|, \qquad i = 1, 2, 3. \quad \text{(D.27)}$$

On the other hand, for terms $\boldsymbol{e}_{\boldsymbol{\omega}}^T\boldsymbol{M}_2^{-1}[\boldsymbol{C}_1(\hat{\boldsymbol{v}})\hat{\boldsymbol{v}} - \boldsymbol{C}_1(\boldsymbol{v})\boldsymbol{v}]$ in (D.25), it holds that

$$\boldsymbol{e}_{\boldsymbol{\omega}}^T\boldsymbol{M}_2^{-1}[\boldsymbol{C}_1(\hat{\boldsymbol{v}})\hat{\boldsymbol{v}} - \boldsymbol{C}_1(\boldsymbol{v})\boldsymbol{v}] \le b_2\|\boldsymbol{e}_{\boldsymbol{\omega}}\| \quad \text{(D.28)}$$

where

$$b_2 \ge \|\boldsymbol{M}_2^{-1}\|(\|\boldsymbol{C}_1(\hat{\boldsymbol{v}})\|\|\hat{\boldsymbol{v}}\| + \|\boldsymbol{C}_1(\boldsymbol{v})\|\|\boldsymbol{v}\|).$$

Note that $\boldsymbol{C}_1(\boldsymbol{v}) = -\boldsymbol{S}(\boldsymbol{M}_{11}\boldsymbol{v})$. Due to (12) and the boundedness of $\boldsymbol{v}$ and $\hat{\boldsymbol{v}}$, the existence of $b_2 \in (0, +\infty)$ is guaranteed.

From Lemma 2 and (D.24), it can be obtained that

$$\|\boldsymbol{e}_{\boldsymbol{\omega}}\| \le \sum_{i=1}^{3} |e_{\omega_i}| \le \frac{1}{2}\sum_{i=1}^{3} e_{\omega_i}^2 + \frac{3}{2} = \rho. \quad \text{(D.29)}$$

It addition

$$\|\boldsymbol{x}\|_p = \left(\sum_{i=1}^{3} |x_i|^p\right)^{1/p}$$

with $p \geq 1$ represents p-norm $\forall \boldsymbol{x} = [x_1, x_2, x_3]^T \in \mathbb{R}^3$. Due to equivalence between any two different norms in $\mathbb{R}^3$, there exists $\sigma_1 > 0$ such that

$$\sum_{i=1}^{3} |e_{\omega_i}|^{3-1/p_2} \leq \sigma_1 \left(\sum_{i=1}^{3} e_{\omega_i}^2\right)^{(3-1/p_2)/2} \leq 2^{(3-1/p_2)/2} \sigma_1 \rho^{(3-1/p_2)/2}. \quad \text{(D.30)}$$

Substituting (D.29) and (D.30) into (D.27) and (D.28), respectively, yields

$$-k_4 \boldsymbol{e}_{\boldsymbol{\omega}}^T \left[\xi_1^{2p_2-1}, \xi_2^{2p_2-1}, \xi_3^{2p_2-1}\right]^T \leq 2^{(3-1/p_2)/2} \sigma_1 k_4 \rho^{(3-1/p_2)/2} + k_4 k_3^{2-1/p_2} \rho \quad \text{(D.31)}$$

$$\boldsymbol{e}_{\boldsymbol{\omega}}^T \boldsymbol{M}_2^{-1} [\boldsymbol{C}_1(\hat{\boldsymbol{v}})\hat{\boldsymbol{v}} - \boldsymbol{C}_1(\boldsymbol{v})\boldsymbol{v}] \leq b_2 \rho. \quad \text{(D.32)}$$

Then, substituting (D.31) and (D.32) into (D.25) yields

$$\dot{\rho} \leq (k_4 k_3^{2-1/p_2} + b_2)\rho + 2^{(3-1/p_2)/2} \sigma_1 k_4 \rho^{(3-1/p_2)/2}. \quad \text{(D.33)}$$

By Lemma 3

$$\rho^b = \rho^b \times 1^{1-b} \leq b\rho + 1 - b \qquad \forall 0 < b \leq 1.$$

Then, it follows from (D.33) that

$$\dot{\rho} \leq \sigma_2 \rho + \sigma_3 \quad \text{(D.34)}$$

where

$$\sigma_2 = k_4 k_3^{2-1/p_2} + b_2 + 2^{(3-1/p_2)/2} \sigma_1 k_4 (3 - 1/p_2)/2$$
$$\sigma_3 = 2^{(3-1/p_2)/2} \sigma_1 k_4 (1/p_2 - 1)/2.$$

Since $\sigma_2, \sigma_3 \in (0, \infty)$, it follows from (D.34) immediately that ρ is bounded, which implies that $\boldsymbol{e}_{\boldsymbol{q}}(t)$ and $\boldsymbol{e}_{\boldsymbol{\omega}}(t)$ are bounded $\forall t \in [0, +\infty)$.

Step 3 [Global Finite-Time Stability of Tracking Error Subsystems (29) and (30)]: From the proof of Steps 1 and 2, $\boldsymbol{e}_{\boldsymbol{r}}(t), \boldsymbol{e}_{\boldsymbol{v}}(t), \boldsymbol{e}_{\boldsymbol{q}}(t)$, and $\boldsymbol{e}_{\boldsymbol{\omega}}(t)$ are bounded, $\forall t \in [0, T_{ob}]$, where T_{ob} is the finite settling-time of observer (42). After T_{ob}, it holds that $\tilde{\boldsymbol{r}}(t) = \tilde{\boldsymbol{v}}(t) = \boldsymbol{0}_{3\times1}$. Then, controllers (46) and (47) reduce to their state feedback counterparts (35) and (39), respectively. From Theorems 1 and 2, in the absence of disturbances $\boldsymbol{\tau}_d$, the states of tracking error subsystems (29) and (30) will globally converge to the equilibrium set

$$Q_1 = \{[\boldsymbol{e}_{\boldsymbol{r}}^T, \boldsymbol{e}_{\boldsymbol{q}}^T, \boldsymbol{e}_{\boldsymbol{v}}^T, \boldsymbol{e}_{\boldsymbol{\omega}}^T]^T | \boldsymbol{e}_{\boldsymbol{r}} = \boldsymbol{e}_{\boldsymbol{v}} = \boldsymbol{e}_{\boldsymbol{\omega}} = \boldsymbol{0}_{3\times1}, \boldsymbol{e}_{\boldsymbol{q}} = [\pm 1, \boldsymbol{0}_{1\times3}]^T\}$$

in finite time. This completes the proof.

Appendix E
Some Remarks

Remark 3 [The Stability of the Closed-Loop System (29) and (35) With External Disturbances]: In the translational subsystem (24), if there exist bounded external disturbances $\boldsymbol{\tau}_{d_1}$ satisfying $\|\boldsymbol{\tau}_{d_1}\| \leq \tilde{L}_1$ with $\tilde{L}_1 > 0$, it follows that there is $L_1 > 0$ such that $\|\boldsymbol{R}(\boldsymbol{q})\boldsymbol{M}_1^{-1}\boldsymbol{\tau}_{d_1}\| \leq L_1$. Still take controller $\boldsymbol{\tau}_1$ as (35). Through the same computation as that in Appendix A, an inequality like (A.16) can be obtained

$$\dot{V}_{tr} \leq -c_1 \sum_{i=1}^{3} \beta_{1i}^{1+p_1} - c_1 \sum_{i=1}^{3} \varphi_i^{1+p_1} + \frac{L_1}{(2-p_1)2^{-p_1} k_1^{1+1/p_1}} \sum_{i=1}^{3} \varphi_i^{2-p_1} \quad \text{(E.1)}$$

where

$$\varphi_i = \beta_{2i}^{1/p_1} + k_1^{1/p_1} \beta_{1i}, \qquad i = 1, 2, 3.$$

By Lemma 3, it can be obtained that

$$\frac{L_1}{(2-p_1)2^{-p_1} k_1^{1+1/p_1}} \left(\varphi_i^{2-p_1} \times 1^{2p_1-1}\right) \leq \frac{c_1}{2} \varphi_i^{1+p_1} + H_1 \quad \text{(E.2)}$$

where the equation shown at the bottom of the page holds. Substituting (E.2) into (E.1) yields

$$\dot{V}_{tr} \leq -c_1 \sum_{i=1}^{3} \beta_{1i}^{1+p_1} - \frac{c_1}{2} \sum_{i=1}^{3} \varphi_i^{1+p_1} + 3H_1. \quad \text{(E.3)}$$

If

$$\|\boldsymbol{\beta}_1\| > \left(\frac{3H_1}{\lambda_1 c_1}\right)^{1/(1+p_1)}$$

with $0 < \lambda_1 < 1$, by Lemma 2, it can be obtained that

$$3H_1 < \lambda_1 c_1 \left(\sum_{i=1}^{3} \beta_{1i}^2\right)^{(1+p_1)/2} \leq \lambda_1 c_1 \sum_{i=1}^{3} \beta_{1i}^{1+p_1}$$

which, together with (E.3), yields

$$\dot{V}_{tr} < -(1-\lambda_1)c_1 \sum_{i=1}^{3} \beta_{1i}^{1+p_1} - \frac{c_1}{2} \sum_{i=1}^{3} \varphi_i^{1+p_1} < 0. \quad \text{(E.4)}$$

Thus, $[\boldsymbol{\beta}_1^T, \boldsymbol{\beta}_2^T]^T$ will converge to the region

$$\Psi_1 = \left\{[\boldsymbol{\beta}_1^T, \boldsymbol{\beta}_2^T]^T \middle| \|\boldsymbol{\beta}_1\| \leq [3H_1/(\lambda_1 c_1)]^{1/(1+p_1)}\right\}$$

in finite time. Similarly, it can be verified that $[\boldsymbol{\beta}_1^T, \boldsymbol{\beta}_2^T]^T$ will also converge to the region

$$\Psi_2 = \left\{[\boldsymbol{\beta}_1^T, \boldsymbol{\beta}_2^T]^T \middle| \|\boldsymbol{\varphi}\| \leq [6H_1/(\lambda_1 c_1)]^{1/(1+p_1)}\right\}$$

$$H_1 = \frac{2^{(2+p_1^2)/(2p_1-1)}(2p_1-1)L_1^{(1+p_1)/(2p_1-1)}}{(1+p_1)^{(1+p_1)/(2p_1-1)}(2-p_1)k_1^{(1+p_1)^2/[p_1(2p_1-1)]}c_1^{(2-p_1)/(2p_1-1)}} > 0.$$

in finite time, where $\boldsymbol{\varphi} = [\varphi_1, \varphi_2, \varphi_3]^T$. By noting that

$$\varphi_i = \beta_{2i}^{1/p_1} + k_1^{1/p_1}\beta_{1i}$$

it follows that

$$|\beta_{2i}| \leq |\varphi_i|^{p_1} + k_1|\beta_{1i}|^{p_1}, \qquad i = 1, 2, 3.$$

If

$$[\boldsymbol{\beta}_1^T, \boldsymbol{\beta}_2^T]^T \in \Psi_1 \bigcap \Psi_2$$

it holds that

$$|\beta_{2i}| \leq [6H_1/(\lambda_1 c_1)]^{p_1/(1+p_1)} + k_1[3H_1/(\lambda_1 c_1)]^{p_1/(1+p_1)}, \qquad i = 1, 2, 3$$

and then

$$\begin{aligned}\|\boldsymbol{\beta}_2\| &\leq \sum_{i=1}^{3} |\beta_{2i}| \\ &\leq 3[6H_1/(\lambda_1 c_1)]^{p_1/(1+p_1)} + 3k_1[3H_1/(\lambda_1 c_1)]^{p_1/(1+p_1)}.\end{aligned}$$

Based on the above analyses, the state $[\boldsymbol{\beta}_1^T, \boldsymbol{\beta}_2^T]^T$ of system (37) will converge to the following region in finite time:

$$\begin{aligned}\Psi = \Bigg\{ \left[\boldsymbol{\beta}_1^T, \boldsymbol{\beta}_2^T\right]^T \Bigg| \|\boldsymbol{\beta}_1\| \leq \left(\frac{3H_1}{\lambda_1 c_1}\right)^{1/(1+p_1)}, \\ \|\boldsymbol{\beta}_2\| \leq 3(2^{p_1/(1+p_1)} + k_1)\left(\frac{3H_1}{\lambda_1 c_1}\right)^{p_1/(1+p_1)} \Bigg\}. \qquad \text{(E.5)}\end{aligned}$$

Due the invertible coordinate transformations (32) between $\boldsymbol{r}, \boldsymbol{v}$ and $\boldsymbol{z}_1, \boldsymbol{z}_2$, and (36) between $\boldsymbol{e}_{\boldsymbol{z}_1}, \boldsymbol{e}_{\boldsymbol{z}_2}$ and $\boldsymbol{\beta}_1, \boldsymbol{\beta}_2$, it can be verified that in the presence of bounded disturbances $\boldsymbol{\tau}_{d_1}$, under controller (35), the state $[\boldsymbol{e}_{\boldsymbol{r}}^T, \boldsymbol{e}_{\boldsymbol{v}}^T]^T$ of translational tracking error subsystem (29) will converge to a bounded region around the origin in finite time and the bound of the region is determined by control parameters k_1, c_1, and p_1 and the bound of $\boldsymbol{\tau}_{d_1}$. Specifically, by the definition of H_1, we have the equation shown at the bottom of the page. Thus, it holds that

$$\lim_{p_1 \to 1/2} \left(\frac{3H_1}{\lambda_1 c_1}\right)^{1/(1+p_1)} = 0 \quad \text{and} \quad \left(\frac{3H_1}{\lambda_1 c_1}\right)^{1/(1+p_1)}$$

is inversely proportional to k_1 and c_1 and directly proportional to the bound of disturbances $\boldsymbol{\tau}_{d_1}$ for fixed λ_1 and p_1. In other words, by appropriately adjusting control parameters k_1, c_1, and p_1 (especially p_1, since k_1 and c_1 cannot be too large due to drawbacks often caused by high gain control, e.g., instability, and control saturation constraint in practice), the steady-state bound of $[\boldsymbol{e}_{\boldsymbol{r}}^T, \boldsymbol{e}_{\boldsymbol{v}}^T]^T$ can be very small.

Remark 4 [The Robustness of the Closed-Loop System (29) and (35)]: When model information is not accurate, the issue of control robustness must be considered. Uncertainties of damping matrix $\boldsymbol{D}_1(\boldsymbol{v})$ and restoring forces $\boldsymbol{g}_1(\boldsymbol{q})$ are considered in the following discussions. Uncertainties of system inertia matrix $\boldsymbol{M}_1$ and matrix of Coriolis and centripetal effects $\boldsymbol{C}_1(\boldsymbol{v})$ [$\boldsymbol{C}_1(\boldsymbol{v})$ relies on $\boldsymbol{M}_1$ since $\boldsymbol{C}_1(\boldsymbol{v}) = -\boldsymbol{S}(\boldsymbol{M}_1\boldsymbol{v})$] are deferred to future work, since it is quite difficult to deal with the multiplicative uncertainties. There are uncertainties in $\boldsymbol{D}_1(\boldsymbol{v})$ and $\boldsymbol{g}_1(\boldsymbol{q})$, i.e.,

$$\begin{aligned}\boldsymbol{D}_1(\boldsymbol{v}) &= \bar{\boldsymbol{D}}_1(\boldsymbol{v}) + \Delta\boldsymbol{D}_1(\boldsymbol{v}) \\ \boldsymbol{g}_1(\boldsymbol{q}) &= \bar{\boldsymbol{g}}_1(\boldsymbol{q}) + \Delta\boldsymbol{g}_1(\boldsymbol{q})\end{aligned}$$

where $\bar{\boldsymbol{D}}_1(\boldsymbol{v})$ and $\bar{\boldsymbol{g}}_1(\boldsymbol{q})$ are the nominal parts and $\Delta\boldsymbol{D}_1(\boldsymbol{v})$ and $\Delta\boldsymbol{g}_1(\boldsymbol{q})$ are the uncertain parts. Specifically, for $\boldsymbol{D}_1(\boldsymbol{v})$

$$d_{v_i} = \bar{d}_{v_i} + \Delta d_{v_i} \quad \text{and} \quad d_{Q_i} = \bar{d}_{Q_i} + \Delta d_{Q_i} q, \qquad i = 1, 2, 3$$

where $\bar{d}_{v_i}$ and $\bar{d}_{Q_i}$ are the nominal parts and Δd_{v_i} and Δd_{Q_i} are the uncertain parts. Due to the presence of uncertainties, controller $\boldsymbol{\tau}_1$ can only utilize the parameter nominal values, i.e., $\boldsymbol{\tau}_1$ given in (35) becomes

$$\begin{aligned}\boldsymbol{\tau}_1 = &-k_2\boldsymbol{M}_1\boldsymbol{R}^T(\boldsymbol{q})\left[\varphi_1^{2p_1-1}, \varphi_2^{2p_1-1}, \varphi_3^{2p_1-1}\right]^T \\ &- \boldsymbol{M}_1\left[\boldsymbol{S}(\boldsymbol{\omega})\boldsymbol{M}_1^{-1}\boldsymbol{R}^T(\boldsymbol{q}) - \boldsymbol{M}_1^{-1}\boldsymbol{S}(\boldsymbol{\omega})\boldsymbol{R}^T(\boldsymbol{q})\right]\boldsymbol{e}_{\boldsymbol{z}_2} \\ &+ \bar{\boldsymbol{D}}_1(\boldsymbol{M}_1^{-1}\boldsymbol{R}^T(\boldsymbol{q})\boldsymbol{z}_2)\boldsymbol{M}_1^{-1}\boldsymbol{R}^T(\boldsymbol{q})\boldsymbol{z}_2 + \bar{\boldsymbol{g}}_1(\boldsymbol{q}) + \boldsymbol{R}^T(\boldsymbol{q})\dot{\boldsymbol{z}}_{2d}\end{aligned} \qquad \text{(E.6)}$$

where the control parameters k_1, k_2 are to be redesigned. Based on the coordinate transformation (36), substituting controller (E.6) into system (34) yields the following system:

$$\dot{\boldsymbol{\beta}}_1 = \boldsymbol{\beta}_2, \dot{\boldsymbol{\beta}}_2 = -k_2[\varphi_1^{2p_1-1}, \varphi_2^{2p_1-1}, \varphi_3^{2p_1-1}]^T + \boldsymbol{\Delta} \qquad \text{(E.7)}$$

where

$$\boldsymbol{\Delta} = [\Delta_1, \Delta_2, \Delta_3]^T = -\boldsymbol{R}(\boldsymbol{q})\boldsymbol{M}_1^{-1}(\Delta\boldsymbol{D}_1(\boldsymbol{v})\boldsymbol{v} + \Delta\boldsymbol{g}_1(\boldsymbol{q}) - \boldsymbol{\tau}_{d_1}).$$

Hence, substituting

$$\dot{\beta}_{2i} = -k_2\varphi_i^{2p_1-1} + \Delta_i, \qquad i = 1, 2, 3$$

into (A.14) yields

$$\begin{aligned}\dot{V}_{tr} \leq &-\left(k_1 - \frac{2^{1-p_1}}{1+p_1} - \frac{2p_1}{1+p_1}\right)\sum_{i=1}^{3}\beta_{1i}^{1+p_1} \\ &+ \left(\frac{2^{1-p_1}p_1}{1+p_1} + \frac{2}{1+p_1} + \frac{2^{2-p_1}}{k_1}\right)\sum_{i=1}^{3}\varphi_i^{1+p_1} \\ &- \frac{k_2}{(2-p_1)2^{-p_1}k_1^{1+1/p_1}}\sum_{i=1}^{3}\varphi_i^{1+p_1} \\ &+ \frac{1}{(2-p_1)2^{-p_1}k_1^{1+1/p_1}}\sum_{i=1}^{3}\varphi_i^{2p_1-1}\Delta_i.\end{aligned} \qquad \text{(E.8)}$$

$$\left(\frac{3H_1}{\lambda_1 c_1}\right)^{1/(1+p_1)} = \left[\frac{2^{(2+p_1^2)/(1+p_1)}3^{(2p_1-1)/(1+p_1)}(2p_1-1)^{(2p_1-1)/(1+p_1)}L_1}{(1+p_1)(2-p_1)^{(2p_1-1)/(1+p_1)}\lambda_1^{(2p_1-1)/(1+p_1)}k_1^{(1+p_1)/p_1}c_1}\right]^{1/(2p_1-1)}.$$

Since the uncertainties and disturbances are bounded, there are

$$H_1, \tilde{H}_1, H_2, \tilde{H}_2 > 0$$

such that

$$|\Delta_i| \leq H_1 \sum_{j=1}^{3} (|\Delta d_{v_j}||v_j| + |\Delta d_{Q_j}|v_j^2) + H_2 \leq \tilde{H}_1 \sum_{i=j}^{3} v_j^2 + \tilde{H}_2, \quad i = 1,2,3.$$

Note that

$$\begin{aligned} \boldsymbol{z}_2 &= \boldsymbol{R}(\boldsymbol{q})\boldsymbol{M}_1\boldsymbol{v} \\ \boldsymbol{z}_{2d} &= \boldsymbol{R}(\boldsymbol{q})\boldsymbol{M}_1\boldsymbol{v}_d \\ \boldsymbol{e}_{\boldsymbol{z}_2} &= \boldsymbol{z}_2 - \boldsymbol{z}_{2d} \end{aligned}$$

and $\boldsymbol{v}_d$ is bounded from Assumption 1. Thus, there are

$$H_3, \tilde{H}_3, H_4, \tilde{H}_4 > 0$$

such that

$$|\Delta_i| \leq H_3 \sum_{j=1}^{3} z_{2j}^2 + H_4 \leq \tilde{H}_3 \sum_{j=1}^{3} e_{z_{2j}}^2 + \tilde{H}_4, \qquad i = 1,2,3.$$

From (36)

$$\boldsymbol{\beta}_2 = \boldsymbol{R}(\boldsymbol{q})\boldsymbol{M}_1^{-1}\boldsymbol{R}^T(\boldsymbol{q})\boldsymbol{e}_{\boldsymbol{z}_2}$$

then there are $H_5, H_6 > 0$ such that

$$|\Delta_i| \leq H_5 \sum_{j=1}^{3} \beta_{2j}^2 + H_6, \qquad i = 1,2,3.$$

Note that

$$\beta_{2j} = (\varphi_j - k_1^{1/p_1}\beta_{1j})^{p_1}.$$

By Lemma 1, it follows that

$$\begin{aligned} |\Delta_i| &\leq H_5 \sum_{j=1}^{3} (\varphi_j - k_1^{1/p_1}\beta_{1j})^{2p_1} + H_6 \\ &\leq 2^{2p_1-1} H_5 \sum_{j=1}^{3} \varphi_j^{2p_1} + 2^{2p_1-1} H_5 k_1^2 \sum_{j=1}^{3} \beta_{1j}^{2p_1} + H_6. \end{aligned} \tag{E.9}$$

From Lemma 3, it holds that

$$\varphi_i^{2-p_1}\beta_{1j}^{2p_1} \leq \frac{2p_1}{1+p_1}\beta_{1j}^{1+p_1} + \frac{2-p_1}{1+p_1}\varphi_i^{1+p_1}, \qquad i,j = 1,2,3.$$

Hence, from (E.8) and (E.9), there are $H_7, H_8, H_9 > 0$ such that

$$\begin{aligned} \dot{V}_{tr} \leq& -(k_1 - H_7)\sum_{i=1}^{3} \beta_{1i}^{1+p_1} + H_8 \sum_{i=1}^{3} \varphi_i^{1+p_1} \\ &- \frac{k_2}{(2-p_1)2^{-p_1}k_1^{1+1/p_1}} \sum_{i=1}^{3} \varphi_i^{1+p_1} + H_9. \end{aligned} \tag{E.10}$$

By taking

$$k_1 \geq H_7 + c_1, k_2 \geq (2-p_1)2^{-p_1}k_1^{1+1/p_1}(H_8 + c_1), \qquad c_1 > 0$$

it follows from (E.10) that

$$\dot{V}_{tr} \leq -c_1 \sum_{i=1}^{3} \beta_{1i}^{1+p_1} - c_1 \sum_{i=1}^{3} \varphi_i^{1+p_1} + H_9. \tag{E.11}$$

Similar to the analyses in Remark 3, under controller $\boldsymbol{\tau}_1$ as (E.6), the state $[\boldsymbol{e}_{\boldsymbol{r}}^T, \boldsymbol{e}_{\boldsymbol{v}}^T]^T$ of translational tracking error subsystem (29) will converge to a bounded region around the origin in finite time and the bound of the region is determined by control parameters k_1, c_1, p_1 and the bounds of the uncertainties and disturbances. Moreover, the steady-state bound of $[\boldsymbol{e}_{\boldsymbol{r}}^T, \boldsymbol{e}_{\boldsymbol{v}}^T]^T$ can be very small by appropriately adjusting k_1, c_1, p_1. Thus, the closed-loop system (29) and (E.6) has very good robustness in the presence of model parameter uncertainties. Actually, a discontinuous term $-k_5\mathrm{sgn}(\varphi_i)$ with appropriate $k_5 > 0$ can be added in controller $u_{1i}, i = 1,2,3$, as (A.15) [represented by $-k_5\boldsymbol{M}_1\boldsymbol{R}^T(\boldsymbol{q})[\mathrm{sgn}(\varphi_1), \mathrm{sgn}(\varphi_2), \mathrm{sgn}(\varphi_3)]^T$ in controller $\boldsymbol{\tau}_1$ as (E.6)] to dominate the uncertainties and disturbances and then improve the robustness of the closed-loop system. The above method is inspired by the sliding-mode control philosophy. However, doing this will lead to chattering, which is undesired in practice.

Remark 5: If $p_1 = 1$, controller $\boldsymbol{\tau}_1$ in (35) reduces to the following controller:

$$\begin{aligned} \boldsymbol{\tau}_1 =& -k_2\boldsymbol{M}_1\boldsymbol{R}^T(\boldsymbol{q})[\varphi_1, \varphi_2, \varphi_3]^T \\ &- \boldsymbol{M}_1[\boldsymbol{S}(\boldsymbol{\omega})\boldsymbol{M}_1^{-1}\boldsymbol{R}^T(\boldsymbol{q}) - \boldsymbol{M}_1^{-1}\boldsymbol{S}(\boldsymbol{\omega})\boldsymbol{R}^T(\boldsymbol{q})]\boldsymbol{e}_{\boldsymbol{z}_2} \\ &+ \boldsymbol{D}_1(\boldsymbol{M}_1^{-1}\boldsymbol{R}^T(\boldsymbol{q})\boldsymbol{z}_2)\boldsymbol{M}_1^{-1}\boldsymbol{R}^T(\boldsymbol{q})\boldsymbol{z}_2 \\ &+ \boldsymbol{g}_1(\boldsymbol{q}) + \boldsymbol{R}^T(\boldsymbol{q})\dot{\boldsymbol{z}}_{2d} \end{aligned} \tag{E.12}$$

where

$$\begin{aligned} &\varphi_i = \left[\boldsymbol{R}(\boldsymbol{q})\boldsymbol{M}_1^{-1}\boldsymbol{R}^T(\boldsymbol{q})\boldsymbol{e}_{\boldsymbol{z}_2}\right]_i + k_1 e_{z_{1i}}, \qquad i = 1,2,3 \\ &k_1 \geq 3/2 + c_1, k_2 \geq k_1^2(3/4 + 1/k_1 + c_1/2), \qquad c_1 > 0. \end{aligned}$$

Actually, controller (E.12) can be regarded to be a conventional backstepping controller. Similar to the proof of Theorem 1, it can be verified that in the absence of external disturbances $\boldsymbol{\tau}_{d_1}$, under controller (E.12), system (34) is globally asymptotically stable with respect to the equilibrium $[\boldsymbol{e}_{\boldsymbol{z}_1}^T, \boldsymbol{e}_{\boldsymbol{z}_2}^T]^T = \boldsymbol{0}_{6\times 1}$, i.e., tracking errors $\boldsymbol{e}_{\boldsymbol{r}}$ and $\boldsymbol{e}_{\boldsymbol{v}}$ of system (29) will globally asymptotically converge to the equilibrium $[\boldsymbol{e}_{\boldsymbol{r}}^T, \boldsymbol{e}_{\boldsymbol{v}}^T]^T = \boldsymbol{0}_{6\times 1}$. Like the analyses in Remark 3, in presence of external disturbances $\boldsymbol{\tau}_{d_1}$, under controller (E.12), the state $[\boldsymbol{e}_{\boldsymbol{r}}^T, \boldsymbol{e}_{\boldsymbol{v}}^T]^T$ of translational tracking error subsystem (29) will converge to a bounded region around the origin in finite time and the bound of the region is determined by control parameters k_1, c_1 and the bound of $\boldsymbol{\tau}_{d_1}$. Specifically, the above bound is directly proportional to $(6^{1/2}L_1)/(\lambda_1^{1/2}k_1^2c_1)$, where $0 < \lambda_1 < 1$ is the same as that defined in Remark 3 and L_1 is the bound of $\boldsymbol{\tau}_{d_1}$. One may argue that by adjusting control parameters k_1 or c_1 to be large enough, both convergence regions under controllers (35) and (E.12) can be rendered to be as small as desired. However, high gain feedback control systems often exhibit instability in actual operations. From the perspectives of stability as well as control saturation constraint in practice, k_1, c_1 cannot be set too large. In this case, for the finite-time controller (35), another parameter, i.e., the fractional power p_1, can be adjusted to enhance the disturbance rejection performance and robustness without obvious increase in the control input. For instance, p_1 can be chosen to be sufficiently close to $1/2$ such that $1/(2p_1-1)$ is sufficiently bigger than 1, which results in the equation shown at the bottom of the page. Therefore, finite-time controller (35) can provide a faster convergence rate, a better disturbance rejection property, and better robustness for system (29) than backstepping controller (E.12).

Remark 6: Similar to the analyses in Remark 3, it can be verified that in the presence of bounded external disturbances $\boldsymbol{\tau}_{d_2}$, the state $[e_q^T, \boldsymbol{e}_{\boldsymbol{\omega}}^T]^T$ of rotational tracking error subsystem (30) will converge to a bounded region around the equilibrium set Q_2 in finite time. Specifically, the bound approaches zero as $p_2 \to 1/2$, and is inversely proportional to the control parameters k_3, c_2 and directly proportional to the bound of disturbances $\boldsymbol{\tau}_{d_2}$. Proof on this is also similar to the proof on part ii) of Theorem 1 in [50]. Due to space limitations, the detailed proof is omitted here. If $p_2 = 1$, controller $\boldsymbol{\tau}_2$ in (39) reduces to the following controller:

$$\begin{aligned}\boldsymbol{\tau}_2 = -k_4\boldsymbol{M}_2[\xi_1,\xi_2,\xi_3]^T + \boldsymbol{C}_1(\boldsymbol{v})\boldsymbol{v} + \boldsymbol{C}_2(\boldsymbol{\omega})\boldsymbol{\omega}\\ + \boldsymbol{D}_2(\boldsymbol{\omega})\boldsymbol{\omega} + \boldsymbol{g}_2(\boldsymbol{q}) + \boldsymbol{M}_2\dot{\boldsymbol{\omega}}_d \quad \text{(E.13)}\end{aligned}$$

where

$$\begin{aligned}&\xi_i = e_{\omega_i} + \operatorname{sgn}(e_\eta(0))k_3 e_{\epsilon_i}, \qquad i = 1,2,3\\ &k_3 \geq 2 + c_2\\ &k_4 \geq k_3^2[3/(2k_3) + 1 + c_2/2], \qquad c_2 > 0\end{aligned}$$

and $e_\eta(0)$ represents the initial value of $e_\eta(t)$. Controller (E.13) can also be regarded to be a conventional backstepping or controller. Similar to proof of Theorem 2, in the absence of external disturbances $\boldsymbol{\tau}_{d_2}$, under controller (E.13), rotational tracking error subsystem (30) is globally asymptotically stable with respect to the equilibrium set Q_2. Like analyses in Remark 5, in the presence of external disturbances $\boldsymbol{\tau}_{d_2}$, under controller (E.13), the state $[\boldsymbol{e}_{\boldsymbol{q}}^T, \boldsymbol{e}_{\boldsymbol{\omega}}^T]^T$ of system (30) will converge to a bounded region around the equilibrium set Q_2 in finite time and the bound of the region is inversely proportional to the control parameters k_3, c_2 and directly proportional to the bound of disturbances $\boldsymbol{\tau}_{d_2}$. Furthermore, compared with backstepping controller (E.13), finite-time controller (39) can achieve a faster convergence rate, a better disturbance rejection property, and better robustness for system (30).

Remark 7: In the presence of bounded external disturbances $\boldsymbol{\tau}_{d_1}, \boldsymbol{\tau}_{d_2}$, through a proof similar to that of Theorem 4, it can be obtained that both the state $[\boldsymbol{e}_{\boldsymbol{r}}^T, \boldsymbol{e}_{\boldsymbol{v}}^T]^T$ of translational tracking error subsystem (29) and the state $[e_q^T, \boldsymbol{e}_{\boldsymbol{\omega}}^T]^T$ of rotational tracking error subsystem (30) are still bounded under controllers (46) and (47), and observer (42) is also globally finite-time convergent with a finite settling time T_{ob}. After T_{ob}, output feedback controllers (46) and (47) reduce to their state feedback counterparts (35) and (39), respectively. Then, from Remarks 3 and 6, the states of both systems (29) and (30) will converge to bounded regions around their equilibria, respectively. Moreover, the bounds of the regions are determined by the control parameters and bounds of the external disturbances.

REFERENCES

[1] S. Soylu, B. J. Buckham, and R. P. Podhorodeski, "A chattering-free sliding-mode controller for underwater vehicles with fault-tolerant infinity-norm thrust allocation," *Ocean Eng.*, vol. 35, no. 16, pp. 1647–1659, Nov. 2008.

[2] G. Bartolini and A. Pisano, "Black-box position and attitude tracking for underwater vehicles by second-order sliding-mode technique," *Int. J. Robust Nonlinear Control*, vol. 20, no. 1, pp. 1594–1609, Sep. 2010.

[3] L. Lapierre and D. Soetanto, "Nonlinear path-following control of an AUV," *Ocean Eng.*, vol. 34, no. 11–12, pp. 1734–1744, Aug. 2007.

[4] K. Teo, E. An, and P. P. J. Beaujean, "A robust fuzzy autonomous underwater vehicle (AUV) docking approach for unknown current disturbances," *IEEE J. Ocean. Eng.*, vol. 37, no. 2, pp. 143–155, Apr. 2012.

[5] J. Petrich and D. J. Stilwell, "Robust control for an autonomous underwater vehicle that suppresses pitch and yaw coupling," *Ocean Eng.*, vol. 38, no. 1, pp. 197–204, Jan. 2011.

[6] G. Antonelli, F. Caccavale, S. Chiaverini, and G. Fusco, "A novel adaptive control law for underwater vehicles," *IEEE Trans. Control Syst. Technol.*, vol. 11, no. 2, pp. 221–232, Mar. 2003.

[7] L. Lapierre and B. Jouvencel, "Robust nonlinear path-following control of an AUV," *IEEE J. Ocean. Eng.*, vol. 33, no. 2, pp. 89–102, Apr. 2008.

[8] S. A. Woods, R. J. Bauer, and M. L. Seto, "Automated ballast tank control system for autonomous underwater vehicles," *IEEE J. Ocean. Eng.*, vol. 37, no. 4, pp. 727–739, Oct. 2012.

[9] B. Miao, T. Li, and W. Luo, "A DSC and MLP based robust adaptive NN tracking control for underwater vehicle," *Neurocomputing*, vol. 111, pp. 184–189, July 2013.

[10] T. I. Fossen, *Marine Control Systems: Guidance, Navigation and Control of Ships, Rigs and Underwater Vehicles*. Trondheim, Norway: Marine Cybernetics, 2002, pp. 194–196.

$$\left[\frac{2^{(2+p_1^2)/(1+p_1)}3^{(2p_1-1)/(1+p_1)}(2p_1-1)^{(2p_1-1)/(1+p_1)}L_1}{(1+p_1)(2-p_1)^{(2p_1-1)/(1+p_1)}\lambda_1^{(2p_1-1)/(1+p_1)}k_1^{(1+p_1)/p_1}c_1}\right]^{1/(2p_1-1)} \ll \frac{6^{1/2}L_1}{\lambda_1^{1/2}k_1^2c_1}$$

with

$$\frac{2^{(2+p_1^2)/(1+p_1)}3^{(2p_1-1)/(1+p_1)}(2p_1-1)^{(2p_1-1)/(1+p_1)}L_1}{(1+p_1)(2-p_1)^{(2p_1-1)/(1+p_1)}\lambda_1^{(2p_1-1)/(1+p_1)}k_1^{(1+p_1)/p_1}c_1} < 1.$$

[11] C. Silpa-Anan, “Autonomous underwater robot: Vision and control,” M.S. thesis, Dept. Syst. Eng., RSISE, Australian Nat. Univ., Canberra, A.C.T., Australia, 2001.
[12] V. Schmidt, T. C. Weber, D. N. Wiley, and M. P. Johnson, “Underwater tracking of Humpback Whales (Megaptera Novaeangliae) with high-frequency pingers and acoustic recording tags,” *IEEE J. Ocean. Eng.*, vol. 35, no. 4, pp. 821–836, Oct. 2010.
[13] N. H. Kussat, C. D. Chadwell, and R. Zimmerman, “Absolute positioning of an autonomous underwater vehicle using GPS and acoustic measurements,” *IEEE J. Ocean. Eng.*, vol. 30, no. 1, pp. 153–164, Jan. 2005.
[14] Ø. Hegrenæs and O. Hallingstad, “Model-aided INS with sea current estimation for robust underwater navigation,” *IEEE J. Ocean. Eng.*, vol. 36, no. 2, pp. 316–337, Apr. 2011.
[15] S. Liu, D. Wang, and E. Poh, “Nonlinear output feedback tracking control for AUVs in shallow wave disturbance condition,” *Int. J. Control*, vol. 81, no. 11, pp. 1806–1823, Nov. 2008.
[16] J. E. Refsnes, A. J. Sorensen, and K. Y. Pettersen, “Model-based output feedback control of slender-body underactuated AUVs: Theory and experiments,” *IEEE Trans. Control Syst. Technol.*, vol. 16, no. 15, pp. 930–946, Sep. 2008.
[17] L. Zhang, X. Qi, and Y. Pang, “Adaptive output feedback control based on DRFNN for AUV,” *Ocean Eng.*, vol. 36, no. 9-10, pp. 716–722, Jul. 2009.
[18] R. Cui, S. S. Ge, B. V. E. How, and Y. S. Choo, “Leader-follower formation control of underactuated autonomous underwater vehicles,” *Ocean Eng.*, vol. 37, no. 17–18, pp. 1491–1502, Dec. 2010.
[19] S. P. Hou and C. C. Cheah, “Can a simple control scheme work for a formation control of multiple autonomous underwater vehicles?,” *IEEE Trans. Control Syst. Technol.*, vol. 19, no. 5, pp. 1190–1201, Sep. 2011.
[20] Y. Wang, W. Yan, and J. Li, “Passivity-based formation control of autonomous underwater vehicles,” *IET Control Theory Appl.*, vol. 6, no. 4, pp. 518–525, Mar. 2012.
[21] S. Li and X. Wang, “Finite-time consensus and collision avoidance control algorithms for multiple AUVs,” *Automatica*, vol. 49, no. 11, pp. 3359–3367, Nov. 2013.
[22] D. A. Smallwood and L. L. Whitcomb, “Adaptive identification of dynamically positioned underwater robotic vehicles,” *IEEE Trans. Control Syst. Technol.*, vol. 11, no. 4, pp. 505–515, Jul. 2003.
[23] J. P. J. Avila, D. C. Donha, and J. C. Adamowski, “Experimental model identification of open-frame underwater vehicles,” *Ocean Eng.*, vol. 60, pp. 81–94, Mar. 2013.
[24] F. Xu, Z. Zou, J. Yin, and J. Cao, “Identification modeling of underwater vehicles' nonlinear dynamics based on support vector machines,” *Ocean Eng.*, vol. 67, pp. 68–76, Jul. 2013.
[25] P. W. J. van de Ven, T. A. Johansen, A. J. Sørensen, C. Flanagan, and D. Toal, “Neural network augmented identification of underwater vehicle models,” *Control. Eng. Practice*, vol. 15, no. 6, pp. 715–725, Jun. 2007.
[26] A. Tiano, R. Sutton, A. Lozowicki, and W. Naeem, “Observer Kalman filter identification of an autonomous underwater vehicle,” *Control. Eng. Practice*, vol. 15, no. 6, pp. 727–739, Jun. 2007.
[27] S. P. Bhat and D. S. Bernstein, “Geometric homogeneity with applications to finite-time stability,” *Math. Control Signal Syst.*, vol. 17, no. 2, pp. 101–127, 2005.
[28] S. Li, S. Ding, and Q. Li, “Global set stabilisation of the spacecraft attitude using finite-time control technique,” *Int. J. Control*, vol. 82, no. 5, pp. 822–836, May 2009.
[29] S. Li, H. Du, and X. Lin, “Finite-time consensus algorithm for multi-agent systems with double-integrator dynamics,” *Automatica*, vol. 47, no. 8, pp. 1706–1712, Aug. 2011.
[30] H. Du, S. Li, and C. Qian, “Finite-time attitude tracking control of spacecraft with application to attitude synchronization,” *IEEE Trans. Autom. Control*, vol. 56, no. 11, pp. 2711–2717, Nov. 2011.
[31] X. Wang, S. Li, and P. Shi, “Distributed finite-time containment control for double-integrator multiagent systems,” *IEEE Trans. Cybern.*, 2013, DOI: 10.1109/TCYB.2013.2288980.
[32] Y. Hong, “Finite-time control for robot manipulators,” *Syst. Control Lett.*, vol. 46, no. 4, pp. 243–253, Jul. 2002.
[33] X. Huang, W. Lin, and B. Yang, “Global finite-time stabilization of a class of uncertain nonlinear systems,” *Automatica*, vol. 41, no. 5, pp. 881–888, May 2005.
[34] X. Wang, X. Sun, S. Li, and H. Ye, “Finite-time position tracking control of rigid hydraulic manipulators based on high-order terminal sliding mode,” *Proc. Inst. Mech. Eng. I, J. Syst. Control Eng.*, vol. 226, no. 3, pp. 394–415, Mar. 2012.
[35] S. Ding, S. Li, and W. X. Zheng, “Nonsmooth stabilization of a class of nonlinear cascaded systems,” *Automatica*, vol. 48, no. 10, pp. 2597–2606, Oct. 2012.
[36] S. Khoo, J. Yin, Z. Man, and X. Yu, “Finite-time stabilization of stochastic nonlinear systems in strict-feedback form,” *Automatica*, vol. 49, no. 5, pp. 1403–1410, May 2013.
[37] Y. Feng, X. Yu, and F. Han, “On nonsingular terminal sliding-mode control of nonlinear systems,” *Automatica*, vol. 49, no. 6, pp. 1715–1722, June 2013.
[38] T. Menard, E. Moulay, and W. Perruquetti, “A global high-gain finite-time observer,” *IEEE Trans. Autom. Control*, vol. 55, no. 6, pp. 1500–1506, Jun. 2010.
[39] Y. Shen, Y. Huang, and J. Gu, “Global finite-time observers for Lipschitz nonlinear systems,” *IEEE Trans. Autom. Control*, vol. 56, no. 2, pp. 418–424, Feb. 2011.
[40] H. Du, C. Qian, S. Yang, and S. Li, “Recursive design of finite-time convergent observers for a class of time-varying nonlinear systems,” *Automatica*, vol. 49, no. 2, pp. 601–609, Feb. 2013.
[41] J. Yang, S. Li, J. Su, and X. Yu, “Continuous nonsingular terminal sliding mode control for systems with mismatched disturbances,” *Automatica*, vol. 49, no. 7, pp. 2287–2291, Jul. 2013.
[42] Y. Feng, X. Yu, and F. Han, “High-order terminal sliding-mode observer for parameter estimation of a permanent-magnet synchronous motor,” *IEEE Trans. Ind. Electron.*, vol. 60, no. 10, pp. 4272–4280, Oct. 2013.
[43] C. Qian and J. Li, “Global finite-time stabilization by output feedback for planar systems without observable linearization,” *IEEE Trans. Autom. Control*, vol. 50, no. 6, pp. 885–890, Jun. 2005.
[44] X. Wang, X. Sun, S. Li, and H. Ye, “Output feedback domination approach for finite-time force control of an electrohydraulic actuator,” *IET Control Theory Appl.*, vol. 6, no. 7, pp. 921–934, May 2012.
[45] M. T. Angulo, L. Fridman, and A. Levant, “Output-feedback finite-time stabilization of disturbed LTI systems,” *Automatica*, vol. 48, no. 4, pp. 606–611, Apr 2012.
[46] A. M. Zou, “Finite-time output feedback attitude tracking control for rigid spacecraft,” *IEEE Trans. Control Syst. Technol.*, vol. 22, no. 1, pp. 338–345, Jan. 2014.
[47] X. Liao, *Mathematical Theory and Application of Stability*. Wuhan, China: Publishing Company of the Center China Normal University, 1988, ch. 4.15.
[48] X. Lin and S. Li, “Finite time set stabilization of Chua's chaotic system,” in *Proc. IEEE Conf. Control Autom.*, Guangzhou, Guangdong, China, May–Jun. 2007, pp. 2890–2893.
[49] G. H. Golub and C. F. Van Loan, *Matrix Computations*. Baltimore, MD, USA: Johns Hopkins Univ. Press, 1996, ch. 2.
[50] S. Li, S. Ding, and Q. Li, “Global set stabilization of the spacecraft attitude control problem based on quaterninon,” *Int. J. Robust Nonlinear Control*, vol. 20, no. 1, pp. 84–105, Jan. 2010.

Shihua Li (M'05–SM'10) received the B.S., M.S., and Ph.D. degrees in automatic control from Southeast University, Nanjing, China, in 1995, 1998, and 2001, respectively.

Since 2001, he has been with the School of Automation, Southeast University, where he is currently a Professor. His main research interests include nonlinear control theory with applications to robot, spacecraft, alternating current (ac) motor, and other mechanical systems.

Xiangyu Wang received the B.S. degree in mathematics from Southeast University, Nanjing, China, in 2009, where he is currently working toward the Ph.D. degree at the School of Automation.

His research interests include nonlinear control theory, distributed cooperative control of multiagent systems, and motion control of autonomous underwater vehicles.

Lijun Zhang (S'91–M'95) received the B.S. degree from Yanan University, Yanan, China, in 1995 and the M.S. and Ph.D. degrees from the Shaanxi Normal University, Xi'an, China, in 2000 and 2003, respectively, all in systems theory.

From August 2003 to July 2005, he was a Postdoctoral Researcher at the Automation Department, Tsinghua University, Beijing, China. From August 2005 to November 2011, he joined Harbin Engineering University, Harbin, China, and served as a Professor. He is currently a Professor at Northwestern Polytechnic University, Xi'an, China. He authored/coauthored more than 60 papers. His current research interests are in nonlinear control theory and applications and acoustic signal processing.

Prof. Zhang is currently an Associated Editor of the *Intelligent Control and Automation*. He also served as a reviewer of the *America Mathematical Review*.